Metabolomic Identification of the Target of the Compounds Modulating Filopodia Protrusion

January 2011

Mitsuhiro Kitagawa

A Thesis for the Degree of Ph.D. in Science

Metabolomic Identification of the Target of the Compounds Modulating Filopodia Protrusion

January 2011

Graduate School of Science and Techonology
Keio University

Mitsuhiro Kitagawa

Contents

Chapter 1

Introduction

Chemical biology

Since genes have been found as the fundamental components of cells, the analysis of genes roles has been widely investigated to understand how they regulate the cellular events (cell growing, survivals, death, migrations, differentiations and etc) that organize our lives. After the human genome project has completed, the functional analysis of the protein has become the main focus in the growing research fields of biology in the post-genome era[1,2]. The proteins produced from the genes codes play the intrinsic roles for determining the cellular events through the sequential assembly of protein-protein interactions, which drafts signal transduction pathways. To realize the role of proteins for the cellular events, genetic study demonstrates as the powerful approach; genes coding the proteins of the interests can be mutated, deleted or knocked down/out to see the effect of the loss of the proteins on the cellular events, and *vice versa* gene overexpression to emphasize the protein role in the cellular events. Indeed, quite large numbers of the proteins have been revealed to regulate the various cellular events. However, according to the whole genome sequencing in the human cells, the number of the proteins is estimated around sub-millions, and roles of many proteins for cellular events are still veiled[1,3].

The research of chemical biology is among the best approaches to investigate the protein function for the cellular events[3-7]. The small molecular compound can bind to proteins and modulate their functions, thus they are used as the bio-probes in the chemical biological study, analogous to the method controlling the gene dosage in the genetic study[6,7]. Indeed, several bioactive compounds became the breakthroughs to

reveal proteins roles for the cellular events. For instance, the chemical biological study using immunosuppressant FK506 revealed the novel mechanism for the immunological systems[8,9]. In the study, Schreiber et al first identified immunophilins as the FK506-binding protein (target protein of FK506)[10] and revealed the complex of FK506-immunophilin as the inhibitor against calcineurin, which brought the FK506-induced immunosuppression[11]. This finding indicated that calcineurin hold the essential role for the immunological system[11,12]. Another example is the discovery of lactacystin. After the proteasomal subunit was identified as the target of lactacystin, the studies on the role of the proteasome-dependent protein degradation in various cellular events became widely expanded because of the easy use of the proteasomal inhibitors including lactacystin[13-15].

Since small molecular compounds can be used as the chemical inhibitor to rapidly control the target protein functions and be easily used and removed, genetics using the chemical inhibitors, termed chemical genetics are largely applicable for understanding the cellular events in molecular level[5,16]. Many chemical inhibitors available to date, however, are far fewer than the number of proteins involved in the complicated regulation of cellular events[5]. Therefore, new chemical inhibitors must be developed in order to advance the applicability of chemical genetic studies to the functional analysis of proteins.

Inhibitor screening

Small molecular compounds huge vary in their structures; variety will be unlimited in

speculation. Thus, there would be small molecular compounds that could be used as the chemical inhibitors against the functions of any proteins coded from genes[17,18]. The study of chemical biology essentially requires the chemical inhibitors, and the natural product takes a quite important role as the small molecular compounds sources for the inhibitor screening throughout history[17,19,20]. Natural products are mainly the second metabolites in bacteria, fungi and plants. They hold unique structural scaffolds and chiral centers, and thus are rich in their structural variety, especially stating unique structures beyond the human imaginations. Indeed, many chemical inhibitors including FK506[21] and lactacystin[22] above and antibiotics, anti-tumor agents and etc were indeed originally found through the natural product screening[23-25]. As the methods of the chemical synthesis have been developed, synthetic library of small molecular compounds also takes an important role for the compounds sources. Diversity-oriented synthesis including the method of the click-chemistry provided huge variety of compounds in shorter research periods as designed[26], and another number of chemical inhibitors was developed from the screening of the synthetic compounds library[27,28]. Today both natural products holding the unique chemical structures and chemical synthesis design of the variety of compounds are two wheels of the compounds sources for the inhibitor screening.

To find a new chemical inhibitor from these compounds sources, screening the compounds is often carried out. Enzyme-based *in vitro* screening assay can explore protein inhibitors. Since either compounds are not always able to penetrate through the cell membrane, or inhibitors sometimes target other proteins in cell system than those

expected in an *in vitro* screening[29,30], they need to confirm whether the inhibitors do indeed target the same proteins in cell system. On the other hand, cell-based screening offers the chemical inhibitors that assure the inhibition in cell systems. However, it requires the target protein identification of the compounds.

As described above, the development of the new chemical inhibitors possesses two issues: finding the bioactive substances from compounds sources and the target protein identification in cell systems. Here the author used the filopodia protrusion assay as the cell-based screening assay in order to obtain the bioactive substances and utilized the metabolome analysis for the target protein identification.

This thesis describes about the screening for the filopodia protrusion inhibitors in Chapter 2, the identification of the target protein of the inhibitors obtained from this screening in Chapter 3 and another screening study using filopodia protrusion assay as same as described in Chapter 2 but the purpose is to obtain the glycolytic inhibitors in Chapter 4. In summary, the author described the challenges to find the chemical inhibitors that could be usable in the study of the chemical biology.

Chapter 2

Screening for the Inhibitors against the Filopodia Protrusion

2-1 Introduction

To obtain the unique bioactive compounds available for the chemical biological study, the author paid attention to filopodia. Filopodia are spike-like cell membrane protrusions that are observed in migratory cells. Their role is described mainly as probing cues of motile cells finding proper path forehead and guiding cells to the right direction, so that they would contribute to the cell motility[31,32]. However, other than the cell migration, filopodia are thought to be also important in a number of cellular and developmental processes, including (i) neuritogenesis[33,34], (ii) axon guidance in neuronal growth cones[35,36], (iii) receptor–ligand endocytosis[37,38], (iv) virus uptake[39,40], (v) detection of pathogen targets for phagocytosis[41,42] and (vi) dorsal closure in *Drosophila* embryos[43,44]. Furthermore, the regulatory mechanism for filopodia protrusion still remains unclear[31,32], and few inhibitors against filopodia protrusion have been reported[45,46]. Therefore, the author tried to obtain the inhibitor against filopodia protrusion that would be a unique chemical probe for the chemical biological research, considering the possibility that it might become a key tool to clarify the regulatory mechanisms behind the filopodia protrusion.

2-2 Results and discussions

2-2-1 Screening, isolation and identification of the filopodia inhibitors

Screening

To screen for the filopodia inhibitors, a screening assay system is required. Human epidermal carcinomas A431 cells highly express the epidermal growth factor (EGF) receptor and became highly chemotactic in response to EGF stimulation[47]. During the process of EGF-induced cell migration in A431 cells, they protrude large spike-like filopodia that can be easily observed under a microscope 30 min after EGF stimulation. The author used this simple assay system to identify compounds from microbial sources that inhibited filopodia protrusion.

After screening over 3,000 microbial broth samples, it was found that one broth from *Lechevalieria* sp. strain 1869-19 strongly inhibited EGF-induced filopodia protrusion in A431 cells (**Fig. 2-1A**).

Isolation 1: the filopodia inhibition was synergistically caused.

To isolate the potential inhibitors in this broth, the broth extracts was separated into six fractions, numbered **I**–**VI**, by silica-gel chromatography with chloroform-methanol elution. However, no single fraction showed inhibitory activity against filopodia protrusion (**Fig. 2-1B**). To examine whether the active substance may have degraded during chromatography, all 6 fractions were re-mixed (recombined fractions were termed “Remix”) and tested for inhibitory activity. The Remix inhibited EGF-induced

filopodia protrusion in the same concentration range as the broth extract (**Fig. 2-1C**). These results suggested that the inhibition of EGF-induced filopodia protrusion was due to the synergistic action of two (or more) substances in the broth extract, and that these "active" substances were separated into different fractions during silica gel chromatography.

To determine which of the 6 fractions contained each active substance, we prepared remixes with one –fraction withdrawn and assessed each such remix for ability or inability to inhibit filopodia protrusion. Withdrawal of fractions **I** (eluted from silica gel column by 100:0 chloroform-methanol) and **IV** (eluted by 100:5 chloroform--methanol) from the Remix resulted in no inhibition of filopodia protrusion (**Table 2-1** and **Fig. 2-1D**), indicating that fractions **I** and **IV** contained active substances. Furthermore, combining fractions **I** and **IV** restored the inhibitory activity to a level comparable to the complete Remix, indicating that the mixture of the active substances in fractions **I** and **IV** was sufficient for inhibition of EGF-induced filopodia protrusion.

Isolation 2: purification

To identify the active substances in fractions **I** and **IV**, further isolation processes were undertaken. Fraction **IV** was subjected to silica gel column chromatography with toluene-acetone elution. Each resulting fraction was assessed for its ability to inhibit filopodia protrusion in the presence of fraction **I**. Fractions eluted with a toluene-acetone mixture at a 3:1 ratio demonstrated inhibition in the presence of fraction **I**, but not in its absence. Fractions showing the filopodia inhibition were

collected and further purified by centrifugal liquid-liquid partition chromatography (CPC) using chloroform-methanol-water (5:4:6, ascending mode) elution, yielding a colorless, amorphous product (**1**). The active substance in fraction **I** was purified by CPC using hexane-ethyl acetate-acetonitrile (5:1:4, ascending mode) elution, yielding pure yellow oil (**2**). The final purification procedure is described in **Fig. 2-2**.

Structural identification

The MS and NMR spectra analysis was enough to identify the substances **1** and **2** as glucopiericidin A[48] and piericidin A[49], respectively. However, since the structural detail became highly important in the next chapter, here the author described the detail, so that it was confirmed that they were identical to those previously reported[48,49].

Compound purity was confirmed by ^{1}H NMR spectra (**Figs. 2-3** and **2-9**). The molecular formulas $C_{31}H_{47}NO_9$ for **1** and $C_{25}H_{37}NO_4$ for **2** were determined from ^{13}C NMR spectra (**Figs. 2-4** and **2-10**) and HRESIMS (m/z 600.3112 $(M + Na)^+$, Calcd 600.3149, and 438.2738 $(M + Na)^+$, Calcd 438.2621, respectively). The assignments of the chemical shifts shown in **Table 2-2** agreed with the previous description of glucopiericidin A and piericidin A. The structural linkages were all confirmed by ^{1}H-^{1}H COSY and HMBC spectra (**Figs. 2-5** to **2-8**, **2-11** and **2-12**). Especially for glucopiericidin A, the hexopyranoside connection was revealed by HMBC correlation from H-1" to C-10 (**Fig. 2-8**). The most important description for stereochemistry of glucopiericidin A follows. Large coupling constants for the protons on the hexopyranoside ring (H-1" ~ H-5") showed that the connected carbon and oxygen

atoms were all equatorial, indicating that it was *β*-glucopyranoside. The value $[\alpha]^{23}_{D}$ -20.3 (*c* 0.24, MeOH) suggested that the stereochemistry of our isolated compound was identical to previously identified glucopiericidin A (10-*O*-*β*-D-glucopiranoside piericidin A)[48] (**Fig. 2-13**).

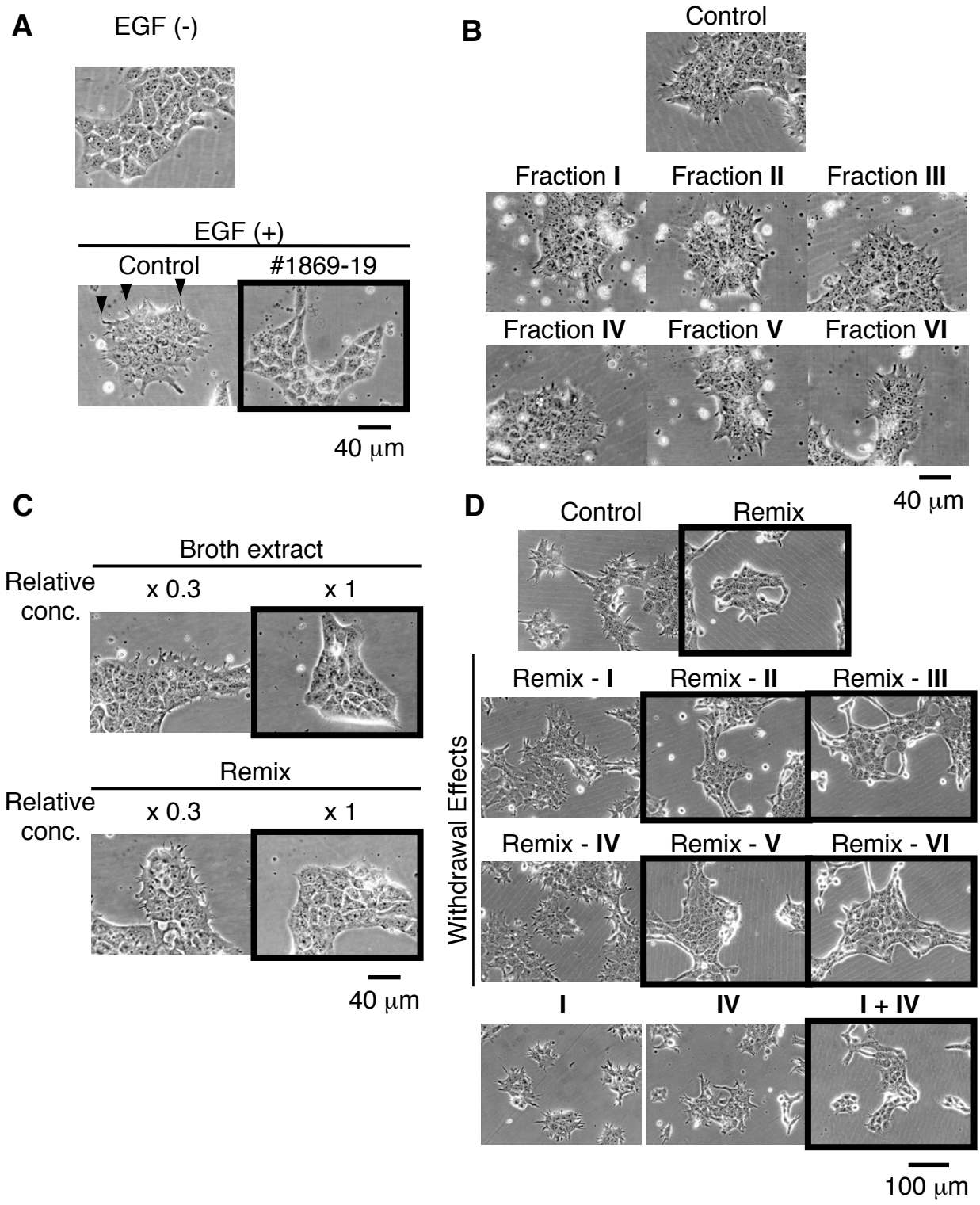

Figure 2-1 Bioassay-guided isolation of the filopodia inhibitor

(**A**) Filopodia inhibition by the hit broth of *Lechevalieria* sp. strain 1869-19. Arrowhead indicates filopodium.
(**B**) Inability to inhibit filopodia in the fractions from silica gel column chromatography.
(**C**) Recovery of the inhibitory activity by re-mixing the fractions of the chromatography.
(**D**) Withdrawing one fraction from Re-mix showed that the mixture of fraction **I** and **IV** was sufficient for the filopodia inhibition. See also **Table 2-1** for the summary of the withdrawal assays.

Table 2-1 Inhibitory activities of remixing silica gel chromatography fractions, and the effect of withholding each fraction from the Remix

Sample #	Fractions Eluted with $CHCl_3$: MeOH						Filopodia Protrusion
	100 : 0 **I**	100 : 1 **II**	100 : 2 **III**	100 : 5 **IV**	100 : 10 **V**	100 : 30 **VI**	
Remix	contained	contained	contained	contained	contained	contained	Inhibition
Remix – **I**		contained	contained	contained	contained	contained	**No inhibition**
Remix – **II**	contained		contained	contained	contained	contained	Inhibition
Remix – **III**	contained	contained		contained	contained	contained	Inhibition
Remix – **IV**	contained	contained	contained		contained	contained	**No inhibition**
Remix – **V**	contained	contained	contained	contained		contained	Inhibition
Remix – **VI**	contained	contained	contained	contained	contained		Inhibition
I + **IV**	contained			contained			**Inhibition**
I	contained						No inhibition
IV				contained			No inhibition

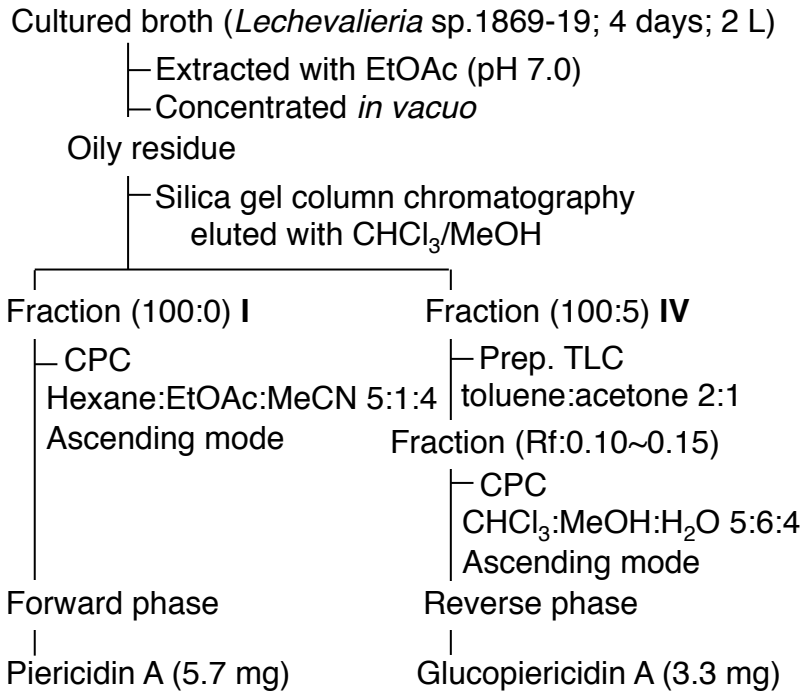

Figure 2-2 Purification procedure of piericidin A and glucopiericidin A.

Figure 2-3 ^{1}H NMR spectrum of glucopiericidin A ($CDCl_3$, 500 MHz)

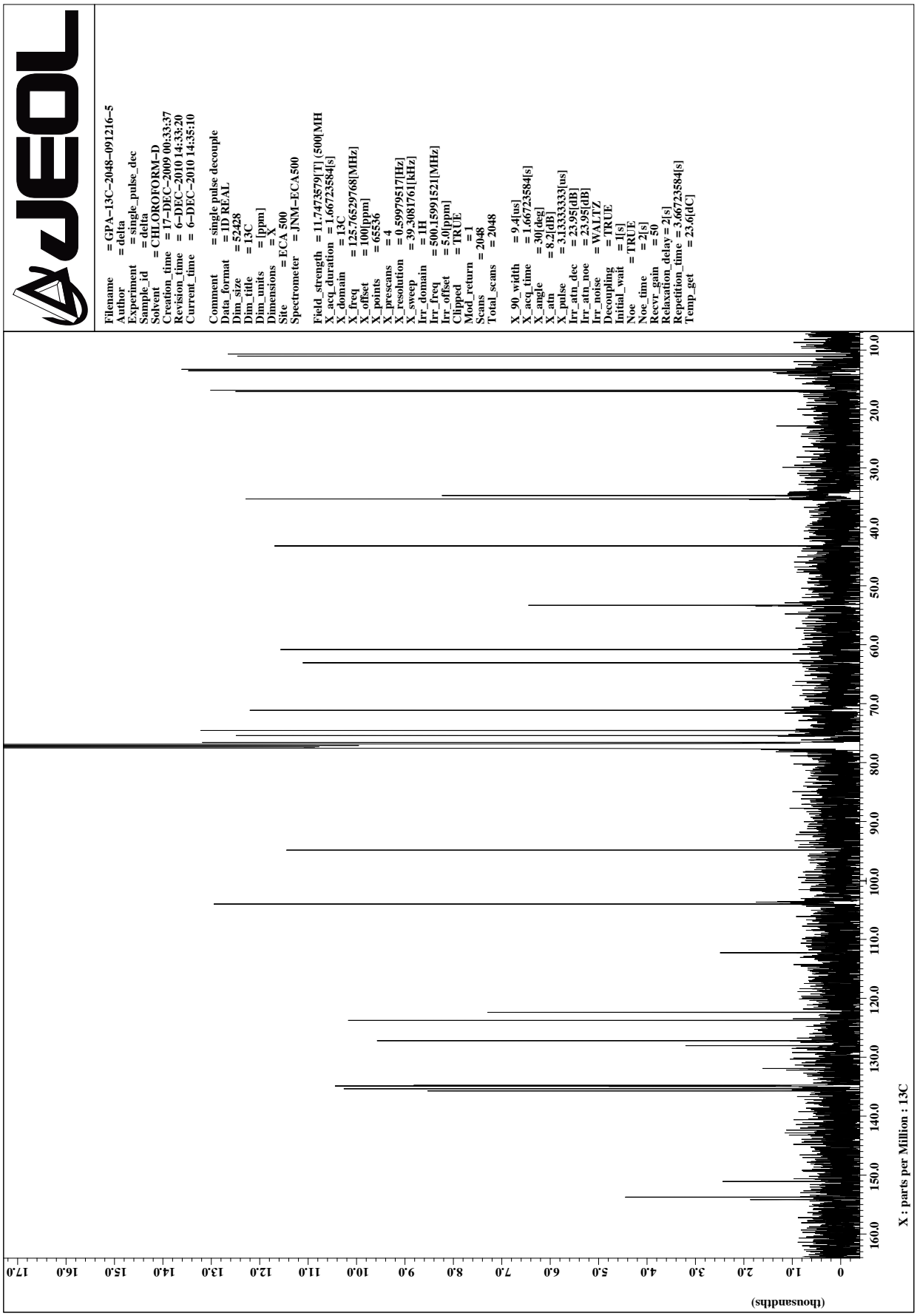

Figure 2-4 ^{13}C NMR spectrum of glucopiericidin A ($CDCl_3$, 125 MHz)

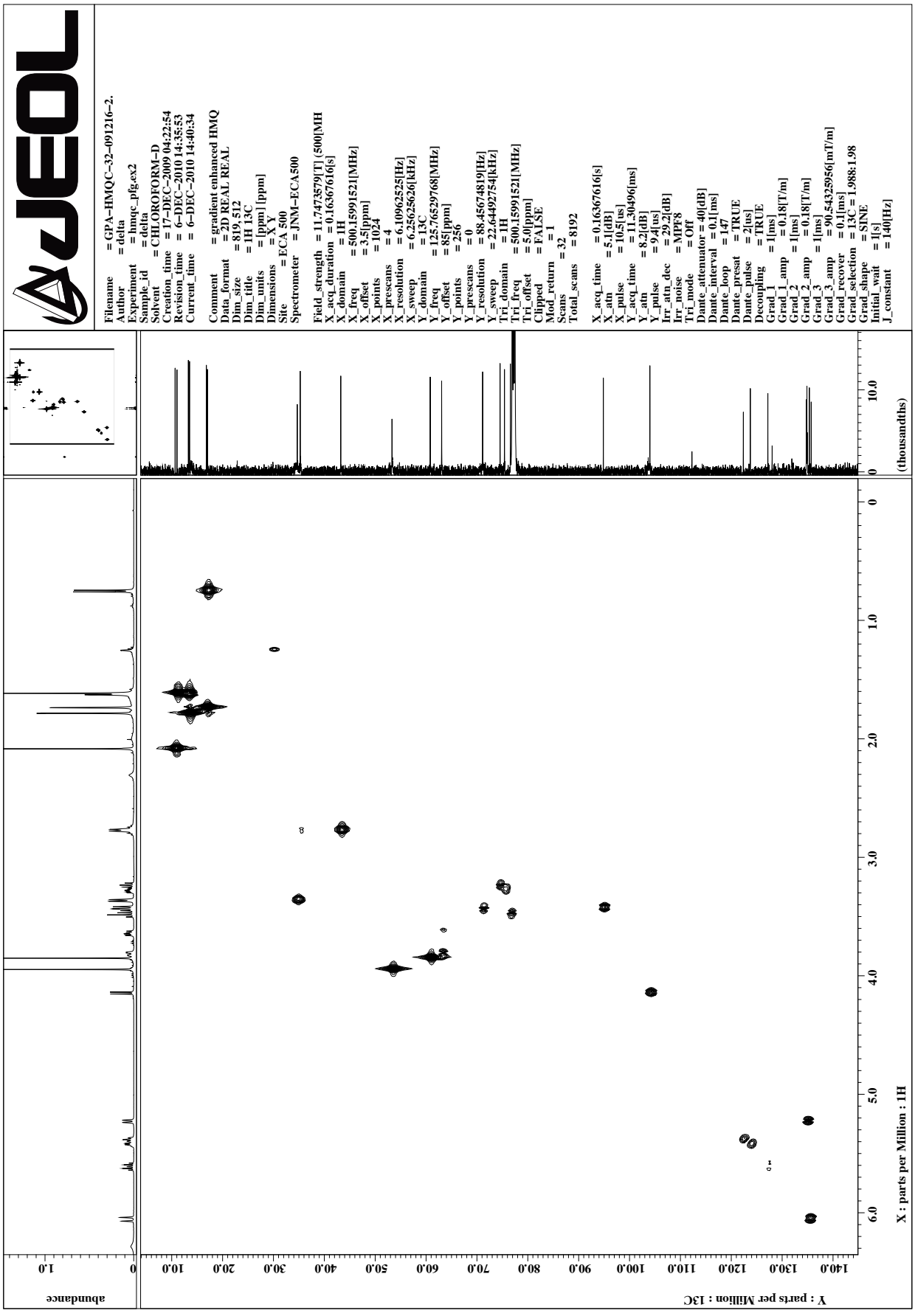

Figure 2-5 HMQC correlation of glucopiericidin A ($CDCl_3$, 500 MHz)

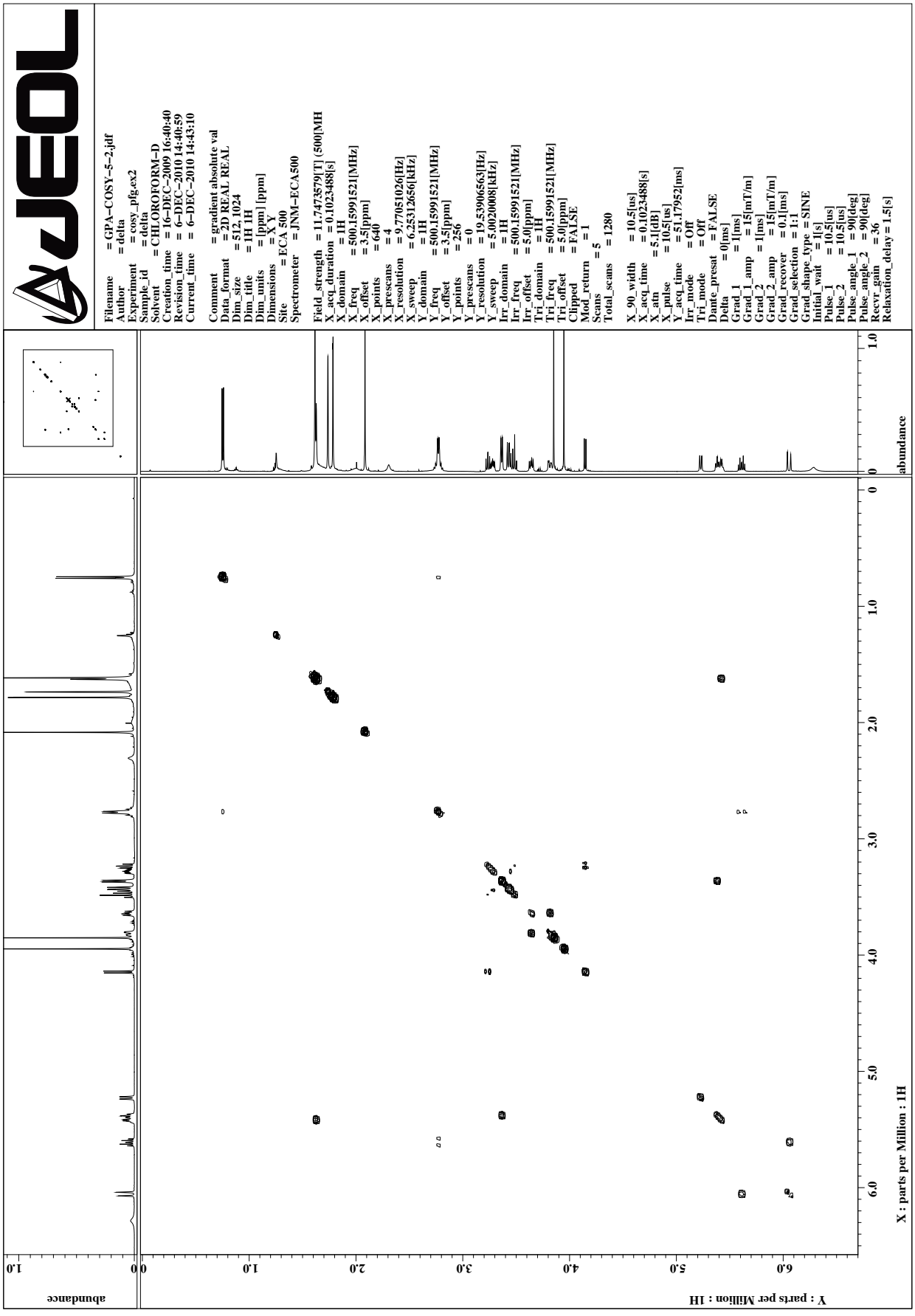

Figure 2-6 ^{1}H-^{1}H COSY correlation of glucopiericidin A ($CDCl_3$, 500 MHz)

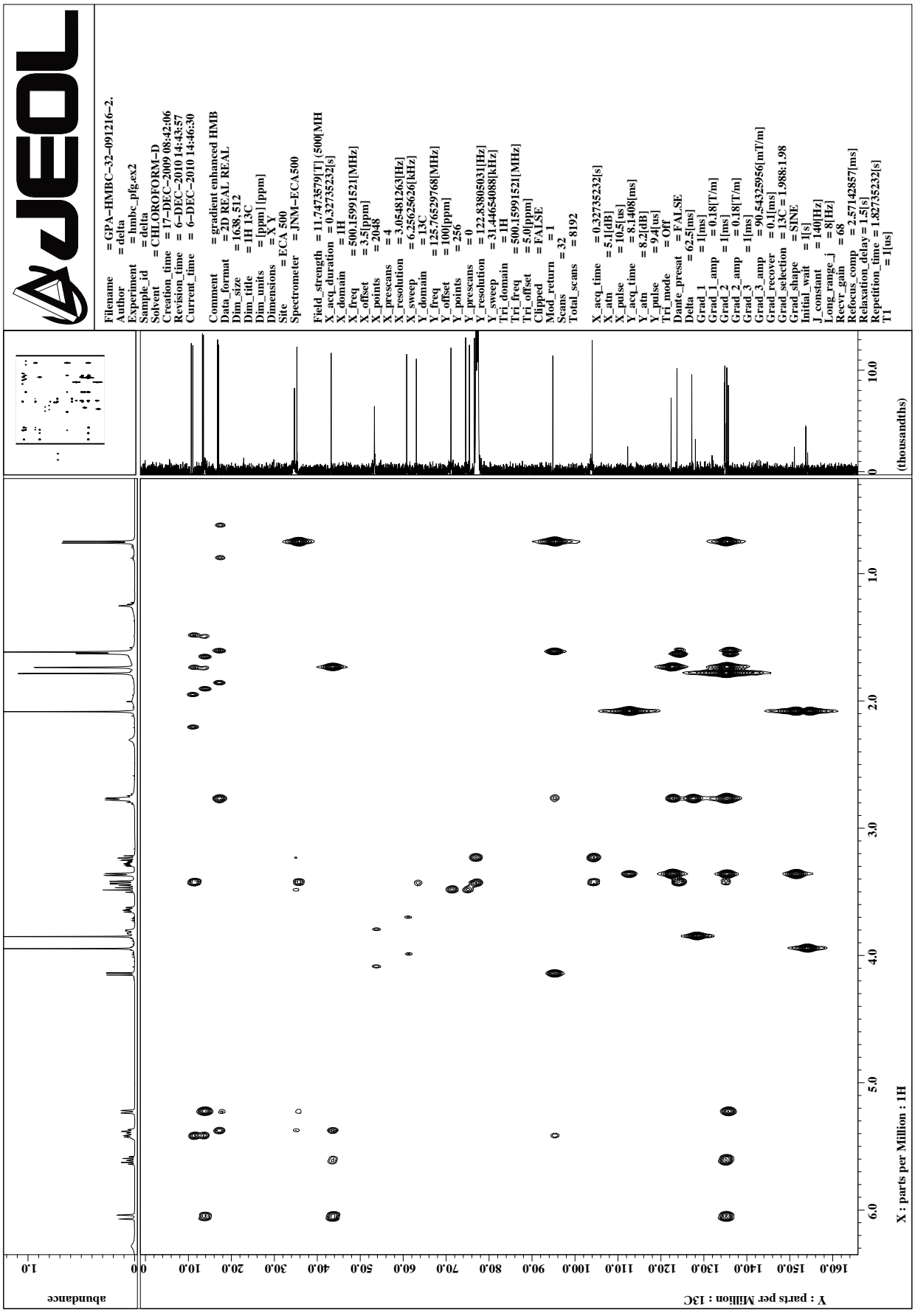

Figure 2-7 HMBC correlation of glucopiericidin A ($CDCl_3$, 500 MHz)

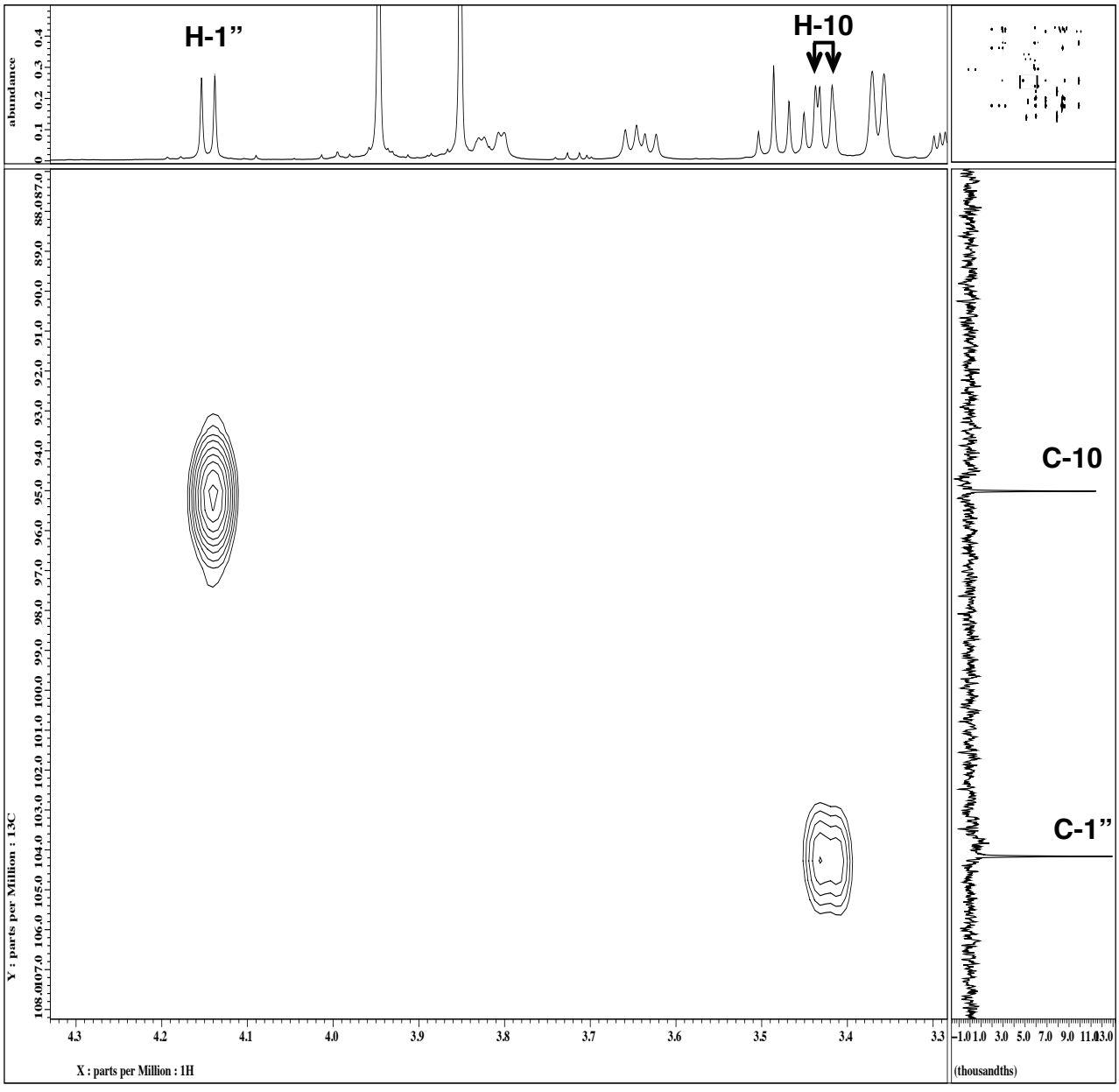

Figure 2-8 HMBC correlation of anomeric H-1” to C-10 in aglycon of glucopiericidin A (expanded from **Figure 2-7**)

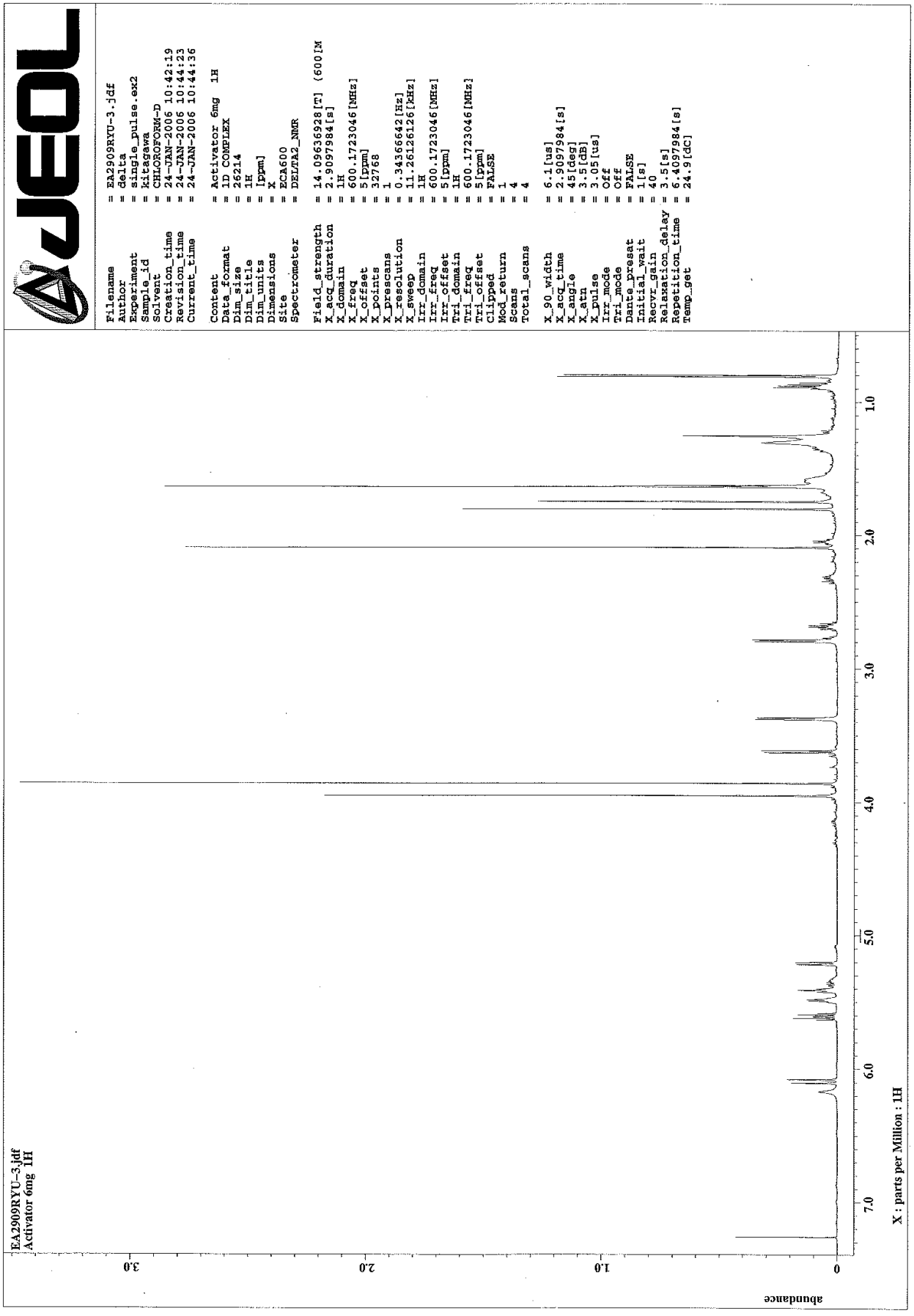

Figure 2-9 ^{1}H NMR spectrum of piericidin A ($CDCl_3$, 600 MHz)

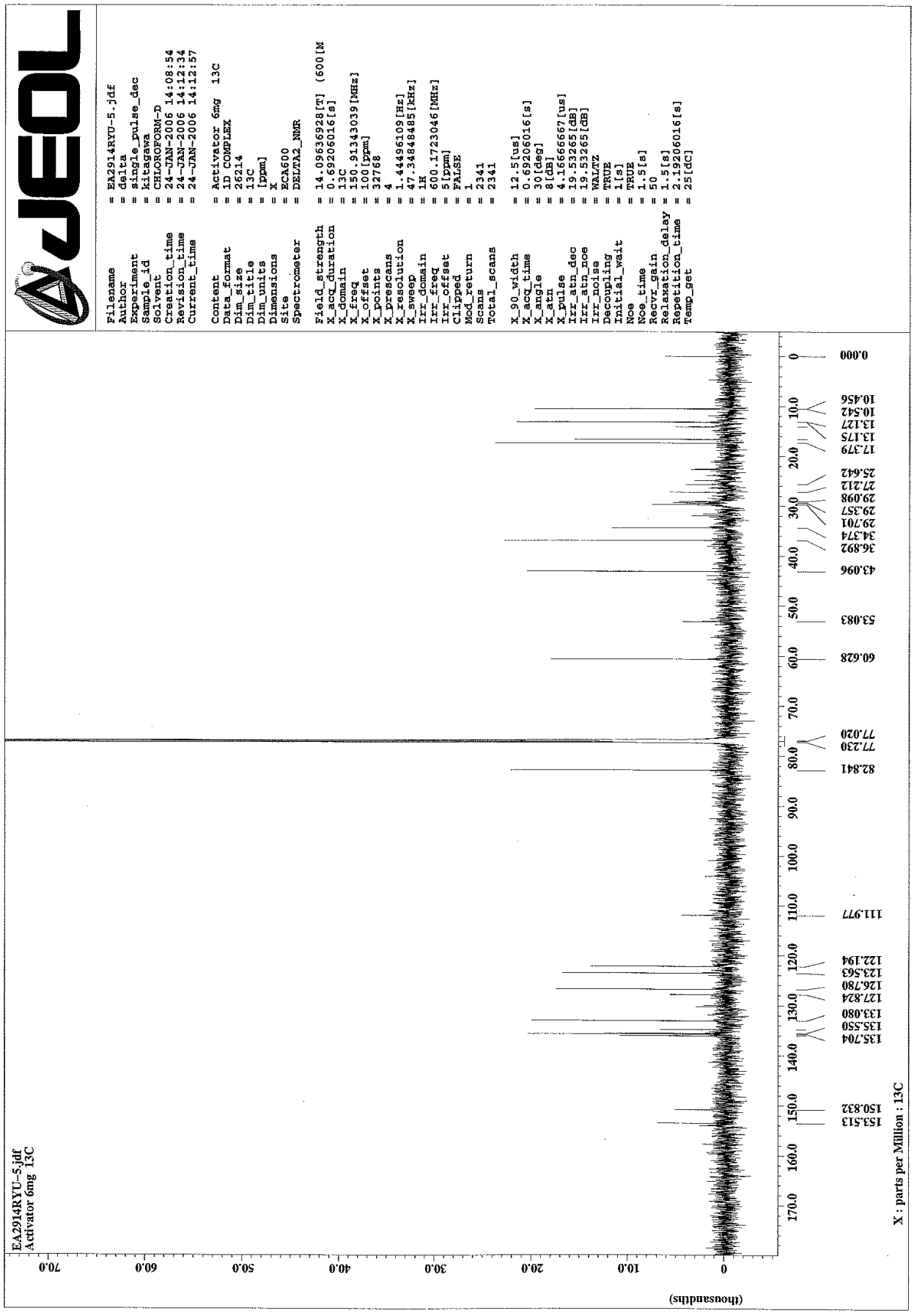

Figure 2-10 ^{13}C NMR spectrum of piericidin A ($CDCl_3$, 150 MHz)

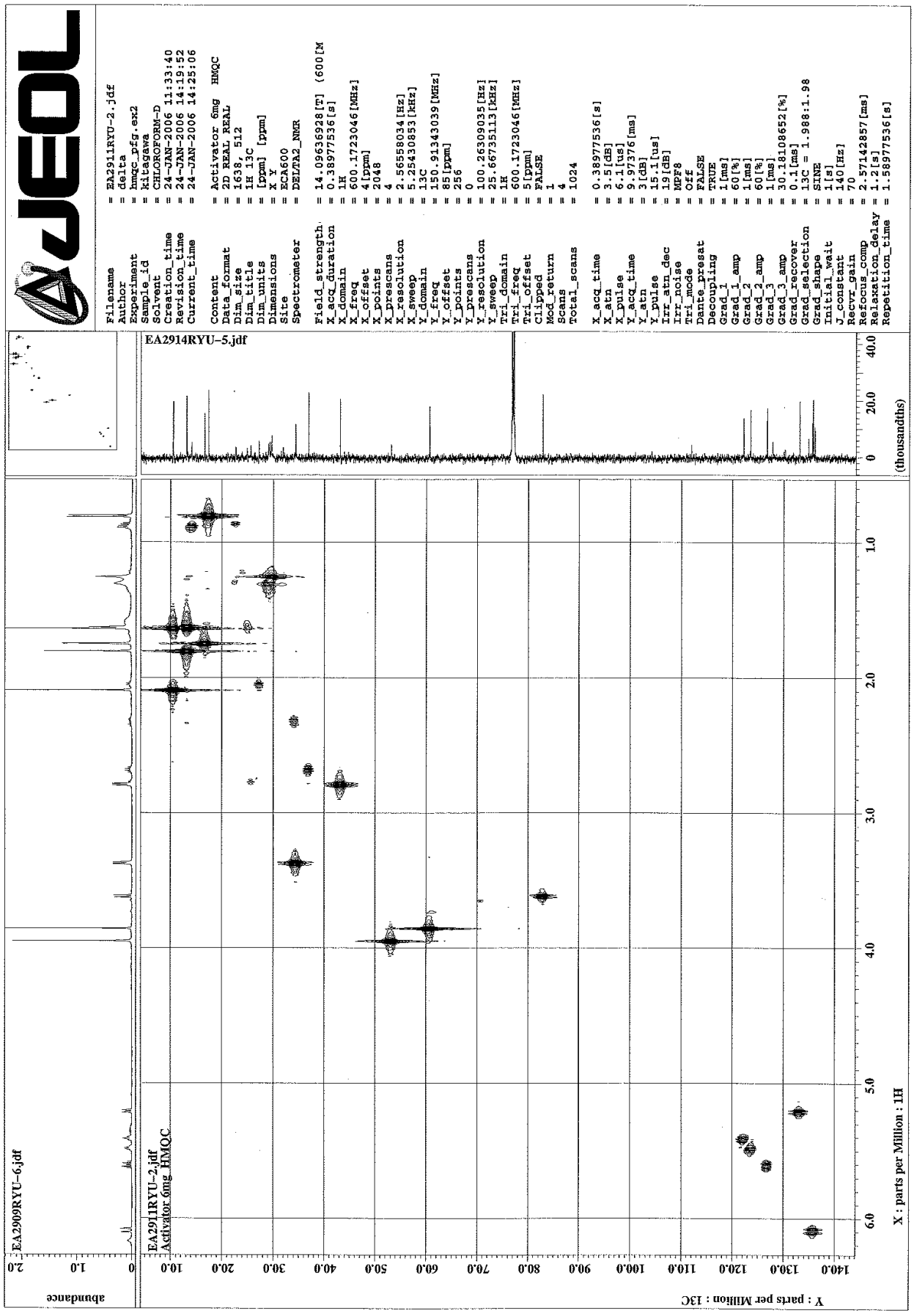

Figure 2-11 HMQC correlation of piericidin A ($CDCl_3$, 600 MHz)

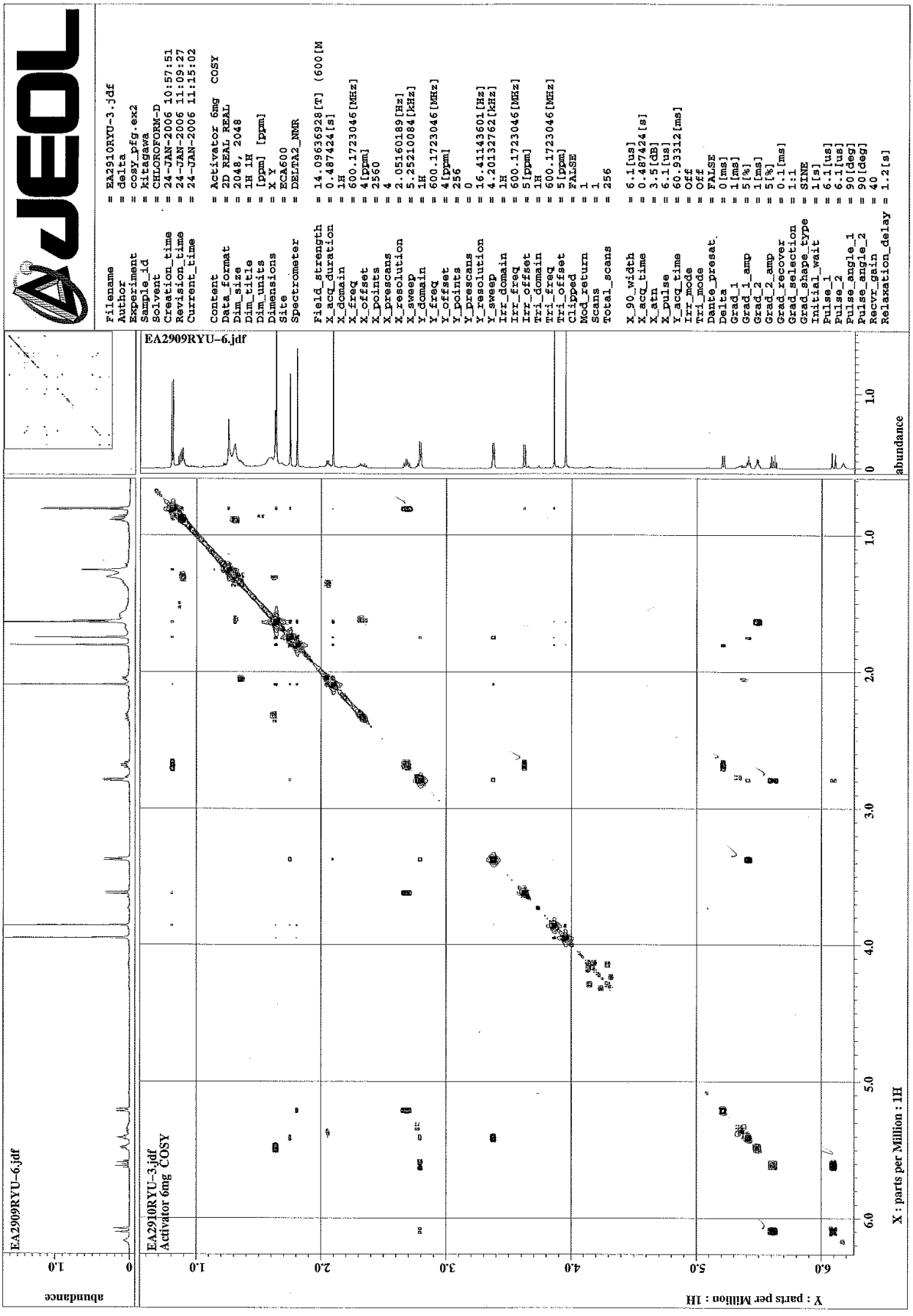

Figure 2-12 ^{1}H-1H COSY correlation of piericidin A ($CDCl_3$, 600 MHz)

Table 2-2 Assignments of ^{13}C and ^{1}H NMR of glucopiericidin A and piericidin A ($CDCl_3$)

position	glucopiericidin A		piericidin A	
	δ_C	δ_H (multiplicity, *J* [Hz])	δ_C	δ_H (multiplicity, *J* [Hz])
1	34.8 (t)	3.36 (2H, d, 6.9Hz)	34.4	3.37 (2H, d, 7.6Hz)
2	122.5 (d)	5.38 (1H, t, 6.9Hz)	122.2	5.41 (1H, t, 7,6Hz)
3	135.1 (s)		135.6	
4	43.4 (t)	2.77 (2H, d, 7.0Hz)	43.1	2.79 (2H, d, 6.8Hz)
5	127.4 (d)	5.61 (1H, dt, 15.4, 7.0Hz)	126.8	5.61 (1H, dt, 15.8, 6.9Hz)
6	135.5 (d)	6.05 (1H, d, 15.4Hz)	135.7	6.09 (1H, d, 15.8Hz)
7	134.9 (s)		134.8	
8	135.0 (d)	5.23 (1H, d, 9.5Hz)	133.1	5.21 (1H, d, 9.8Hz)
9	35.4 (d)	2.77 (1H, m)	36.9	2.69 (1H, m)
10	95.0 (d)	3.43 (1H, d, 9.7Hz)	82.8	3.62 (1H, d, 9.2Hz)
11	135.9 (s)		136.0	
12	123.9 (d)	5.42 (1H, q, 6.0Hz)	123.6	5.49 (1H, m)
13	13.7 (q)	1.62 (3H, d, 6.0Hz)	13.1	1.63 (3H, d, 6.6Hz)
14	11.2 (q)	1.61 (3H, s)	10.5	1.64 (3H, s)
15	17.2 (q)	0.75 (3H, d, 6.9Hz)	17.4	0.81 (3H, d, 7.2Hz)
16	17.0 (q)	1.78 (3H, s)	16.6	1.75 (3H, s)
17	13.4 (q)	1.74 (3H, s)	13.2	1.81 (3H, s)
1'	151.2 (s)		150.8	
2'	112.4 (s)		112.0	
3'	154.3 (s)		154.0	
4'	128.2 (s)		127.8	
5'	153.9 (s)		153.5	
6'	10.8 (q)	2.08 (3H, s)	10.5	1.64 (3H, s)
7'	61.0 (q)	3.85 (3H, s)	60.6	3.86 (3H, s)
8'	53.5 (q)	3.95 (3H, s)	53.1	3.95 (3H, s)
1"	104.2 (d)	4.14 (1H, d, 7.9Hz)		
2"	74.7 (d)	3.23 (1H, dd, 8.9, 7.9Hz)		
3"	75.6 (d)	3.48 (1H, dd, 8.9, 9.2Hz)		
4"	71.3 (d)	3.43 (1H, t, 9.2Hz)		
5"	76.7 (d)	3.28 (1H, ddd, 3.3, 6.4, 9.2Hz)		
6"	63.2 (t)	3.64 (1H, dd, 6.4, 11,5Hz), 3.81 (1H, dd, 3.3, 11.5Hz)		

Chemical shifts in ppm from TMS as an internal standard

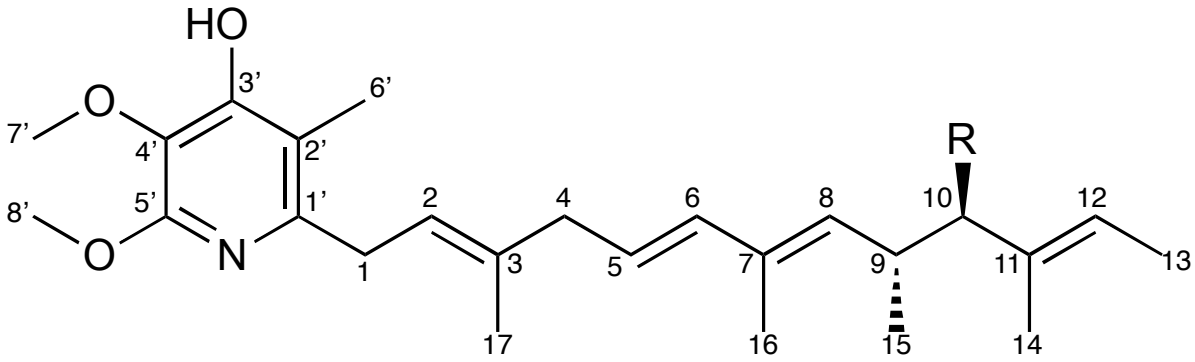

glucopiericidin A

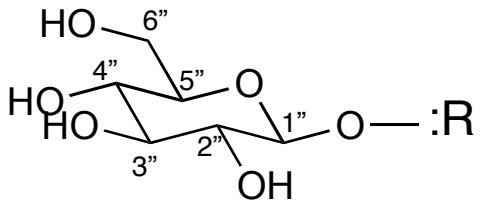

piericidin A

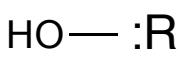

Figure 2-13 structures of glucopiericidin A and piericidin A

2-2-2 Synergistic inhibition of the filopodia protrusion by piericidin A & glucopiericidin A

Next, the author examined the inhibitory activity of GPA and PA against filopodia protrusion (**Figs. 2-14** and **2-15**). Neither GPA alone nor PA alone at concentrations up to 500 nM and 2.3 μM, respectively, showed inhibitory activity. When combined, however, much lower concentrations of GPA (17 nM) and PA (0.68 nM) produced inhibition of filopodia protrusion. The colony numbers of cells with filopodia fell down by the co-treatment of GPA & PA at those concentrations (**Fig. 2-15**). Hence, the author isolated two natural products that inhibit EGF-induced filopodia protrusion in a synergistic manner.

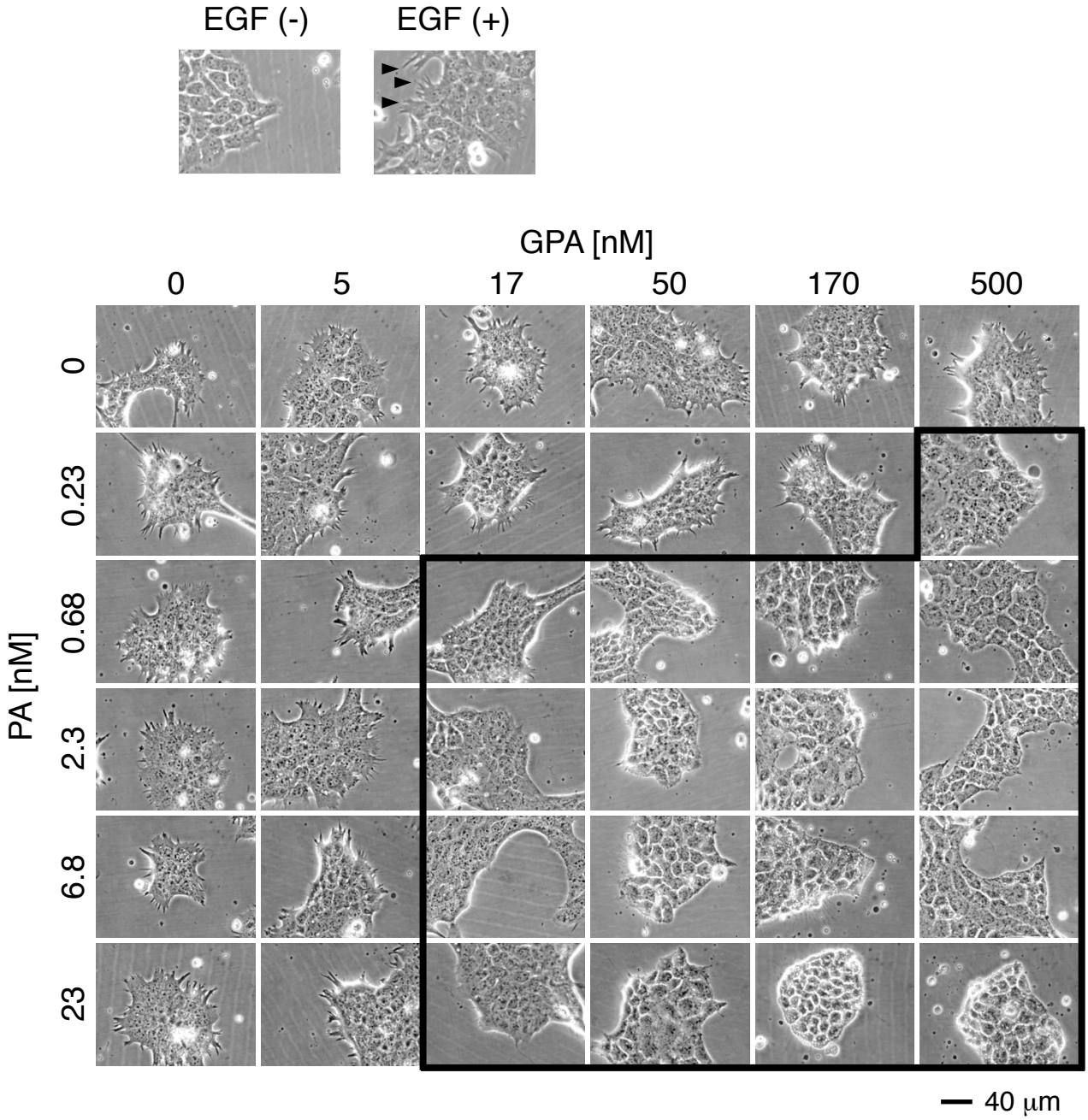

Figure 2-14 Synergistic inhibitory activity of glucopiericidin A & piericidin A in combination against the EGF-induced filopodia protrusion in A431 cells

Cells were treated with varied concentrations of PA and GPA for 30 min, then stimulated by EGF (30 ng ml^{-1}) for 30 min to protrude filopodia (as shown by arrowhead in control picture above). Frameless photos indicate cells with filopodia, while the framed photos indicate cells in which filopodia protrusion was inhibited. Note that co-treatment with GPA & PA inhibited filopodia protrusion while single treatment with each did not, indicating that GPA and PA act synergistically. Photos represent the results of three independent experiments.

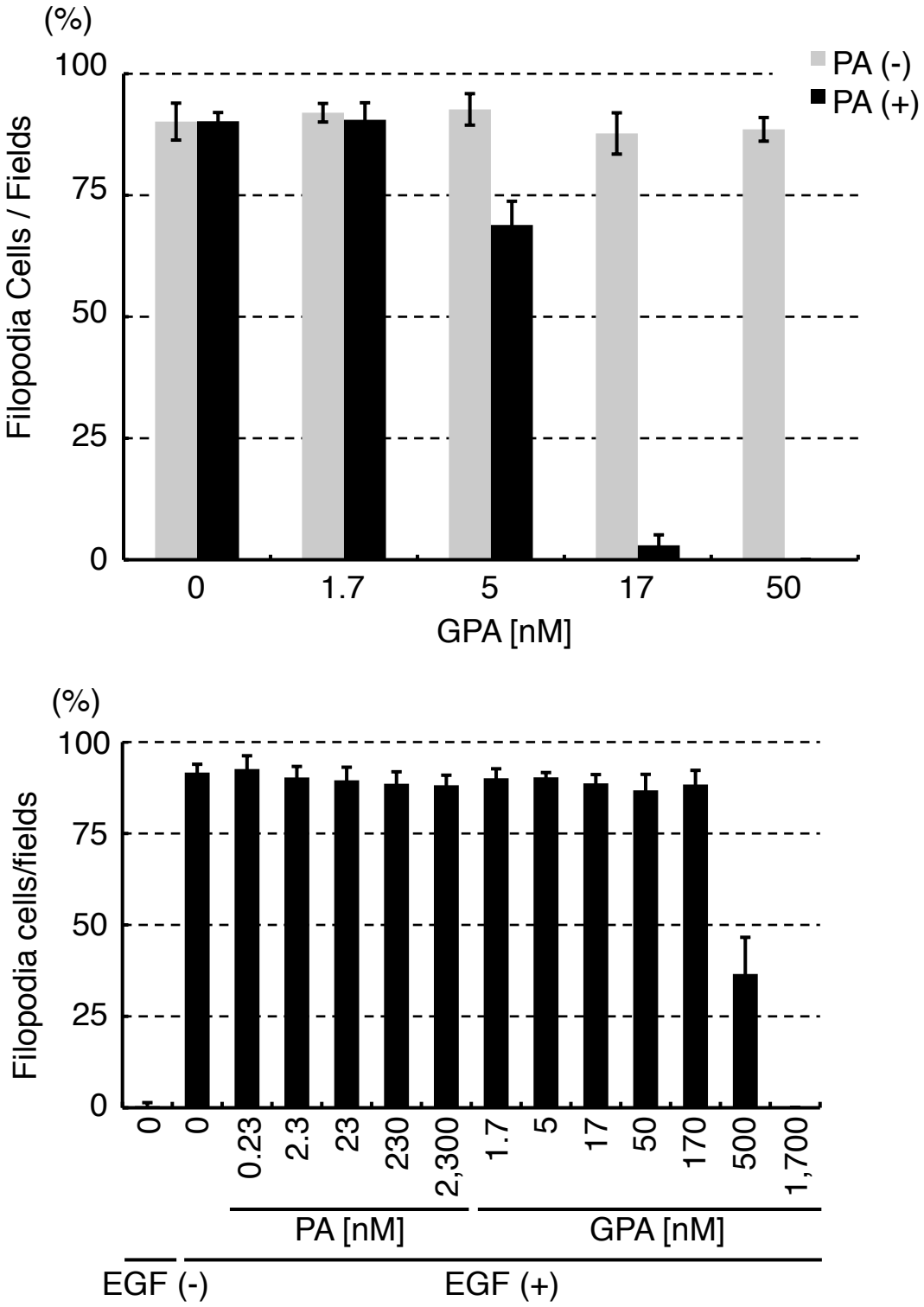

Figure 2-15 Quantification of the filopodia inhibition by glucopiericidin A and piericidin A

The number of A431 colonies with filopodia were determined microscopically, and the rate of inhibition [filopodia colonies] / [total colonies] in a field was calculated. (upper panel) Effect of GPA in the co-treatment with PA (0.68 nM). (lower panel) Effect of single treatment with GPA or PA: bars, SD (n = 9). The same result was obtained in duplicate.

2-3 Experimental procedures

Cell culture

Human epidermal carcinoma A431 cells were grown in DMEM containing 5% calf serum, 2.5 g l^{-1} sodium bicarbonate, penicillin G (100 units ml^{-1}) and kanamycin (0.1 g l^{-1}).

Filopodia protrusion assay

Cells were seeded sparsely at 5×10^4 cells ml^{-1} (250 μl per well in 48-well plates. Sparse cell seeding was maintained throughout this study). After one day, the growth media was changed to CS 0.2% DMEM and the cells were incubated for 12-18 h. Cells were then treated with the assay samples for 30 min, followed by stimulation with 30 ng ml^{-1} of EGF (Sigma) for 30 min and observed under microscopy.

For screening, isolation from the broth and evaluation of compounds, cells with complete absence of filopodia were judged to be filopodia inhibited. To quantify the filopodia cell population, filopodia protrusion was induced in the same manner as above except that cells were seeded on glass cover slips in 12-well plates. The cells formed colonies on the cover slips, and filopodia cell colonies were then counted. Colony counts were done in nine fields chosen at random for one sample.

Fermentation

The producing strain was elucidated to be *Lechevalieria* sp. by 16S rRNA analysis, as

described in detail elsewhere. The strain was cultured in media consisting of galactose 2%, dextrin 2%, soy peptone (Difco) 1%, cornstarch liquor (Oji Cornstarch) 0.5%, $(NH_4)_2SO_4$ 0.2% and $CaCO_3$ 0.2% (pH 7.2), and shaken at 180 rpm for 2 days at 27°C. This seed culture was transferred into the fermentation media at 2%. The media consisted of potato starch 1.5%, soy bean meal (toast soya, Nisshin Oillio) 0.75%, corn starch liquor (Oji Cornstarch) 0.25%, yeast extract (Oriental) 0.1%, NaCl 0.15%, $MgSO_4$ $7H_2O$ 0.025%, $CoCl_2$ $6H_2O$ 0.0005% and $CaCO_3$ 0.15% (pH 7.2). The fermentation was carried out at 180 rpm for 4 days at 27°C.

Broth extracts

Two liters of *Lechevalieria* sp. strain 1869-19 culture broth was centrifuged to separate the mycelial cake from the supernatant. The mycelial cake was sonicated in ethanol and filtered. The filtrate was concentrated under reduced pressure to remove the ethanol and then combined with the broth supernatant because the inhibitory activities of the supernatant and the mycelium were in the same range. This solution was then extracted twice with ethyl acetate (2.0 l), and the organic layer was concentrated until a brown oily residue remained.

Structural analysis of glucopiericidin A and piericidin A

The structural determination of glucopiericidin A and piericidin A was performed by MS (Thermo Fisher Scientific LTQ Orbitrap mass spectrometer) and NMR (data acquisition with JEOL JNM-ECA500, 600 and analysis with DELTA NMR Processing

and Control Software) spectra. For the stereochemistry of glucopiericidin A, the specific optical rotation was measured by the polarimeter (Jasco P1030 spectropolarimeter, light path 100 mm).

Chapter 3

Metabolomic Identification of the Target of the Filopodia Protrusion Inhibitor Glucopiericidin A

3-1 Introduction

For the study of the chemical biology, the author had obtained the unique bioactive substances herein. Glucopiericidin A (GPA) and piericidin A (PA) were structurally highly related and showed the synergistic filopodia inhibition by the treatment of A431 cells with their combination. To expand the chemical biological study hereafter, the important matter is to identify the target protein of the substance and to know the reason why the target protein inhibition by the substance cause the cellular effect, in this case the filopodia inhibition. Once these are revealed, not only the importance of the target proteins and the mechanisms for the EGF-induced filopodia protrusion in A431 cells would be proposed, but also it would be encouraged to know in expansion whether they are important in the other case of the filopodia protrusion and cell migration. Moreover, the target-identified bioactive substances are widely applicable as the chemical inhibitors and used in the experimental study other than the filopodia to control the function of their target proteins and to reveal its important role for the cellular event of the interests. Therefore here in Chapter 3, the author concentrated to reveal the target proteins of glucopiericidin A and piericidin A to know why they synergistically inhibited the filopodia protrusion and to provide them as the useful chemical tools for the other research in expansion. As the matter of fact, the case for piericidin A was quite simply described since it was a well-known inhibitor. The chapter mainly described about the target identification of glucopiericidin A.

Approaches for the target identification of the chemical substances

There is no general protocol for the target protein identification of the inhibitor. Many reports describe the methods and technologies for the target protein identification of the chemical inhibitor[7,50], which are fundamentally categorized into two approaches; direct and indirect[50].

Direct approaches: In the direct approach, the target proteins bound to the inhibitor are directly identified. For instance, the inhibitor-immobilized beads or a column is used[11,51]. The cell lysate including the target proteins are loaded onto the inhibitor-immobilized beads/column, and the target protein will be purified based on the affinity between the inhibitor and the target protein. The purified protein can be directly identified by mass spectrometry (MS). Importantly, the techniques of chemical synthesis provide great helps for the preparation of the inhibitor-immobilized beads/column, but it must be prepared absolutely without the loss of the target recognition maintained by the original structure of the inhibitor[52]. To clear this matter, forehead to the preparation, the Structure-Activity Relationship (SAR) study is often operated to realize the important functional group within the original inhibitor structure, and to identify the unimportant partial structure that can be modified by the chemical synthesis for the inhibitor-immobilized beads/column without loss of the target recognition[52,53]. In the other cases, radioisotope- or fluorescent-labeled inhibitors are chemically synthesized for the target protein visualization. The mixture of cell lysate and the labeled inhibitor are proceeded to SDS-PAGE, and the visualized band can be cut off and eluted from the SDS-PAGE gel that can be directly identified by MS[28]. In

any cases, the direct approach provides the direct-binding target protein of the chemical inhibitor, and thus is quite powerful. The slight drawback is that this requires the techniques of chemical synthesis for the labeled or beads/column-immobilized inhibitor. In some cases especially of natural products, the chiral centers and unique structural scaffolds make synthesis difficult.

Indirect approaches: In the indirect approaches, the candidates of the target protein are provided by profiling the biological data of the chemical substances of the interests[50,54]. Once the chemical substance of interests was found to perturb some cellular event for which the regulatory signaling pathway is known, all the proteins included in this signaling pathway are the target candidates. Examining the effect of the substance on each step of the pathway will reveal the *bona fide* target[55]. In other cases, the structures of the chemical substances are quite informative. Takemoto et al. revealed that the novel cell migration inhibitor moverastin targets farnesyl-transferase (FTase), according to the knowledge that moverastin structurally belongs to the cylindrol family chemical substances, many of which were reported to inhibit FTase[56]. The methods belonging to the indirect approaches are not limited as described above but quite rich in its variety. One interesting bioinformatic approach is reported by Yaguchi et al[57]. The research team first collected the list of EC_{50} values of the cell proliferation assay for the large variety of target-identified inhibitors. Using 39 human cancer cell lines termed JFCR39, each target-identified inhibitor owns 39 EC_{50} values. Next they compared the list of 39 EC_{50} values of each target-identified inhibitor to those of the novel substance of interest ZSTK474 and lead the conclusion that the pattern of EC_{50} values of

ZSTK474 against JFCR39 resembled to that of PI3K inhibitor. Finally they experimentally confirmed that ZSTK474 is the novel PI3K inhibitor by *in vitro* PI3K enzyme assay[57,58]. Similar approaches using the bioinformatics are recently introduced[58,59]. Likewise, the indirect approaches lead toward the target identification through the large number of the biological data. In some researches, omics studies (e.g. proteomics, transcriptomics, metabolomics) can aid the indirect approaches on the comprehensive investigation of a substance's effect on the large numbers of biological steps in the signal transductions pathways and in the cell-event-regulating systems.

Metabolomics for the target identification of the chemical inhibitor

Because of the results described in the next session, the author employed an indirect approach, using metabolomics to identify the target of glucopiericidin A derived from natural product screening. Metabolomics technologies have advanced tremendously in recent years, and capillary electrophoresis time-of-flight mass spectrometry (CE-TOFMS) has emerged as a powerful new tool for the comprehensive analysis of cellular metabolites[60,61]. The use of CE-TOFMS to understand global metabolism at the system level has become widespread[62-65]. Analysis of the metabolome with CE-TOFMS also revealed metabolic changes induced by drug compounds[64]. Thus, despite a lack of reports describing the identification of chemical inhibitor targets using metabolomic analysis, such efforts would be worthwhile.

Here Chapter 3 mainly describes the target identification of glucopiericidin A, especially with the use of CE-TOFMS metabolome analysis as a new approach for it

and discuss the mechanism underlying the synergistic filopodia inhibition by glucopiericidin A and piericidin A below.

3-2 Results

3-2-1 Mode of action of piericidin A

The author investigated the mechanisms underlying the synergistic inhibition of filopodia protrusion using co-treatment with glucopiericidin A (GPA) and piericidin A (PA). Since PA is a known inhibitor of the mitochondrial respiratory chain complex I[49,66], the author hypothesized that inhibition of mitochondrial respiration by PA was required for the observed synergistic inhibition of filopodia protrusions when cells were co-treated with GPA and PA. To test this hypothesis, it was examined whether other inhibitors of mitochondrial respiration would inhibit filopodia protrusion in combination with GPA. As expected, rotenone, another complex I inhibitor, showed the synergistic inhibition in combination with GPA (**Fig. 3-1**). In addition, antimycin A, a mitochondrial respiratory chain complex III inhibitor, and oligomycins, complex V inhibitors, also inhibited filopodia protrusion synergistically with GPA (**Fig. 3-1**). These results suggested that suppression of mitochondrial respiration is responsible for the synergistic filopodia inhibition seen with GPA and PA. Conversely, although GPA is the glucopyranoside derivative of PA, GPA showed low inhibitory activity against mitochondrial respiration (about 500-fold weaker than PA, see **Fig. 3-2**). The weak inhibition of mitochondrial respiration suggested that GPA must contribute to inhibition of filopodia protrusion through a different mode of action.

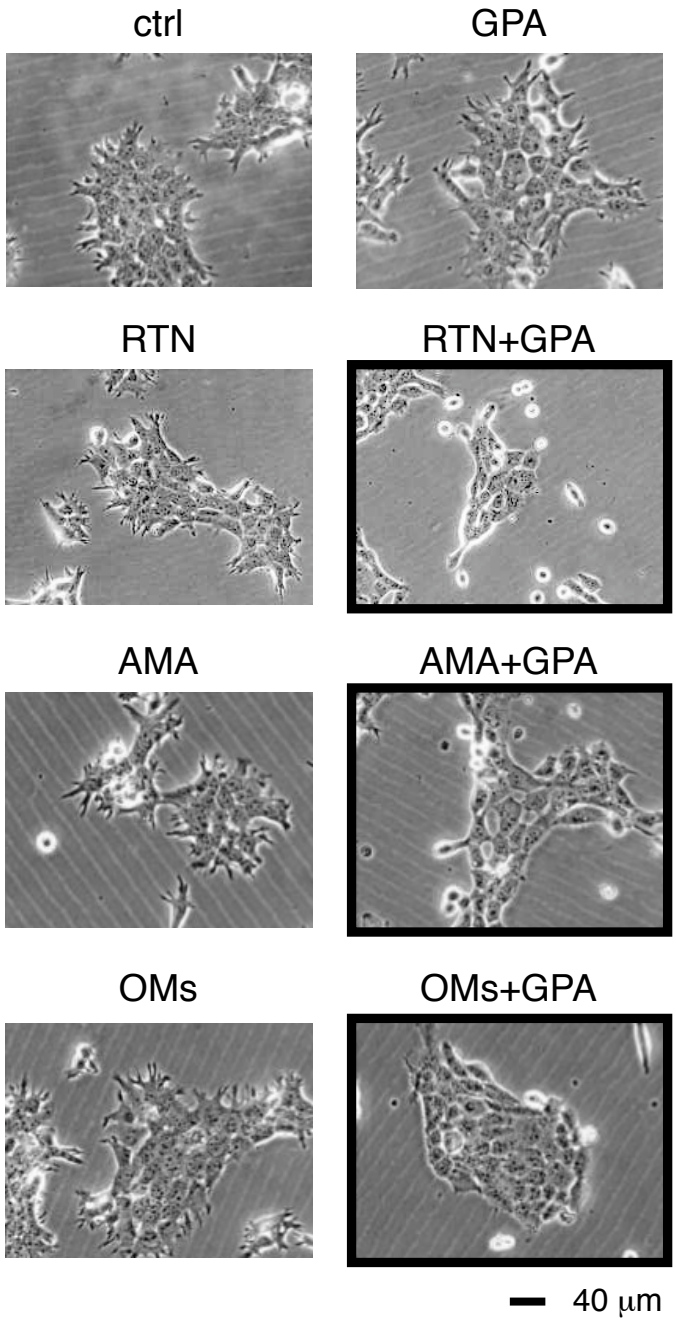

Figure 3-1 Inhibitors of mitochondrial respiration caused the synergistic filopodia inhibition with GPA.

PA was known as the inhibitor against complex I in respiratory chains. Other Mitochondrial inhibitors were tested: RTN (rotenone: complex I inhibitor 100 nM), AMA (antimycin A: complex III inhibitor 10 ng ml^{-1}), and OMs (oligomycins: complex V inhibitor 10 ng ml^{-1}). Frameless photos, cells with filopodia; the framed photos, filopodia inhibition. Same result was obtained in duplicate.

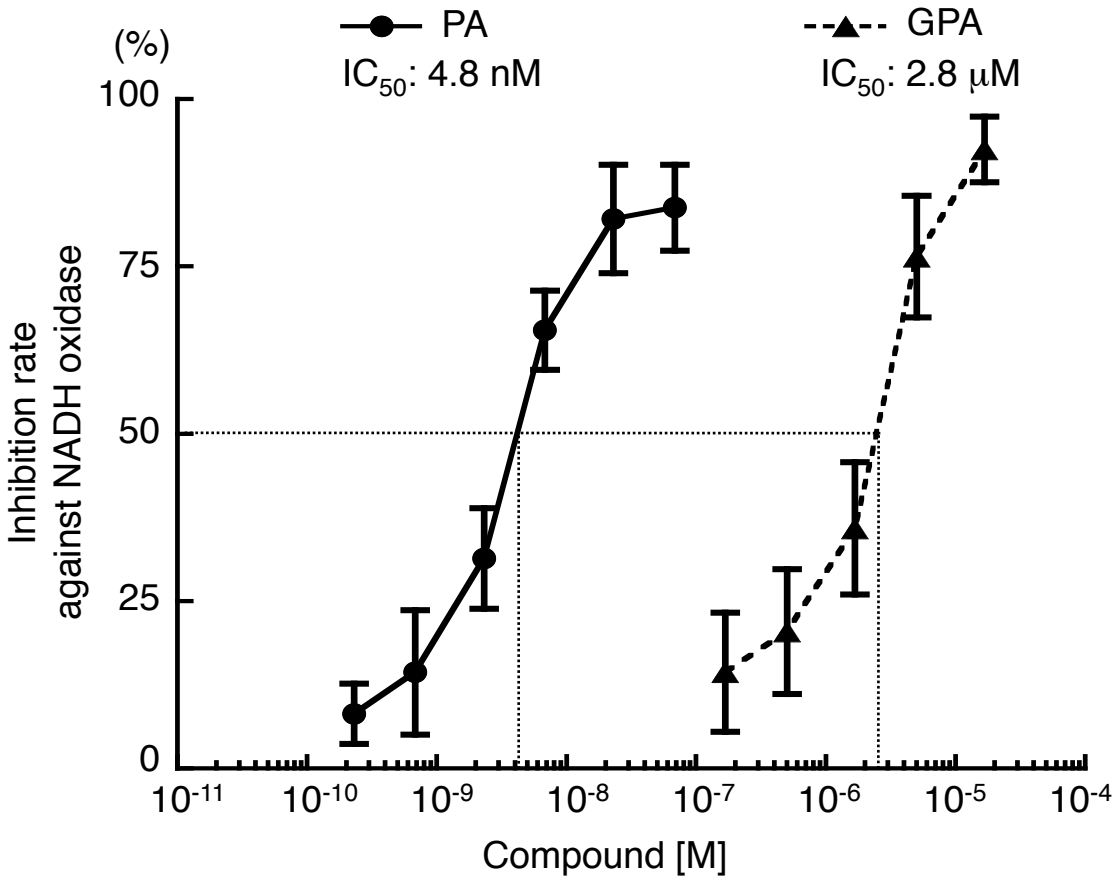

Figure 3-2 Inhibitory activity against mitochondrial NADH oxidase.

The inhibitory activity of PA and GPA against mitochondrial NADH oxidase activity *in vitro* was determined. Inhibitory activity of GPA was quite low (IC_{50} value: 2.8 μM), while structurally related PA showed strong inhibition (IC_{50} value: 4.8 nM): bars, SD (n = 4).

3-2-2 Mode of action of glucopiericidin A

(1) Chemical genomic screening

The author conducted chemical genomic screening to investigate the mode of action whereby GPA contributes to the inhibition of filopodia protrusion. In this screening, the biological profile of target-identified inhibitors of filopodia inhibition was compared with that of GPA in order to find target-identified inhibitors with the same bioactivity as GPA, considering the possibility that GPA might target the same molecules as these other inhibitors. About 200 target-identified compounds were assessed for their ability to inhibit EGF-induced filopodia protrusion in the presence of PA (**Table 3-1**). As a result of this analysis, it was found that 2-deoxyglucose (2DG), a known suppressor of glycolysis[67], was the sole compound able to inhibit protrusion in combination with PA (**Fig. 3-3**).

This raised the possibility that glycolytic suppression could be involved in the synergistic inhibition of filopodia protrusion seen with PA. Additionally, filopodia protrusion has been described as an ATP-dependent process[68-70]. Thus, it could be hypothesized that PA and 2DG inhibit filopodia protrusion by decreasing cellular ATP levels through simultaneous blockage of two ATP-producing metabolic pathways: glycolysis (2DG) and mitochondrial respiration (PA). In support of this hypothesis, the author found that 2DG did indeed decrease cellular ATP levels synergistically with PA (**Fig. 3-4**). Therefore it was suspected that GPA might also decrease cellular ATP levels, resulting in inhibition of filopodia protrusion in the same manner as 2DG. As shown in

Fig. 3-4, treatment of A431 cells with GPA also caused a drastic decrease in cellular ATP with PA, suggesting that GPA might perturb the ATP-producing metabolic pathways, most likely glycolysis, resulting in the filopodia protrusion inhibition in the presence of PA.

Table 3-1 Compounds for chemical genomic screening.

The inhibition of filopodia protrusion in the absence ("single") or the presence of mitochondrial respiratory inhibitor ("with MRI*") are shown.
Hit criteria: The compound with smaller EC_{100} value "with MRI*" than in a "single" treatment.

Compound		EC_{100}			Compound		EC_{100}		
name	category	single	with MRI*		name	category	single	with MRI*	
5-FU	thymidylate synthetase	-	-		Pifithrin-a (cyclic)	p53	-	-	
Bestatin	aminopeptidase B	-	-		PRIMA-1	p53 activator	-	-	
Bleomycin sulfate	DNA	-	-		Finasteride	5a-reductase	-	-	
Cisplatin	DNA	-	-		Aminoglutethimide	aromatase	-	-	
Methotrexate	DHFR	-	-		Formestane	aromatase	-	-	
Mitomycin C	DNA	-	-		Mifepristone	progesterone receptor	-	-	
Flutamide	AR	-	-		TOFA	acetyl-CoA carboxylase	-	-	
Daunorubicin, HCl	DNA	-	-		Amastatin	aminopeptidase A	-	-	
Doxorubicin, HCl	DNA	-	-		Actinonin	aminopeptidase M	-	-	
Tamoxifen, citrate	ER	-	-		HA 14-1	Bcl-2	-	-	
Vinblastin	tublin polymerization	-	-		BH3I-1	Bcl-XL	-	-	
Camptothecin	topo I	-	-		LFM-A13	BTK	-	-	
Aclarubicin	topo I/II	-	-		Terreic acid	BTK	-	-	
Etoposide (VP-16)	topo II	-	-		E-64d	calpain	-	-	
2',5'-dideoxyadenosine	adenylcyclase	-	-		ALLN	calpain, cathepsin B, L	-	-	
AKT inhibitor	AKT	-	-		CA-074	cathepsin B	-	-	
NL-71-101	AKT	-	-		Pepstatin A	cathepsin D	-	-	
AG957	Bcr-Abl	-	-		Z-GLF-CMK	cathepsin G	-	-	
KN93	CAMKII	-	-		RS 102895	CCR2	-	-	
Z-VAD-FMK	caspase	-	-		SB 328437	CCR3	-	-	
Kenpaullone	CDC2	-	-		SB 225002	CXCR2	-	-	
Purvalanol A	CDK2	-	-		AMD3100 - 8HCl	CXCR4	-	-	
3-ATA	CDK4	-	-		NSC95397	Cdc25	-	-	
Olomoucine	CDKs	-	-		SC-ααα9	Cdc25A	-	-	
TBB	CKII	-	-		Amiloride	Na channel	-	-	
Sulindac sulfide	COX-1	-	-		Lidocaine	Na channel	-	-	
Valeryl salicylate	COX-1	-	-		Ouabain	Na/K ATPase	-	-	
NS-398	COX-2	-	-		Sanguinarine	Na/K/Mg ATPase	-	-	
Theophylline	cyclicphosphodiesterase	-	-		Glibenclamide	K channel	-	-	
Azacytidine	DNA methyltransferase	-	-		Dequalinium	K channel	-	-	
Aphidicolin	DNA polymerase	-	-		Diazoxide	K channel opener	-	-	
AG1478	EGFR	0.1 μM	0.1 μM		Inostamycin	PI turnover	1 μg/ml	1 μg/ml	
Genistein	EGFR, topoII	-	-		Nigericin	K ionophore	3 μM	3 μM	
SU5402	FGFR	-	-		Valinomycin	K ionophore	-	-	
SU9518	PDGFR	-	-		Diltiazem	Ca channel	-	-	
Manumycin A	farnesyltransferase	-	-		Nifedipine	Ca channel	-	-	
SU1498	Flk-1	-	-		Verapamil	Ca channel, MDR	-	-	
GGTI-286	GGTase I	-	-		PGP-4008	MDR	-	-	
Dexamethasone	GR	-	-		Fumitremorgin C	BCRP	-	-	
GSK-3 inhibitor II	GSK-3	-	-		A23187	Ca ionophore	0.1 μM	0.1 μM	T**
SB 415286	GSK-3	-	-		Ionomycin	Ca ionophore	0.1 μM	0.1 μM	T**
LiCl	GSK-3	-	-		t-Butylhydroquinone	Ca-ATPase	-	-	
Scriptaid	HDAC	-	-		Thapsigargin	SERCA	-	-	T**
Trichostatin A	HDAC	10 μg/ml	10 μg/ml		N-phenylanthranilic acid	Cl channel	-	-	
AG825	HER2, EGFR	-	-		DIDS	Cl channel	-	-	
Alendronate	HMG-CoA reductase	-	-		SB 218078	Chk 1	-	-	
Lovastatin	HMG-CoA reductase	-	-		Debromohymenialdisine	Chk 1, 2	-	-	
Risedronate	HMG-CoA reductase	-	-		Rotenone	mitochondrial complex I	-	-	
17-AAG	HSP90	-	-		Antimycin A1	mitochondrial complex III	10 μg/ml	10 μg/ml	T**
Herbimycin A	HSP90	-	-	T**	Oligomycin	mitochondrial complex V	10 μg/ml	10 μg/ml	
Radicicol	HSP90	-	-	T**	1400W, HCl	iNOS	-	-	
2-deoxyglucose	**glycolysis**	**-**	**10 mM**	***HIT***	AMT, HCl	iNOS	-	-	

(*continuing*)

Table 3-1 Compounds for chemical genomic screening (*continued*)

Compound		EC_{100}		Compound		EC_{100}	
Name	Category	single	with MRI*	Name	Category	single	with MRI*
Damnacanthal	lck (p56), TYK	-	-	R59022	DAG kinase	-	-
Cerulenin	FAS	-	-	Dioctanoylglycol	DAG kinase	-	-
C75	fatty acid synthase	-	-	RHC80267	DAG lipase	-	-
Cucurbitacin I	Jak-2	0.3 μM	0.3 μM	Xanthohumol	DAG acyltransferase	-	-
PD 98059	MEK	-	-	Deoxynojirimycin	Glucosidase I, II	-	-
U0126	MEK	-	-	Swainsonine	α-Mannosidase	-	-
Fumagillin	MetAP	-	-	LY 83583	Guanylate cyclase	-	-
GM 6001	MMP	-	-	ODQ	Guanylate cyclase	-	-
Aminoguanidine	NOS	-	-	Anacardic acid	HAT	-	-
PD169316	p38 (MAPK)	-	-	Chetomin	HIF	0.3 μM	0.3 μM
SB 203580	p38 (MAPK)	-	-	Dimethyloxalylglycine	HIF-1a hydroxylase	-	-
NU1025	PARP	-	-	HR22C16	Kinesin Eg5	-	-
Benzamide	PARP-1	-	-	Monastrol	Kinesin Eg5	-	-
D609	PC-PLC	-	-	Nordihydroguaiaretic acid	Lipoxygenase	-	-
IBMX	PDE	-	-	AA-861	5-Lipoxygenase	-	-
Ro-20-1724	PDE (cAMP)	-	-	ETYA	12, 15-Lipoxygenase	-	-
Zaprinast	PDE (cGMP)	-	-	Baicalein	12-Lipoxygenase	-	-
AG1296	PDGFR	-	-	Nutlin-3	Mdm2	-	-
LY294002	PI3K	-	-	MDM2 inhibitor	Mdm2	-	-
wortmannin	PI3K	-	-	Phenelzine	Monoamine oxidase	-	-
H-89, HCl	PKA	-	-	Deprenyl	Monoamine oxidase B	-	-
Bisindolylmaleimide I	PKC	-	-	Decylubiquinone	MPTP	-	-
H-7	PKC, PKA	-	-	Ro 5-4864	MPTP	-	-
Staurosporine	PKC, PKA, PKG, MLCK	-	-	Lonidamine	MPTP opener	-	-
cPLA2 inhibitor	PLA2	-	-	ML-7	Myosin light chain kinase	-	-
OBAA	PLA2	-	-	Benzylguanine	MGMT	-	-
Cantharidin	PP2A	-	-	DFMO	Ornithine decarboxylase	-	-
Cytostatin	PP2A	-	-	KT 5823	PKG	-	-
Okadaic acid	PP1, PP2A	-	-	Rp-8-CPT-cGMPS	PKG	-	-
Cyclosporin A	PP2B/cyclophilin	-	-	MK 886	PPAR-α, FLAP	-	-
FK-506	PP2B/FKBP	-	-	Clofibrate	PPAR-α activator	-	-
Lactacystin	Proteasome	-	-	BADGE	PPAR-γ	-	-
MG-132	Proteasome	-	-	Troglitazone	PPAR-γ activator	-	-
Hydroxyurea	Ribonucleotide reductase	-	-	AZT	Reverse transcriptase	-	-
HA1077	ROCK	-	-	Nalidixic acid	Reverse transcriptase	-	-
Y27632	ROCK	-	-	α-Amanitin	RNA polymerase	-	-
PP1 (analog)	Src, Fyn, Lck	-	-	MST-312	Telomerase	-	-
PP-H	Src, Fyn, Lck	-	-	β-Rubromycin	Telomerase	-	-
Nocodazole	Tubulin depolymerization	-	-	SB 431542	TGF-β receptor	-	-
Taxol	Tubulin depolymerization	-	-	N1,N12-Diethylspermine	SSAT activator	-	-
Dephostatin	Tyr phosphatase (PTP)	-	-	Fumonisin B1	Sphingosine N-acyltransferase	-	-
Leptomycin B	CRM1	-	- T**	Tunicamycin	Glycosylation	10 μg/ml	10 μg/ml
AG1024	IGF-1R	-	-	SP600125	JNK	30 μM	30 μM
BAFILOMYCIN A	V-ATPase	-	-	Rapamycin	mTOR	-	-

*MRI: Complex I inhibitor PA (0.68 nM) or rotenone (10 nM)
**T: Toxic representing the cells with abnormal morphology

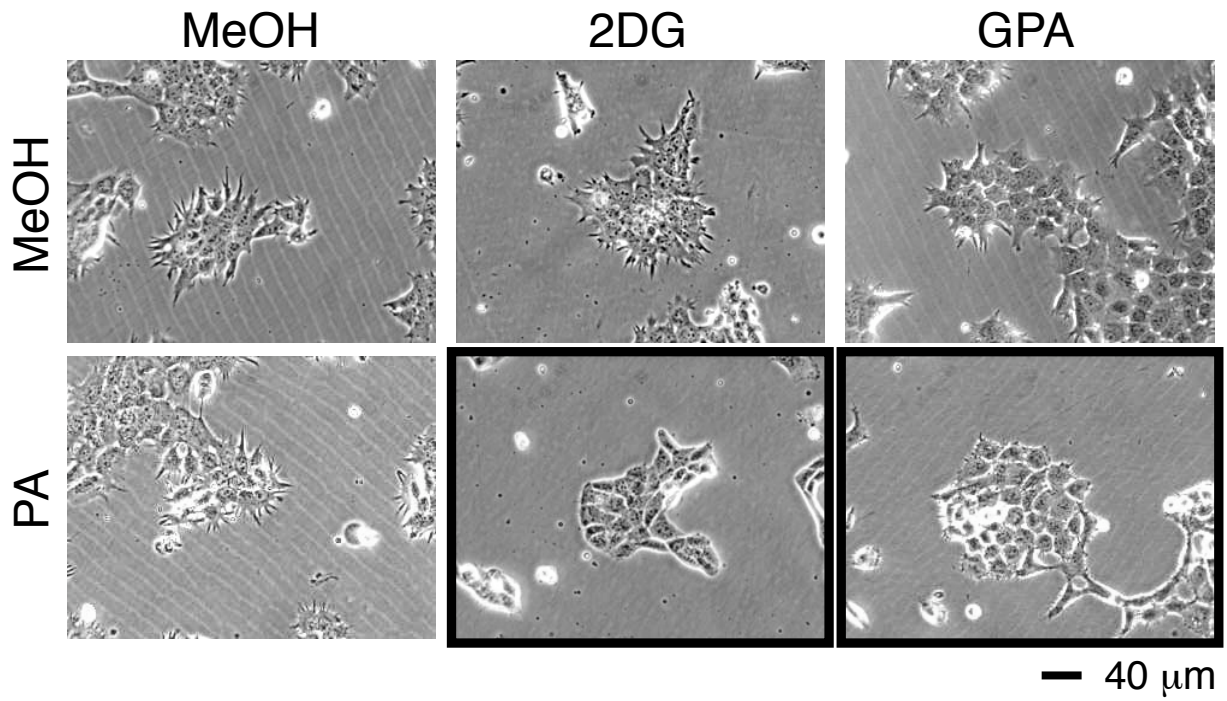

Figure 3-3 Hexokinase inhibitor 2-deoxy-D-glucose synergistically inhibited filopodia protrusion in the presence PA, similar to the effect observed with GPA.

Among about 200 target-identified inhibitors, 2-deoxy-D-glucose, a suppressor of glycolysis, was as the sole compound able to show the synergistic filopodia inhibition with PA, which was the same effect as GPA. This indicated that the glycolysis might have a key for the mode of action of GPA. (PA 0.68 nM, GPA 17 nM and 2DG 10 mM) Frameless photos, cells with filopodia; the framed photos, filopodia inhibition. Same result was obtained in duplicate.

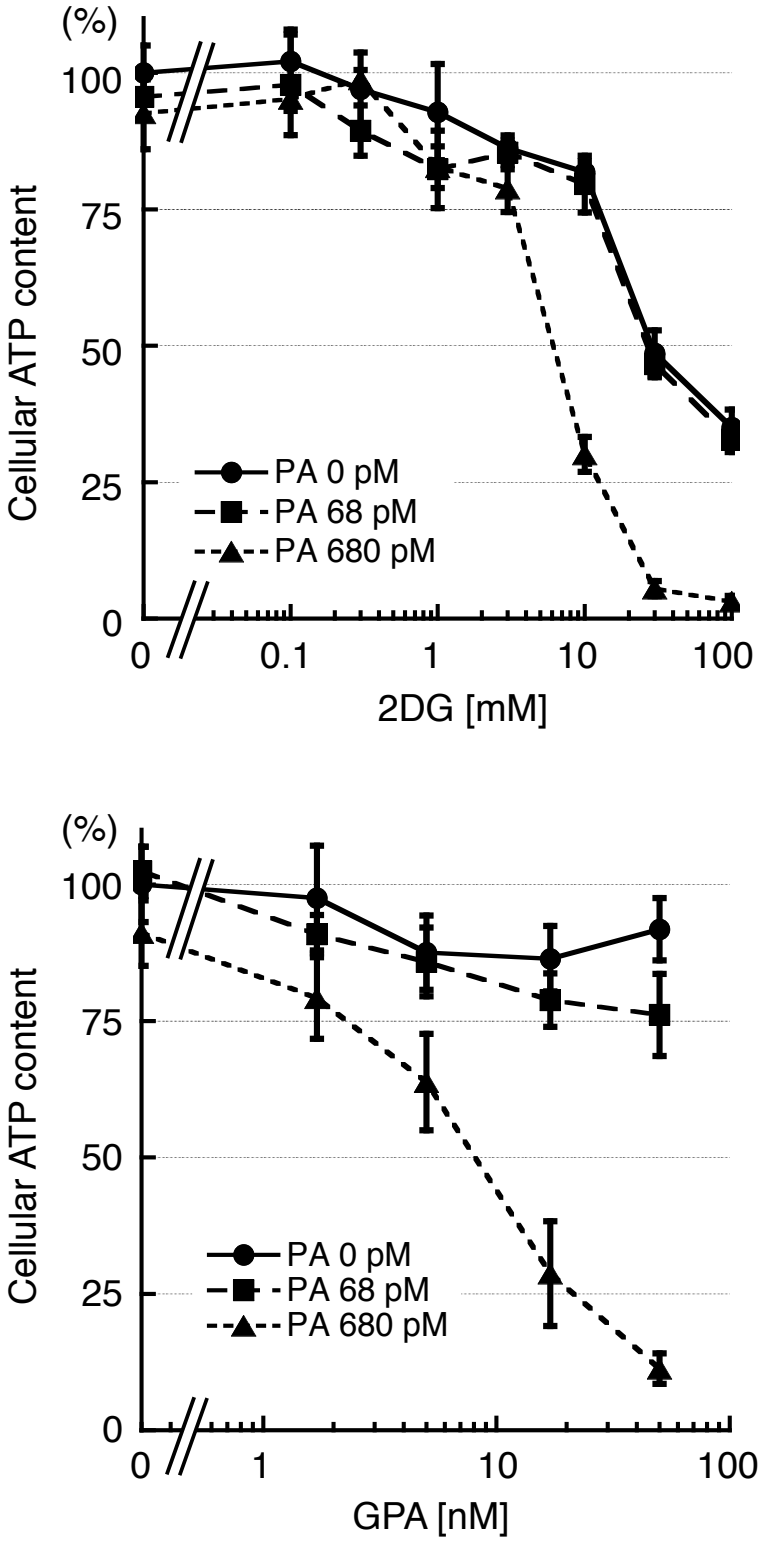

Figure 3-4 GPA appears to suppress glycolysis

It was known that glycolytic suppression causes a drastic decrease in cellular ATP under the suppression of mitochondrial respiration (upper panel). Glucopiericidin A also decreased the cellular ATP in the presence of mitochondrial respiratory inhibitor piericidin A (lower panel). Error bars: standard deviation (n = 3). Same result was obtained in duplicate

3-2-2 Mode of action of glucopiericidin A

(2) Metabolome analysis

One possible approach to address the issue of whether GPA actually perturbs glycolysis is to assess the effect of GPA on global metabolism and on glycolysis in particular, by measuring the metabolome using CE-TOFMS. In CE-TOFMS, metabolites are separated by capillary electrophoresis (CE) on the basis of their charge and size, and then detected as peaks in MS[61]. Metabolites are identified by comparing CE migration time and molecular weight with that of standards, and are quantified by peak intensity in reference to standard calibration curves. The author used this approach to quantitatively examine the differences in metabolite levels between control and GPA-treated cells.

Using the CE-TOFMS approach, around 4,000 (3,853–4,848) peaks were detected in each sample (control and GPA-treated, n = 4). A reference set of 112 standards was used to identify the metabolites of glycolysis and related pathways (pentose phosphate pathway, TCA cycle, nucleotide synthesis, amino acid and others, see **Table 3-2**, **Figs. 3-5** to **3-7**). A total of 83 peaks were quantitatively identified, and 24 metabolites were found to significantly differ between control and GPA-treated samples (for the entire list with exact *p* values, see **Table 3-2** and **Fig. 3-6**), which are mapped in the overview in **Fig. 3-7** (pathway information was referred to KEGG [http://www.genome.jp/kegg/pathway.html]). The results showed that GPA significantly decreased the amount of glycolytic end-products (pyruvate: 61.5%, $p = 1.8 \times 10^{-3}$ and lactate: 40.3%, $p = 8.7 \times 10^{-5}$). Moreover, another glycolytic parameter, the

lactate/pyruvate ratio[71], was also significantly decreased (**Fig. 3-8**). These results strongly suggested that GPA inhibited glycolysis. Besides, the effect of PA and co-treatment of PA&GPA on the metabolome were also examined, and it showed the decrease in these parameters in PA-changed metabolome map (**Table 3-3**, **Figs. 3-9** and **3-10**).

Upon determining that GPA inhibits glycolysis, the author then examined which reaction step in glycolysis was blocked by GPA as a means of identifying the GPA target. To reveal particular GPA-induced changes in glucose metabolism, control and GPA-treated A431 cells were treated with [1,2,3,4,5,6-^{13}C]-glucose (full-label), and then the [^{13}C]-incorporated metabolites within those cells were quantified by CE-TOFMS. Incorporation of [^{13}C]-labeled glucose into any metabolites of glycolysis was decreased in GPA-treated cells (**Table 3-4** and **Fig. 3-11**), indicating that the glycolytic influx was lowered by GPA treatment. Since the metabolite closest to glucose in the glycolytic pathway is glucose-6-phosphate (G6P), these results suggest that GPA acts on the steps proceeding from glucose uptake to G6P production.

Table 3-2 Absolute metabolite concentrations in control and GPA-treated cells.

class	Metabolites (abbrev.)	μM / cells : ave. (± s.d.)		fold	*t*-test	
		ctrl	GPA		*p*	*p*<0.05
Glycolysis	Glucose 6-phosphate (Glc6P)	0.452 (± 0.055)	0.400 (± 0.027)	0.885	1.5.E-01	
Glycolysis	Fructose 6-phosphate (Frc6P)	0.267 (± 0.037)	0.168 (± 0.078)	0.628	1.4.E-01	
Glycolysis	Fructose 1,6-diphosphate (Frc(1,6)P)	0.253 (± 0.049)	0.203 (± 0.064)	0.802	2.3.E-02	yes
Glycolysis	Dihydroxyacetone phosphate (DHAP)	n.d.	n.d.			
Glycolysis	2,3-Diphosphoglycerate ((2,3)BPG)	0.248 (± 0.038)	n.d.	ct>GPA		
Glycolysis	3-Phosphoglycerate (3PG)	0.781 (± 0.149)	0.556 (± 0.086)	0.712	7.3.E-02	
Glycolysis	Phosphoenolpyruvate (PEP)	0.176 (± 0.032)	0.299 (± 0.087)	1.70	8.3.E-02	
Glycolysis	Pyruvate (Pyr)	1.58 (± 0.09)	0.970 (± 0.074)	0.615	1.8.E-03	yes
Glycolysis	Lactate (Lac)	64.4 (± 4.6)	26.0 (± 2.9)	0.403	8.7.E-05	yes
Glycolysis	Glucose 1-phosphate (G1P)	0.190 (± 0.045)	0.211 (± 0.072)	1.11	7.0.E-01	
Glyoxylate	Glycolate	n.d.	n.d.			
Glyoxylate	Glyoxylate	n.d.	n.d.			
	Glycerophosphorate (Glycerol-P)	0.665 (± 0.109)	0.464 (± 0.126)	0.697	3.0.E-02	yes
TCA cycle	Citrate	6.95 (± 0.40)	5.69 (± 0.61)	0.819	2.3.E-02	yes
TCA cycle	cis-Aconitate	0.092 (± 0.029)	0.087 (± 0.03)	0.943	8.0.E-01	
TCA cycle	Isocitrate	n.d.	n.d.			
TCA cycle	2-Oxoglutarate	6.27 (± 1.21)	5.87 (± 1.04)	0.937	4.4.E-01	
TCA cycle	Succinate	5.84 (± 0.36)	13.6 (± 0.8)	2.33	6.4.E-04	yes
TCA cycle	Fumarate	1.95 (± 0.33)	2.94 (± 0.52)	1.50	6.0.E-03	yes
TCA cycle	Malate	7.26 (± 2.05)	12.5 (± 2.3)	1.71	1.8.E-03	yes
Pentose phosphate	Gluconate	1.12 (± 0.05)	1.21 (± 0.18)	1.08	2.6.E-01	
Pentose phosphate	6-Phosphogluconate (6PGlcA)	0.223 (± 0.037)	0.070 (± 0.015)	0.316	2.9.E-02	yes
Pentose phosphate	Ribulose 5-phosphate (Rbl5P)	0.733 (± 0.118)	0.801 (± 0.128)	1.09	1.4.E-01	
Pentose phosphate	Ribose 5-phosphate (Rb5P)	0.259 (± 0.058)	0.224 (± 0.118)	0.867	3.8.E-01	
Pentose phosphate	Sedoheptulose 7-phosphate (SedHpt7P)	0.596 (± 0.176)	0.689 (± 0.200)	1.15	2.4.E-02	yes
Pentose phosphate	Erythrose 4-phosphate (Erth4P)	n.d.	n.d.			
Pentose phosphate	PRPP	n.d.	n.d.			
amino acid	Ala	24.5 (± 0.7)	22.3 (± 1.6)	0.909	7.9.E-02	
amino acid	Arg	3.45 (± 0.20)	4.05 (± 0.77)	1.17	1.3.E-01	
amino acid	Asn	1.53 (± 0.37)	3.46 (± 0.61)	2.26	7.2.E-04	yes
amino acid	Asp	14.4 (± 3.7)	50.3 (± 8.4)	3.49	7.5.E-04	yes
amino acid	Cys	0.213 (± 0.053)	0.143 (± 0.068)	0.671	1.8.E-01	
amino acid	Gln	295 (± 15)	293 (± 16)	0.993	8.0.E-01	
amino acid	Glu	438 (± 23)	445 (± 21)	1.01	5.5.E-01	
amino acid	Gly	146 (± 8)	207 (± 83)	1.42	2.5.E-01	
amino acid	His	12.8 (± 1.2)	13.5 (± 1.4)	1.05	2.7.E-01	
amino acid	Ile	40.4 (± 2.6)	41.9 (± 3.2)	1.03	2.4.E-01	
amino acid	Leu	42.1 (± 2.2)	43.2 (± 4.0)	1.02	4.8.E-01	
amino acid	Lys	8.69 (± 0.76)	10.3 (± 1.8)	1.18	1.8.E-01	
amino acid	Met	12.7 (± 3.0)	14.8 (± 2.8)	1.16	2.9.E-01	
amino acid	Phe	31.7 (± 2.7)	33.4 (± 2.7)	1.05	1.7.E-01	
amino acid	Pro	25.8 (± 1.3)	19.3 (± 1.2)	0.748	5.7.E-03	yes
amino acid	Ser	35.6 (± 1.1)	33.3 (± 1.2)	0.936	1.1.E-02	yes
amino acid	Thr	89.2 (± 5.4)	87.4 (± 7.5)	0.980	5.5.E-01	
amino acid	Trp	5.24 (± 0.37)	5.51 (± 0.50)	1.05	1.6.E-01	
amino acid	Tyr	33.7 (± 2.3)	34.9 (± 3.3)	1.03	2.3.E-01	
amino acid	Val	46.3 (± 3.0)	48.8 (± 4.5)	1.05	2.0.E-01	
purine	Adenine	0.093 (± 0.029)	0.096 (± 0.028)	1.03	7.9.E-01	
purine	Adenosine	0.026 (± 0.006)	0.035 (± 0.007)	1.35	5.2.E-02	
purine	AMP	0.772 (± 0.156)	1.03 (± 0.15)	1.32	6.3.E-04	yes
purine	ADP	6.05 (± 0.78)	6.75 (± 0.59)	1.11	1.6.E-02	yes
purine	ATP	43.4 (± 2.8)	40.8 (± 5.2)	0.941	2.7.E-01	
purine	cAMP	0.735 (± 0.133)	0.849 (± 0.255)	1.15	5.8.E-01	
purine	dATP	0.564 (± 0.044)	0.518 (± 0.037)	0.918	1.5.E-03	yes
purine	Guanine	n.d.	n.d.			
purine	Guanosine	n.d.	n.d.			
purine	GMP	0.202 (± 0.044)	0.231 (± 0.019)	1.14	3.6.E-01	
purine	GDP	1.35 (± 0.12)	1.43 (± 0.04)	1.05	3.2.E-01	
purine	GTP	9.89 (± 1.69)	8.00 (± 1.52)	0.809	2.0.E-02	yes
purine	cGMP	0.466 (± 0.038)	0.547 (± 0.064)	1.17	1.3.E-01	
purine	Hypoxanthine	n.d.	n.d.			
purine	IMP	0.245 (± 0.029)	0.246 (± 0.046)	1.00	9.7.E-01	
purine	Inosine	n.d.	n.d.			

(*continuing*)

Table 3-2 Absolute metabolite concentrations in control and GPA-treated cells. (*continued*)

class	Metabolites (abbrev.)	μM / cells : ave (± s.d.) ctrl	GPA	fold	*t*-test *p*	*p*<0.05
pyrimidine	Cytidine	n.d.	n.d.			
pyrimidine	Cytosine	n.d.	n.d.			
pyrimidine	CMP	0.171 (± 0.027)	0.208 (± 0.026)	1.21	1.9.E-01	
pyrimidine	CDP	0.588 (± 0.068)	0.732 (± 0.161)	1.24	7.0.E-02	
pyrimidine	CTP	7.64 (± 0.30)	7.07 (± 0.52)	0.925	4.2.E-02	yes
pyrimidine	dCTP	0.197 (± 0.020)	0.191 (± 0.015)	0.971	7.2.E-01	
pyrimidine	dTMP	0.070 (± 0.018)	0.120 (± 0.016)	1.70	1.0.E-02	yes
pyrimidine	dTDP	0.085 (± 0.025)	0.073 (± 0.025)	0.853	3.9.E-01	
pyrimidine	dTTP	0.685 (± 0.041)	0.547 (± 0.047)	0.799	2.7.E-02	yes
pyrimidine	Uridine	n.d.	n.d.			
pyrimidine	Uracil	n.d.	n.d.			
pyrimidine	UTP	22.8 (± 2.0)	22.2 (± 1.7)	0.973	7.1.E-01	
Urea cycle	Citrulline	0.965 (± 0.243)	1.10 (± 0.22)	1.14	2.3.E-03	yes
Urea cycle	Ornithine	0.550 (± 0.126)	0.418 (± 0.040)	0.760	6.0.E-02	
	Putrescine	0.511 (± 0.099)	0.564 (± 0.133)	1.10	3.4.E-01	
	GABA	0.078 (± 0.011)	0.099 (± 0.020)	1.27	1.0.E-01	
Coenzyme	Acetyl CoA	n.d.	n.d.			
Coenzyme	CoA	0.521 (± 0.080)	0.490 (± 0.043)	0.941	2.4.E-01	
Coenzyme	Malonyl CoA	5.28 (± 0.50)	5.28 (± 0.53)	1.00	9.8.E-01	
Coenzyme	FAD	n.d.	n.d.			
Coenzyme	NAD	4.46 (± 0.76)	3.78 (± 0.95)	0.847	1.3.E-01	
Coenzyme	NADH	0.717(± 0.135)	0.567 (± 0.137)	0.791	6.5.E-03	yes
Coenzyme	NADP	0.439 (± 0.088)	0.375 (± 0.100)	0.855	2.3.E-02	yes
Coenzyme	NADPH	0.390 (± 0.185)	0.348 (± 0.082)	0.892	5.1.E-01	
redox	Glutathione, oxidized (GSSG)	24.8 (± 5.7)	25.6 (± 8.0)	1.03	6.2.E-01	
redox	Glutathione, reduced (GSH)	193 (± 5)	193 (± 9)	1.00	9.0.E-01	
redox	r-Glu-cys	1.97 (± 0.21)	2.24 (± 0.41)	1.13	8.0.E-02	
taurine	Cysteine sulfinate (Cys sulfinate)	n.d.	n.d.			
taurine	Hypotaurine	0.425 (± 0.100)	0.414 (± 0.132)	0.975	7.5.E-01	
taurine	Taurine	2.00 (± 0.49)	2.23 (± 0.31)	1.11	2.5.E-01	
tyrosine	DOPA	n.d.	n.d.			
tyrosine	Tyramine	n.d.	n.d.			
	2-Aminoisobutyrate (2AB)	n.d.	n.d.			
	2-Oxopentanoate (2OP)	1.29 (± 0.15)	1.23 (± 0.26)	0.958	5.3.E-01	
	3-Aminopyrrolidine (3AP)	1.67 (± 1.04)	1.79 (± 1.22)	1.07	3.6.E-01	
	Glu-2aminobutyrate (Glu2AB)	n.d.	n.d.			
	Ophthalmate	n.d.	n.d.			
	beta-Alanine	16.5 (± 2.1)	18.0 (± 2.9)	1.08	1.5.E-01	
	Creatine	25.3 (± 4.1)	44.9 (± 6.3)	1.77	1.6.E-03	yes
	Carnosine	n.d.	n.d.			
	Cystathionine	1.20 (± 0.22)	1.36 (± 0.20)	1.13	7.7.E-02	
	Homocysteine (HomoCys)	n.d.	n.d.			
	Homoserine	n.d.	n.d.			
	S-Adenosylhomocysteine (S-Ahcys)	0.035 (± 0.011)	0.047 (± 0.008)	1.34	1.4.E-01	
	S-Adenosylmethionine (S-Amet)	1.80 (± 0.17)	1.89 (± 0.27)	1.05	3.3.E-01	
	Spermidine	2.83 (± 0.50)	2.24 (± 0.67)	0.792	8.9.E-02	
	Spermine	0.113 (± 0.006)	0.092 (± 0.007)	0.817	4.3.E-02	yes
	Hydroxyproline (Pro-OH)	n.d.	n.d.			
	Anthranilate	n.d.	n.d.			

n.d. : not detected
s.d. : standard deviation (n = 4)
significance was determined by Student's *t*-test.

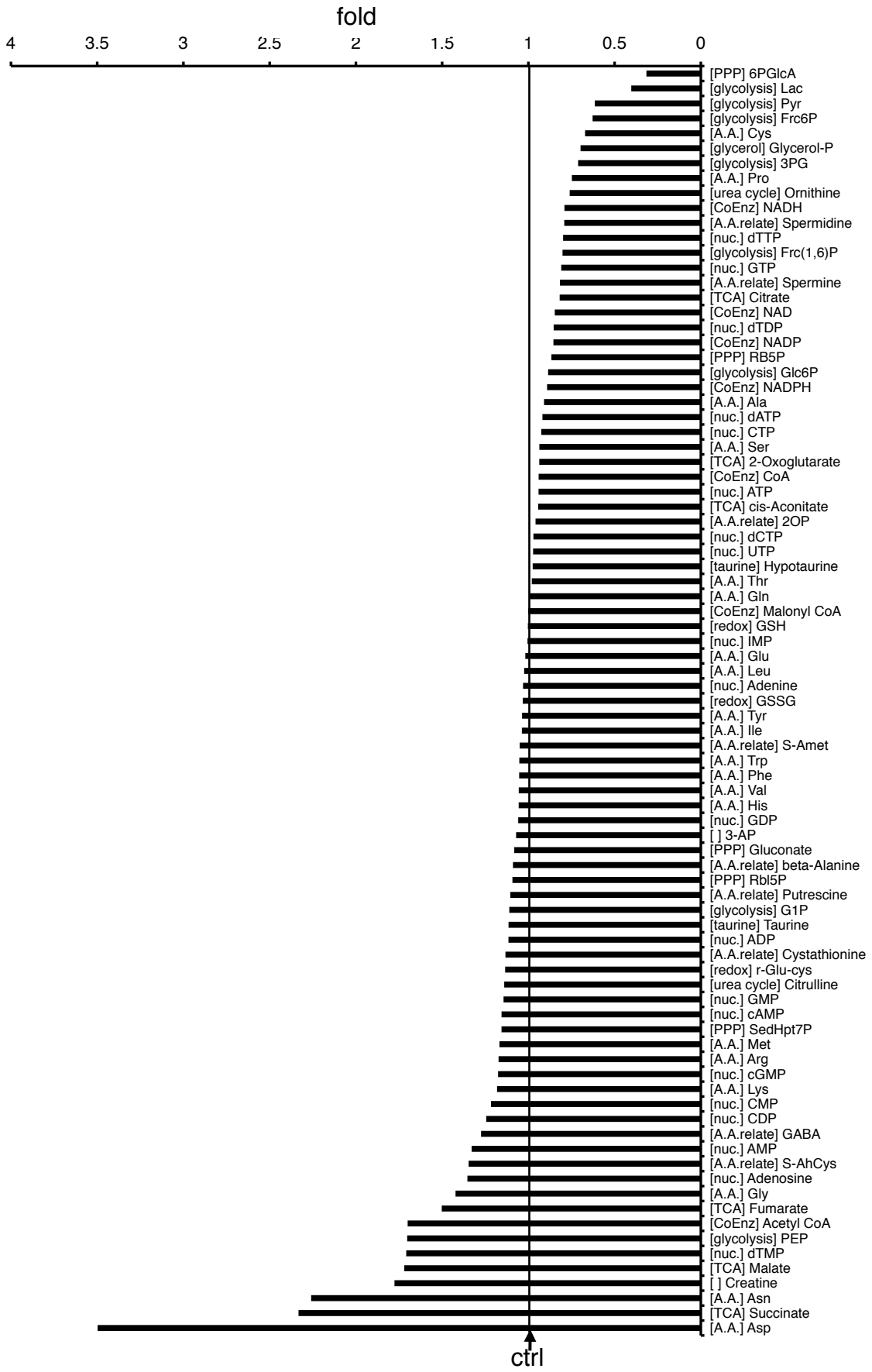

Figure 3-5 Fold changes in metabolites levels in GPA-treated A431 cells

Metabolites in **Table 3-2** were ordered in ascending sequence. Metabolites were categorized as glycolysis, TCA [tricarboxilic acid cycle], PPP [pentose phosphate pathway], nuc. [nucleotide synthesis], CoEnz [coenzyme], A.A. [amino acids], A.A. relate [amino acid conversion, degradation, etc], urea cycle and redox, shown in parentheses.

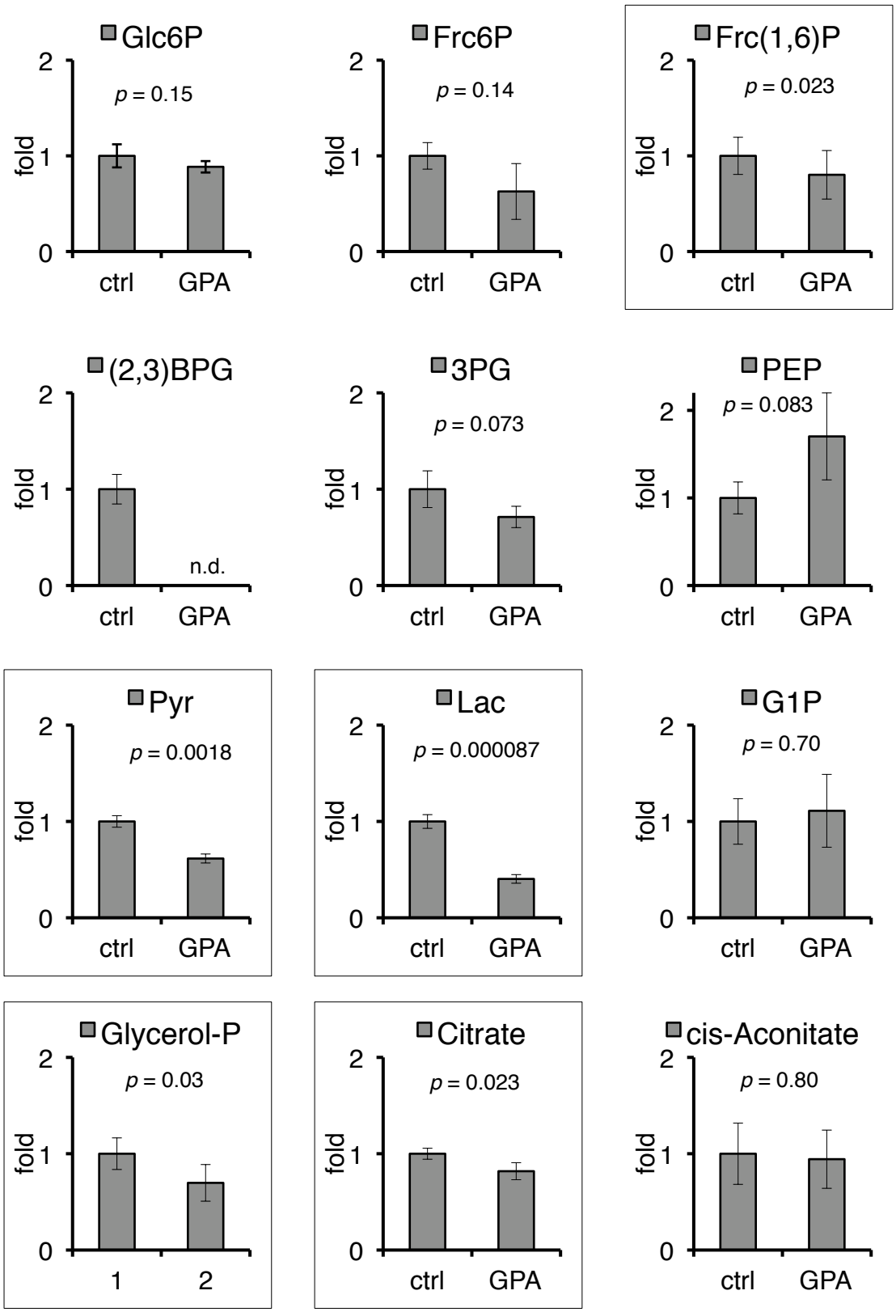

Figure 3-6 Fold changes in metabolites levels in GPA-treated A431 cells (1/7)

Framed graphs indicate the significant difference between metabolites in control and GPA-treated cells. bars: SD (n = 4). Significance was determined by Student's *t*-test

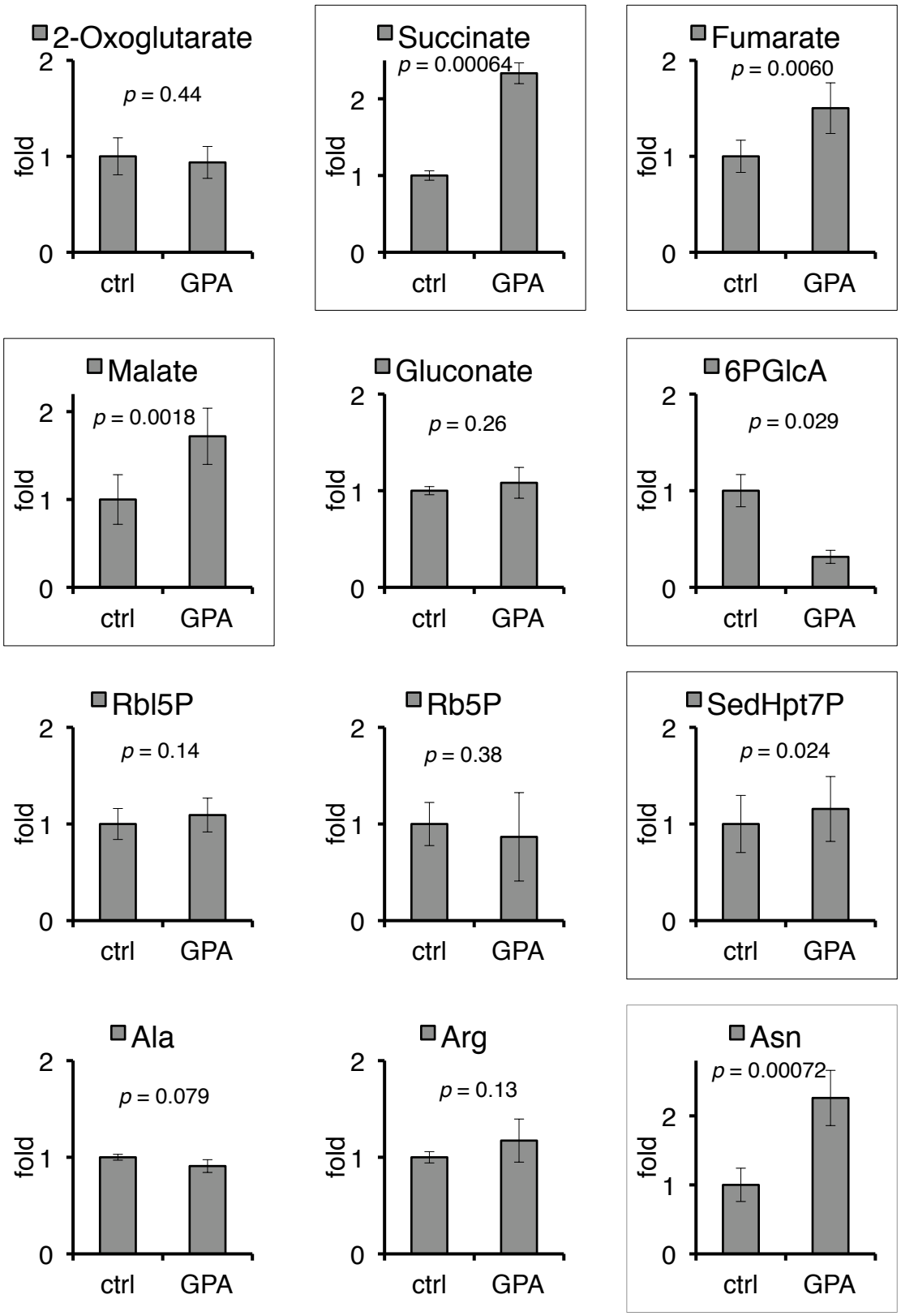

Figure 3-6 Fold changes in metabolites levels in GPA-treated A431 cells (2/7)

Framed graphs indicate the significant difference between metabolites in control and GPA-treated cells. bars: SD (n = 4). Significance was determined by Student's *t*-test

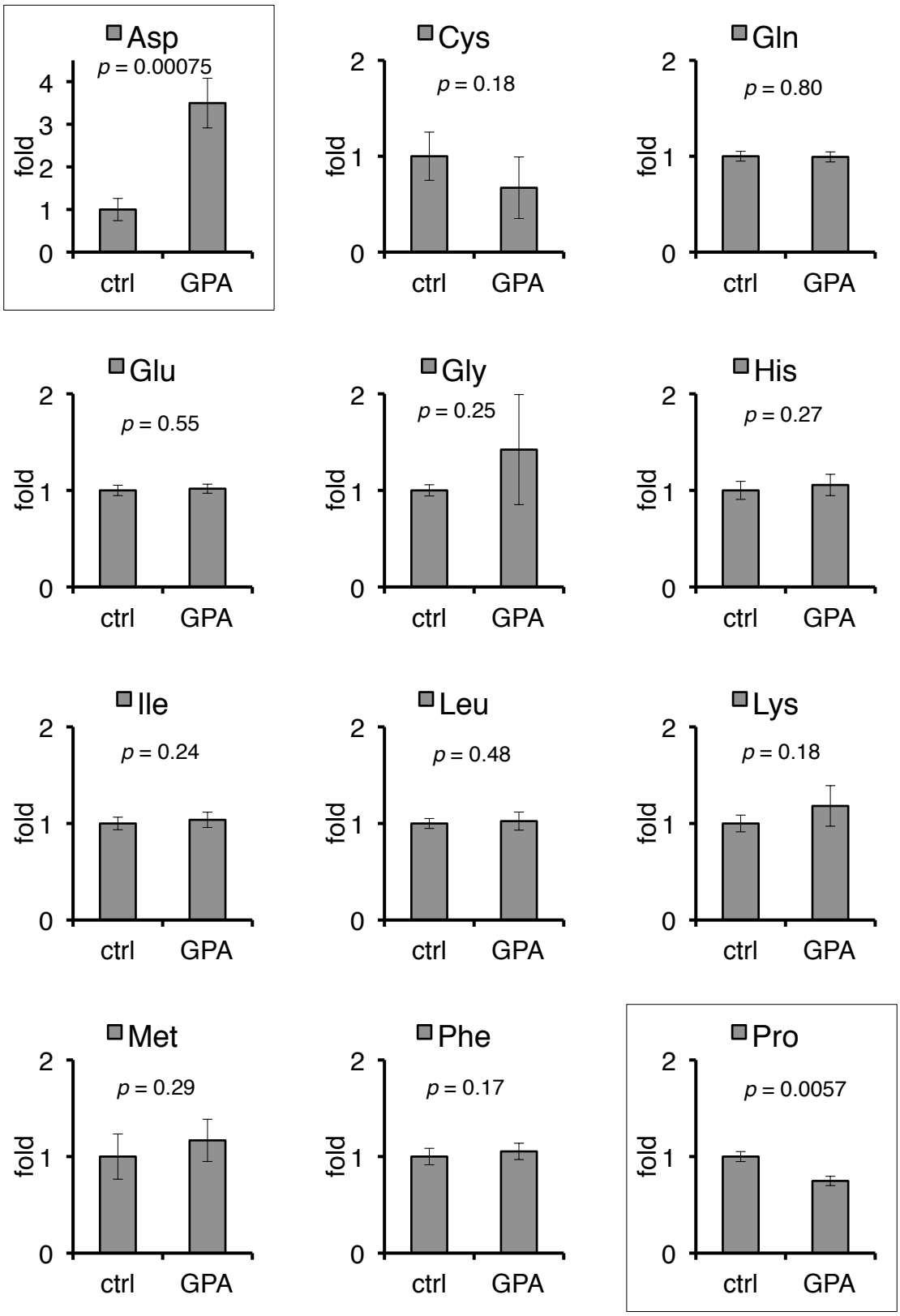

Figure 3-6 Fold changes in metabolites levels in GPA-treated A431 cells (3/7)

Framed graphs indicate the significant difference between metabolites in control and GPA-treated cells. bars: SD (n = 4). Significance was determined by Student's *t*-test

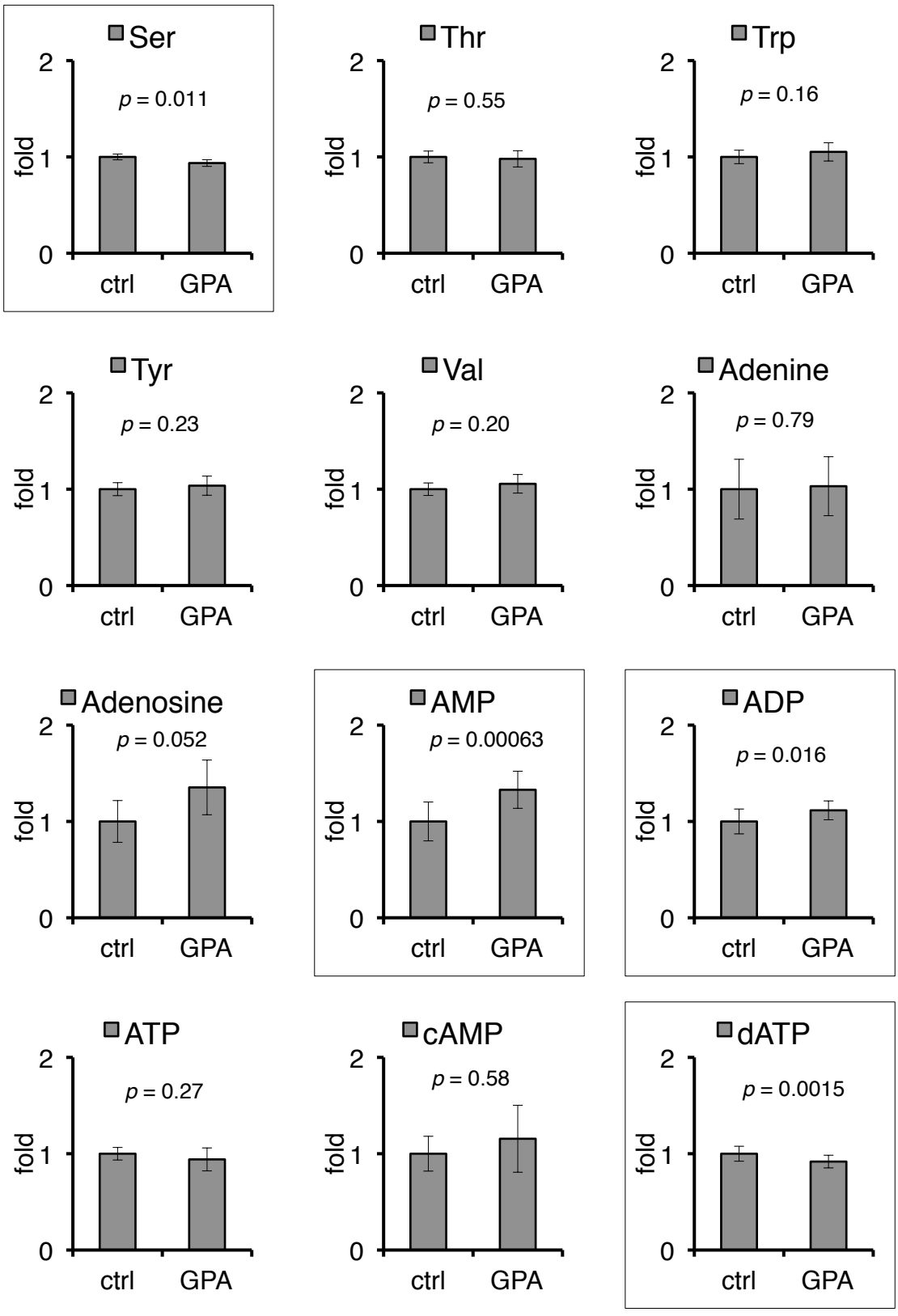

Figure 3-6 Fold changes in metabolites levels in GPA-treated A431 cells (4/7)

Framed graphs indicate the significant difference between metabolites in control and GPA-treated cells. bars: SD (n = 4). Significance was determined by Student's *t*-test

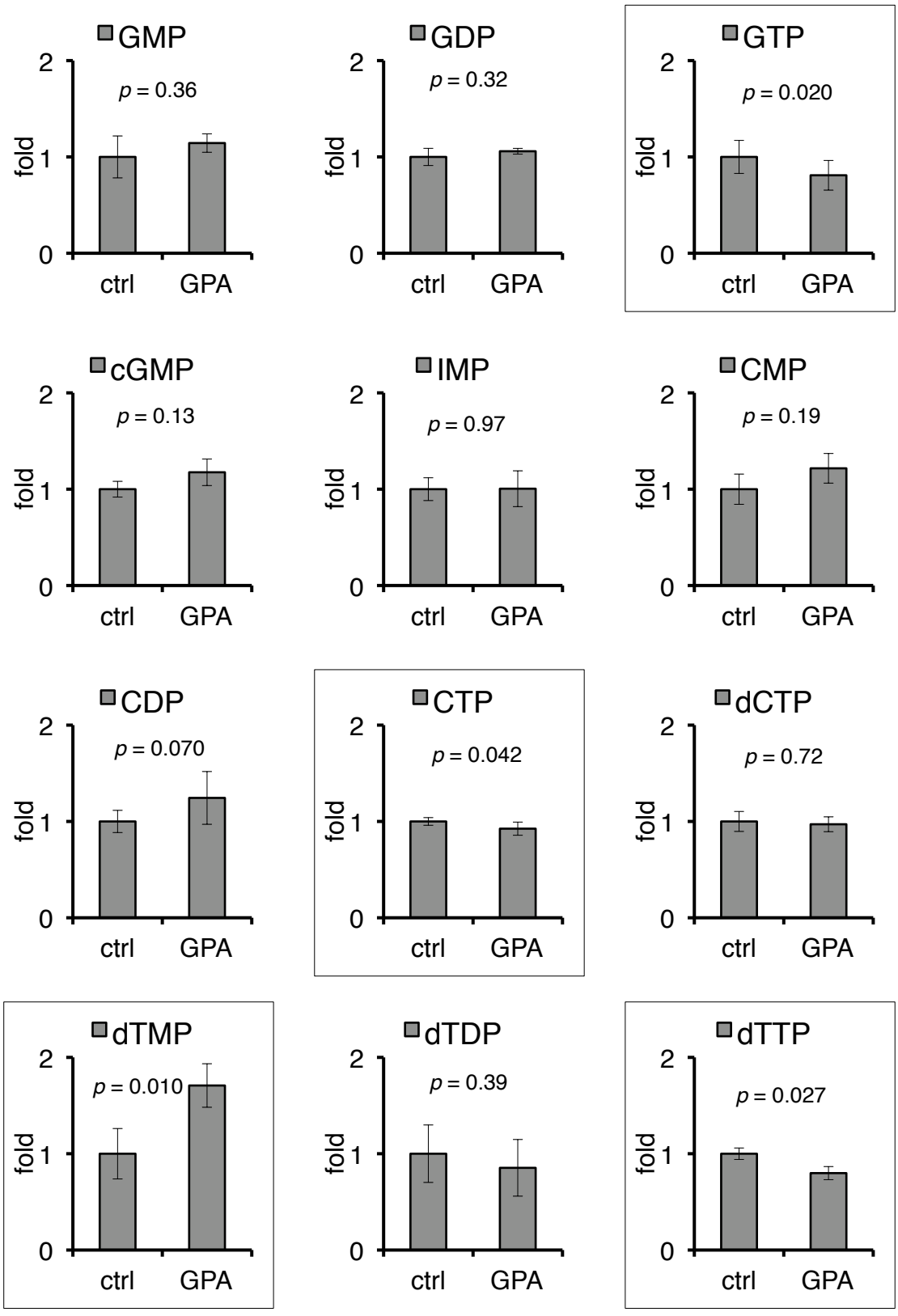

Figure 3-6 Fold changes in metabolites levels in GPA-treated A431 cells (5/7)

Framed graphs indicate the significant difference between metabolites in control and GPA-treated cells. bars: SD (n = 4). Significance was determined by Student's *t*-test

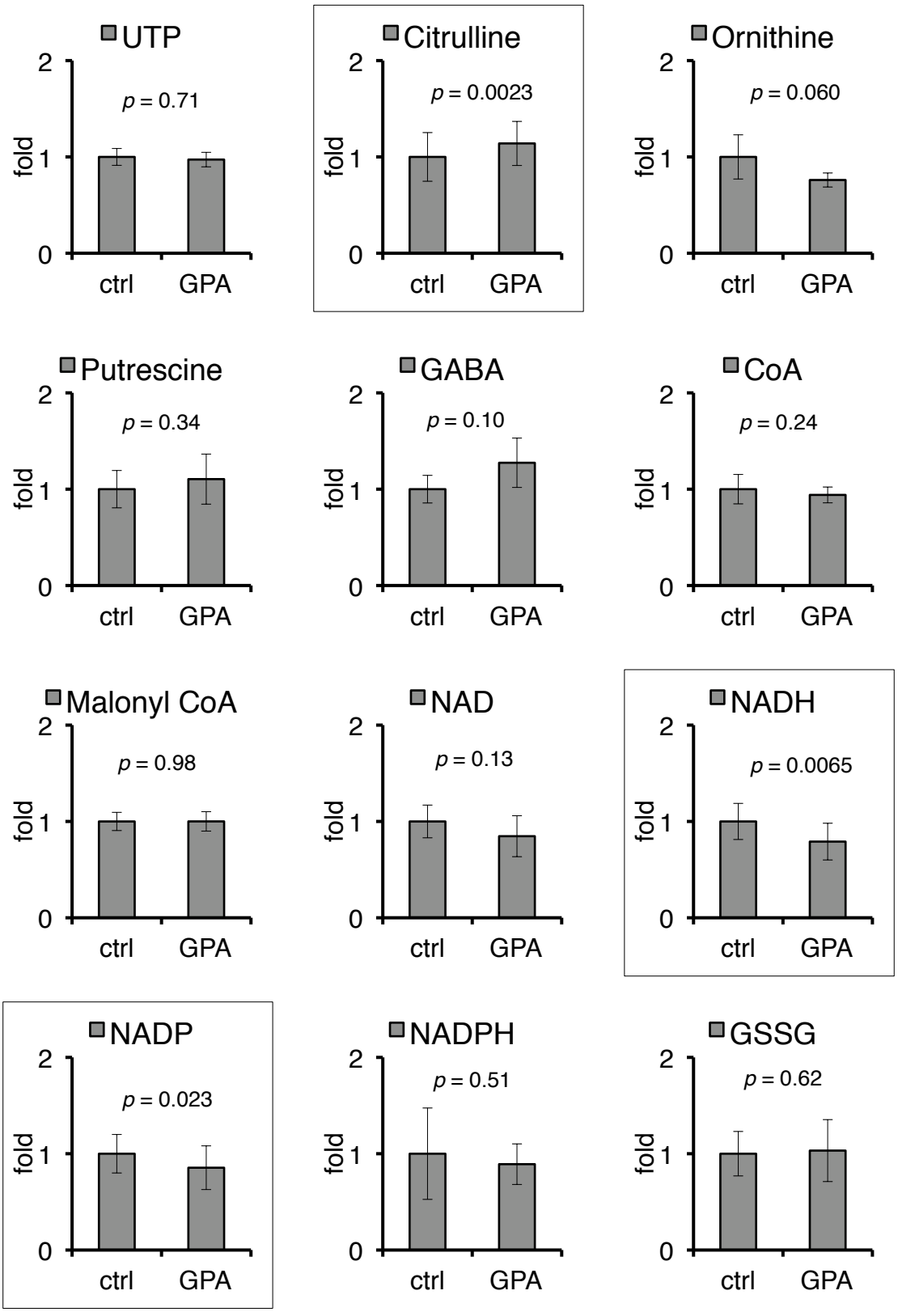

Figure 3-6 Fold changes in metabolites levels in GPA-treated A431 cells (6/7)

Framed graphs indicate the significant difference between metabolites in control and GPA-treated cells. bars: SD (n = 4). Significance was determined by Student's *t*-test

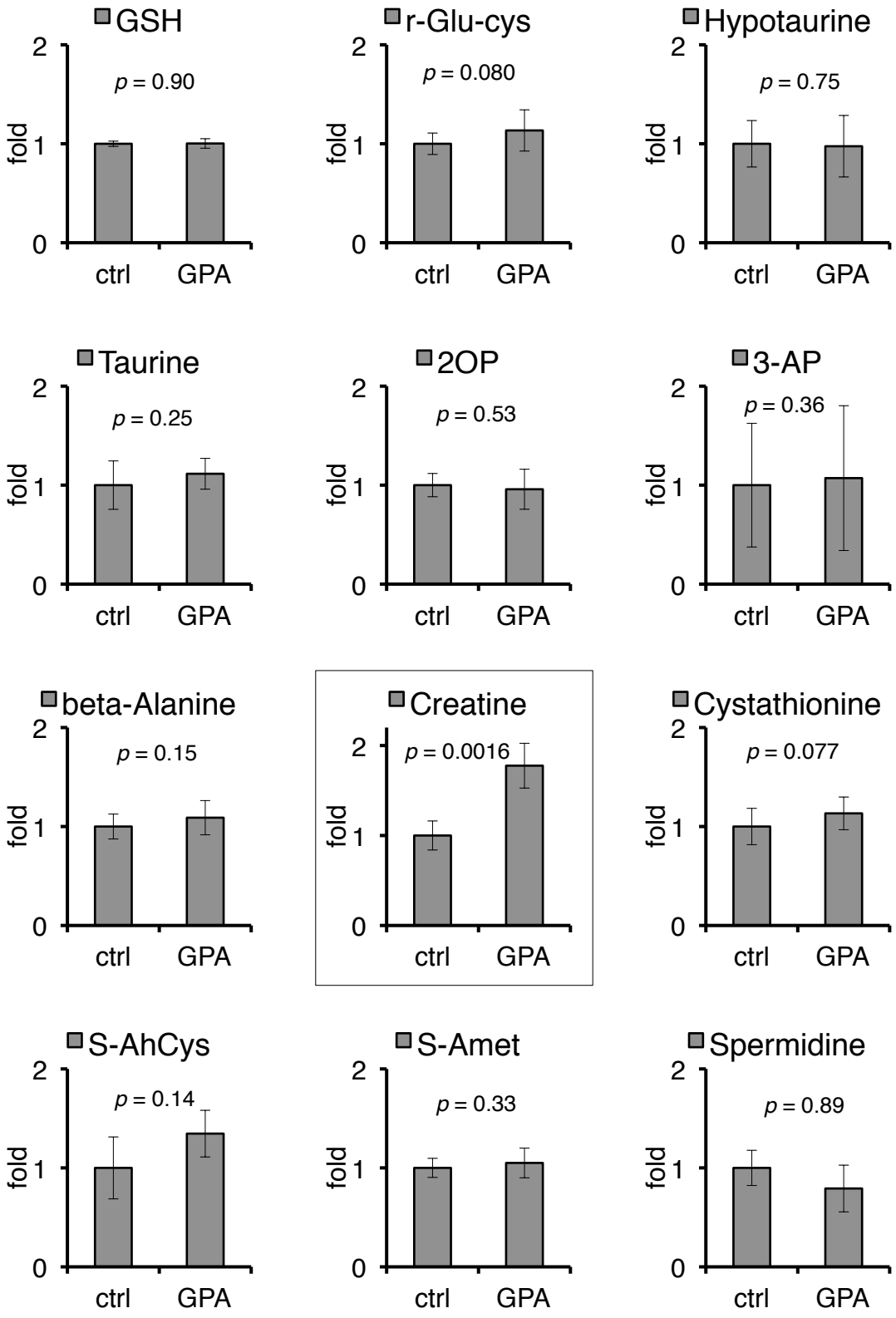

Figure 3-6 Fold changes in metabolites levels in GPA-treated A431 cells (7/7)

Framed graphs indicate the significant difference between metabolites in control and GPA-treated cells. bars: SD (n = 4). Significance was determined by Student's *t*-test

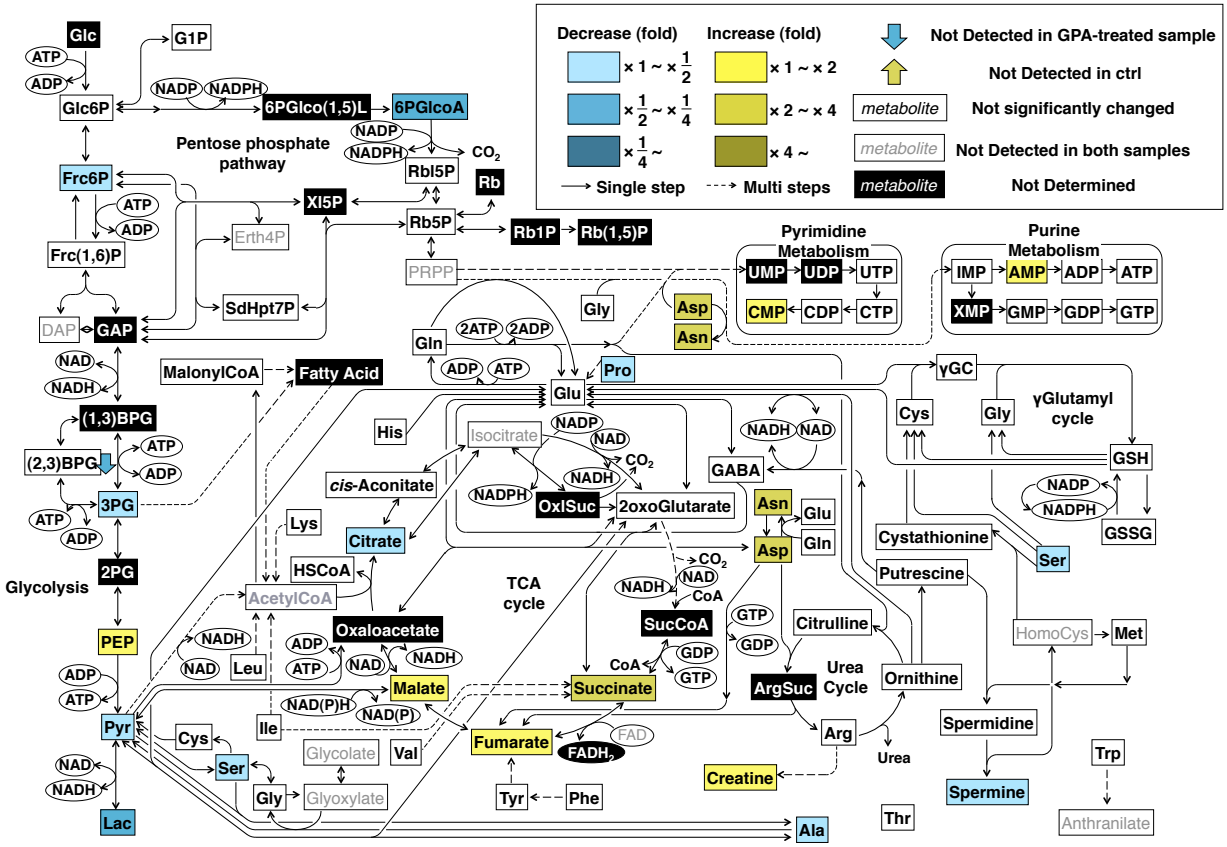

Figure 3-7 Snapshot picture of GPA-changed metabolome.

The global metabolites in GPA-treated A431 cells (30 min treatment) were extracted and analyzed by CE-TOFMS, and compared with that of control cells. Significantly decreased metabolites in GPA-treated cells are shown as , and (> 50%, > 25%, and < 25%, respectively), and significantly increased metabolites are shown as , and (< 200%, < 400%, and > 400%, respectively). Significance was determined by Student's *t*-test (n = 4, $p < 0.05$). The entire set of results with exact *p* values and list of metabolite abbreviations are listed in **Table 3-2**. (See also **Fig. 3-8** for lactate / pyruvate ratio in addition)

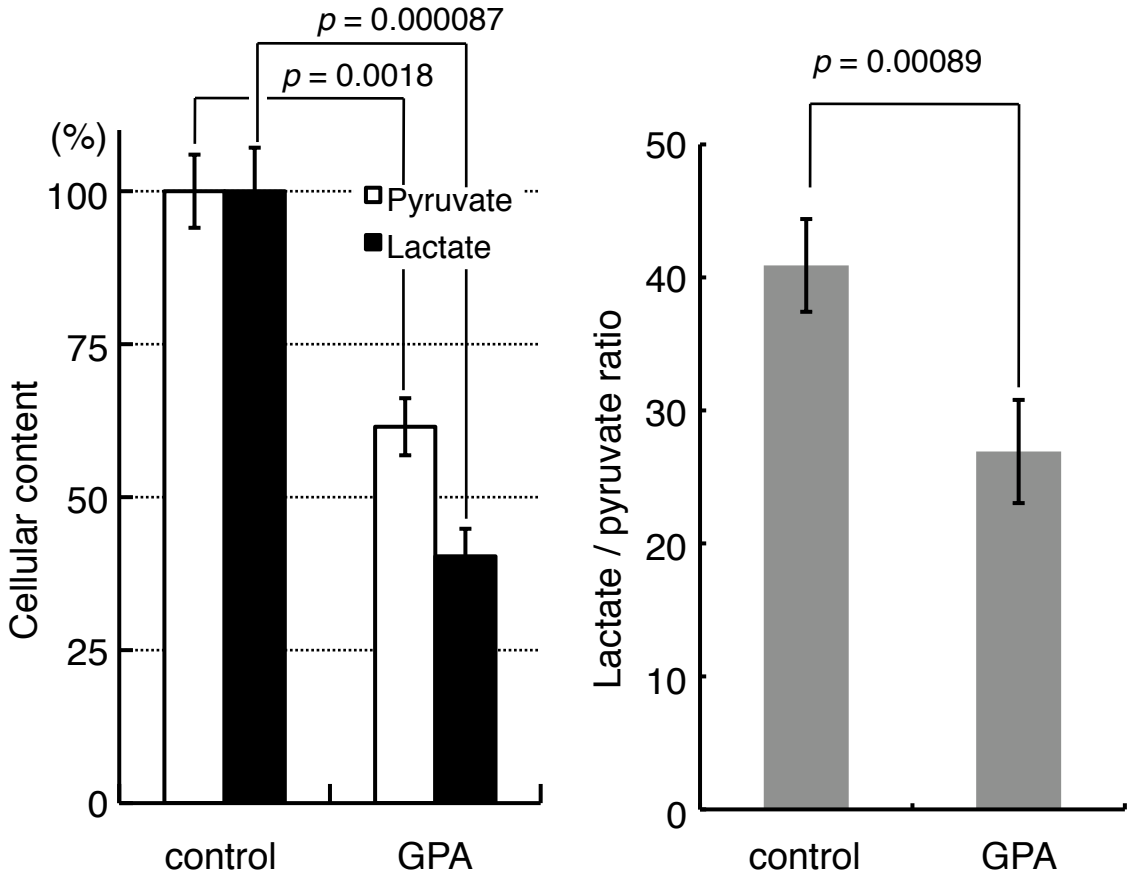

Figure 3-8 Decrease in glycolytic parameter by GPA treatment

As the glycolytic parameter, pyruvate, lactate levels and lacate / pyruvate ration were shown. They were all significantly decreased, indicating that GPA suppresses glycolysis. bars: SD (n = 4)

Table 3-3 Absolute metabolite concentrations in PA-treated and PA&GPA-cotreated cells.

class	Metabolites (abbrev.)	μM (± s.d.) PA	fold ctrl	*t*-test *p*	*p*<0.05	μM (± s.d.) PA&GPA	fold ctrl
Glycolysis	Glucose 6-phosphate (Glc6P)	0.446 (± 0.081)	0.987	8.9E-01		0.355 (± 0.065)	0.785
Glycolysis	Fructose 6-phosphate (Frc6P)	0.274 (± 0.037)	1.02	7.8E-01		0.249 (± 0.090)	0.933
Glycolysis	Fructose 1,6-diphosphate (Frc(1,6)P)	0.270 (± 0.111)	1.07	6.4E-01		0.182 (± 0.051)	0.722
Glycolysis	Dihydroxyacetone phosphate (DHAP)	n.d.				n.d.	
Glycolysis	2,3-Diphosphoglycerate ((2,3)BPG)	0.186 (± 0.018)	0.752	1.7E-01		n.d.	ct>PA&GPA
Glycolysis	3-Phosphoglycerate (3PG)	0.669 (± 0.142)	0.857	9.1E-03	yes	0.105 (± 0.049)	0.134
Glycolysis	Phosphoenolpyruvate (PEP)	0.129 (± 0.050)	0.733	9.4E-02		n.d.	ct>PA&GPA
Glycolysis	Pyruvate (Pyr)	1.48 (± 0.39)	0.936	5.7E-01		0.936 (± 0.293)	0.593
Glycolysis	Lactate (Lac)	78.5 (± 9.0)	1.22	2.0E-02	yes	30.0 (± 4.7)	0.467
Glycolysis	Glucose 1-phosphate (G1P)	0.139 (± 0.039)	0.730	1.8E-01		0.283 (± 0.070)	1.49
Glyoxylate	Glycolate	n.d.				n.d.	
Glyoxylate	Glyoxylate	n.d.				n.d.	
	Glycerophosphorate (Glycerol-P)	0.620 (± 0.187)	0.932	5.9E-01		0.199 (± 0.030)	0.299
TCA cycle	Citrate	0.984 (± 0.198)	0.141	4.9E-05	yes	1.16 (± 0.14)	0.168
TCA cycle	cis-Aconitate	n.d.	ct>PA				ct>PA&GPA
TCA cycle	Isocitrate	n.d.				n.d.	
TCA cycle	2-Oxoglutarate	6.06 (± 0.73)	0.966	8.2E-01		1.14 (± 0.16)	0.182
TCA cycle	Succinate	2.79 (± 0.84)	0.477	5.3E-03	yes	2.47 (± 0.80)	0.423
TCA cycle	Fumarate	1.88 (± 0.33)	0.964	4.4E-02	yes	1.30 (± 0.17)	0.666
TCA cycle	Malate	6.93 (± 1.02)	0.954	5.8E-01		4.03 (± 0.93)	0.555
Pentose phosphate	Gluconate	1.06 (± 0.15)	0.945	4.3E-01		1.06 (± 0.18)	0.945
Pentose phosphate	6-Phosphogluconate (6PGlcA)	0.269 (± 0.060)	1.21	1.6E-01		0.037 (± 0.003)	0.165
Pentose phosphate	Ribulose 5-phosphate (Rbl5P)	1.19 (± 0.20)	1.62	2.8E-03	yes	1.36 (± 0.25)	1.86
Pentose phosphate	Ribose 5-phosphate (Rb5P)	0.431 (± 0.080)	1.66	4.7E-02	yes	0.608 (± 0.153)	2.35
Pentose phosphate	Sedoheptulose 7-phosphate (SedHpt7P)	0.680 (± 0.218)	1.14	2.2E-01		1.55 (± 0.35)	2.60
Pentose phosphate	Erythrose 4-phosphate (Erth4P)	n.d.				n.d.	
Pentose phosphate	PRPP	n.d.				n.d.	
amino acid	Ala	26.9 (± 2.5)	1.10	1.4E-01		28.8 (± 3.3)	1.17
amino acid	Arg	4.08 (± 0.67)	1.18	8.1E-02		8.17 (± 1.05)	2.37
amino acid	Asn	1.20 (± 0.26)	0.785	1.5E-02	yes	3.82 (± 0.60)	2.50
amino acid	Asp	5.30 (± 0.99)	0.368	8.2E-03	yes	27.6 (± 2.3)	1.92
amino acid	Cys	0.263 (± 0.112)	1.23	3.1E-01		0.341 (± 0.103)	1.60
amino acid	Gln	302 (± 32)	1.03	6.5E-01		328 (± 40)	1.11
amino acid	Glu	468 (± 38)	1.07	1.8E-01		473 (± 47)	1.08
amino acid	Gly	129 (± 11)	0.883	5.6E-02		137 (± 14)	0.941
amino acid	His	13.1 (± 2.0)	1.02	7.5E-01		17.6 (± 1.9)	1.375
amino acid	Ile	41.7 (± 5.7)	1.03	5.9E-01		54.2 (± 7.8)	1.344
amino acid	Leu	44.7 (± 6.8)	1.06	4.4E-01		59.2 (± 8.4)	1.406
amino acid	Lys	10.2 (± 1.6)	1.17	1.9E-01		19.9 (± 3.5)	2.285
amino acid	Met	14.9 (± 4.0)	1.17	3.6E-01		17.7 (± 5.0)	1.390
amino acid	Phe	32.9 (± 4.9)	1.04	5.2E-01		40.5 (± 5.9)	1.278
amino acid	Pro	28.3 (± 3.2)	1.10	1.5E-01		17.6 (± 2.7)	0.684
amino acid	Ser	41.8 (± 2.7)	1.18	2.6E-02	yes	41.4 (± 4.8)	1.16
amino acid	Thr	92.4 (± 13.1)	1.04	5.5E-01		99.6 (± 13.7)	1.12
amino acid	Trp	5.36 (± 0.72)	1.02	5.7E-01		6.67 (± 0.84)	1.27
amino acid	Tyr	34.2 (± 5.6)	1.02	7.9E-01		44.0 (± 5.9)	1.31
amino acid	Val	48.0 (± 7.1)	1.04	5.9E-01		62.5 (± 8.6)	1.35
purine	Adenine	0.095 (± 0.025)	1.02	7.0E-01		0.149 (± 0.046)	1.61
purine	Adenosine	0.057 (± 0.022)	2.19	4.0E-02	yes	0.122 (± 0.054)	4.71
purine	AMP	4.25 (± 0.76)	5.51	4.6E-03	yes	16.5 (± 1.1)	21.4
purine	ADP	13.1 (± 1.8)	2.16	1.1E-03	yes	16.4 (± 1.6)	2.70
purine	ATP	30.4 (± 3.6)	0.701	1.6E-03	yes	15.0 (± 1.6)	0.346
purine	cAMP	0.831 (± 0.110)	1.13	4.5E-01		0.892 (± 0.066)	1.21
purine	dATP	0.399 (± 0.059)	0.708	1.4E-02	yes	0.228 (± 0.04)	0.403
purine	Guanine	n.d.				n.d.	
purine	Guanosine	n.d.				n.d.	
purine	GMP	0.843 (± 0.141)	4.18	3.8E-03	yes	2.72 (± 0.24)	13.5
purine	GDP	2.97 (± 0.19)	2.20	1.4E-03	yes	3.85 (± 0.54)	2.86
purine	GTP	7.08 (± 1.29)	0.716	1.6E-03	yes	3.64 (± 0.49)	0.368
purine	cGMP	0.444 (± 0.039)	0.953	5.8E-01		0.464 (± 0.063)	0.997
purine	Hypoxanthine	n.d.				n.d.	
purine	IMP	1.16 (± 0.33)	4.75	1.0E-02	yes	2.84 (± 0.33)	11.6
purine	Inosine	n.d.				n.d.	

(*continuing*)

Table 3-3 Absolute metabolite concentrations in PA-treated and PA&GPA-cotreated cells. (*continued*)

class	Metabolites (Abbrev.)	μM (± s.d.) PA	fold ctrl	*t*-test *p*	*p*<0.05	μM (± s.d.) PA&GPA	fold ctrl
pyrimidine	Cytidine	n.d.				n.d.	
pyrimidine	Cytosine	n.d.				n.d.	
pyrimidine	CMP	0.710 (± 0.087)	4.16	5.1E-04	yes	0.718 (± 0.045)	4.20
pyrimidine	CDP	1.46 (± 0.23)	2.48	6.8E-03	yes	0.62 (± 0.09)	1.05
pyrimidine	CTP	5.06 (± 0.82)	0.663	2.9E-03	yes	1.25 (± 0.10)	0.163
pyrimidine	dCTP	0.119 (± 0.033)	0.605	2.0E-02	yes	0.048 (± 0.015)	0.244
pyrimidine	dTMP	0.174 (± 0.032)	2.47	7.9E-03	yes	0.169 (± 0.023)	2.40
pyrimidine	dTDP	0.136 (± 0.043)	1.59	2.1E-01		0.158 (± 0.042)	1.86
pyrimidine	dTTP	0.443 (± 0.072)	0.646	8.5E-04	yes	0.215 (± 0.039)	0.314
pyrimidine	Uridine	n.d.				n.d.	
pyrimidine	Uracil	n.d.				n.d.	
pyrimidine	UTP	16.5 (± 2.7)	0.722	7.9E-03	yes	3.27 (± 0.28)	0.143
Urea cycle	Citrulline	0.877 (± 0.086)	0.908	5.2E-01		1.35 (± 0.32)	1.40
Urea cycle	Ornithine	0.474 (± 0.106)	0.862	5.2E-02		0.514 (± 0.098)	0.934
	Putrescine	0.470 (± 0.285)	0.920	8.0E-01		0.572 (± 0.122)	1.12
	GABA	0.093 (± 0.011)	1.20	7.8E-02		0.064 (± 0.015)	0.829
Coenzyme	Acetyl CoA	0.025 (± 0.004)	ct>PA			0.031 (± 0.004)	ct>PA&GPA
Coenzyme	CoA	0.487 (± 0.118)	0.933	2.9E-01		0.391 (± 0.065)	0.749
Coenzyme	Malonyl CoA	3.59 (± 0.11)	0.680	3.4E-03	yes	1.63 (± 0.29)	0.308
Coenzyme	FAD	n.d.				n.d.	
Coenzyme	NAD	3.83 (± 0.95)	0.860	3.7E-02	yes	4.29 (± 0.80)	0.963
Coenzyme	NADH	1.11 (± 0.30)	1.54	5.7E-02		0.680 (± 0.104)	0.948
Coenzyme	NADP	0.356 (± 0.039)	0.811	1.2E-01		0.340 (± 0.089)	0.774
Coenzyme	NADPH	0.314 (± 0.119)	0.805	5.3E-01		0.138 (± 0.037)	0.355
redox	Glutathione, oxidized (GSSG)	28.2 (± 6.4)	1.14	3.0E-01		32.2 (± 6.9)	1.30
redox	Glutathione, reduced (GSH)	186 (± 16)	0.965	5.2E-01		173 (± 16)	0.898
redox	r-Glu-cys	2.63 (± 0.50)	1.34	2.1E-02	yes	3.12 (± 0.35)	1.58
taurine	Cysteine sulfinate	n.d.				n.d.	
taurine	Hypotaurine	0.442 (± 0.167)	1.04	7.7E-01		0.382 (± 0.171)	0.899
taurine	Taurine	2.20 (± 0.51)	1.10	2.5E-02	yes	1.53 (± 0.64)	0.766
tyrosine	DOPA	n.d.				n.d.	
tyrosine	Tyramine	n.d.				n.d.	
	2-Aminoisobutyrate (2AB)	n.d.				n.d.	
	2-Oxopentanoate (2OP)	0.971 (± 0.234)	0.756	1.4E-01		0.406 (± 0.074)	0.315
	3-Aminopyrrolidine (3AP)	2.17 (± 1.27)	1.30	7.7E-02		2.28 (± 1.67)	1.37
	Glu-2aminobutyrate (Glu2AB)	n.d.				n.d.	
	Ophthalmate	n.d.				n.d.	
	beta-Alanine	16.3 (± 2.8)	0.985	7.9E-01		15.5 (± 2.3)	0.940
	Creatine	33.6 (± 6.9)	1.33	1.3E-02	yes	55.1 (± 7.1)	2.18
	Carnosine	n.d.				n.d.	
	Cystathionine	1.32 (± 0.23)	1.10	9.2E-03	yes	1.39 (± 0.23)	1.16
	Homocysteine (HomoCys)	n.d.				n.d.	
	Homoserine	n.d.				n.d.	
	S-Adenosylhomocysteine (S-Ahcys)	0.043 (± 0.011)	1.22	4.5E-01		0.048 (± 0.011)	1.38
	S-Adenosylmethionine (S-Amet)	1.82 (± 0.37)	1.01	8.5E-01		2.34 (± 0.56)	1.30
	Spermidine	2.37 (± 0.31)	0.837	1.1E-01		1.85 (± 0.48)	0.656
	Spermine	0.074 (± 0.003)	0.659	3.2E-02	yes	0.070 (± 0.005)	0.618
	Hydroxyproline (Pro-OH)	n.d.				n.d.	
	Anthranilate	n.d.				n.d.	

n.d. : not detected

s.d. : standard deviation (n = 4)

For PA-changed metabolites, significance was determined by Student's *t*-test

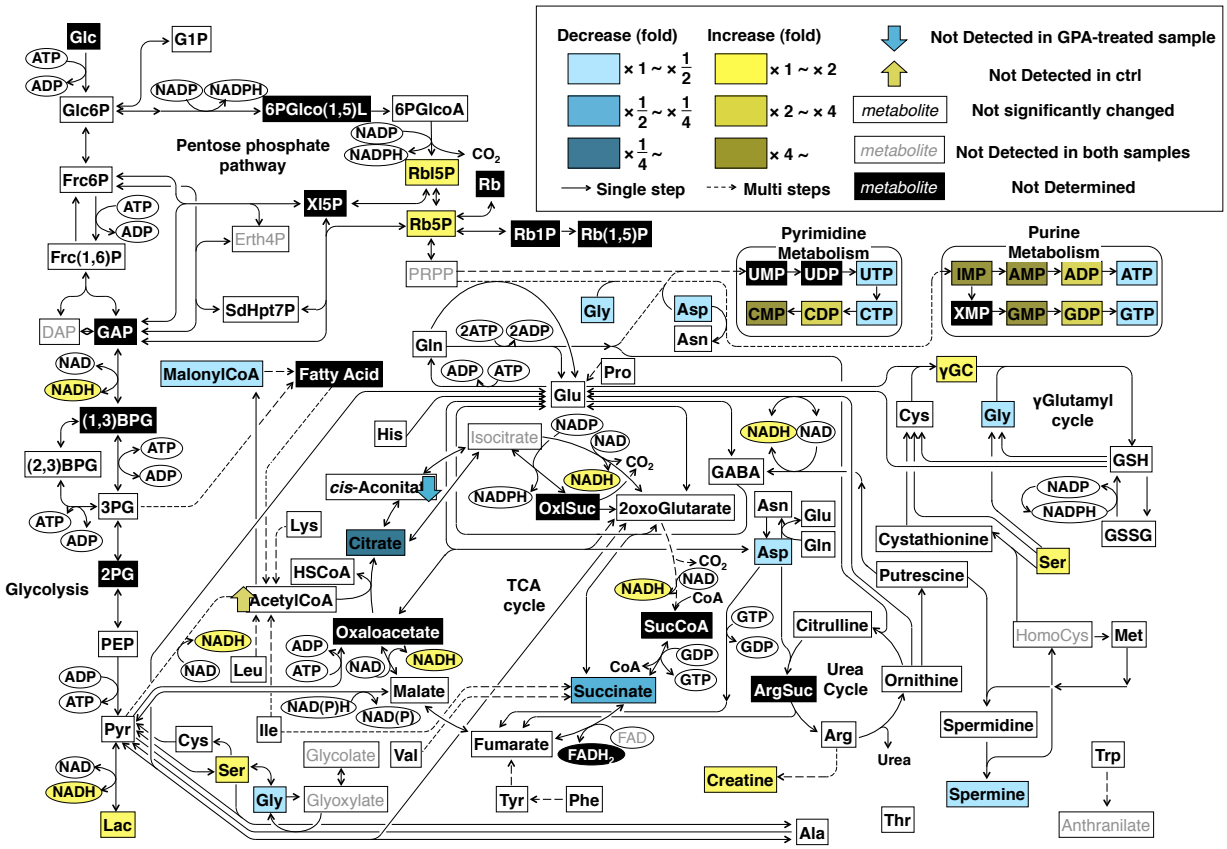

Figure 3-9 Snapshot picture of PA-changed metabolome.

The global metabolites in PA-treated A431 cells (30 min treatment) were extracted and analyzed by CE-TOFMS, and compared with that of control cells. Significantly decreased metabolites in GPA-treated cells are shown as , and (> 50%, > 25%, and < 25%, respectively), and significantly increased metabolites are shown as , and (< 200 %, < 400%, and > 400%, respectively). Significance was determined by Student's *t*-test (n = 4, $p < 0.05$).

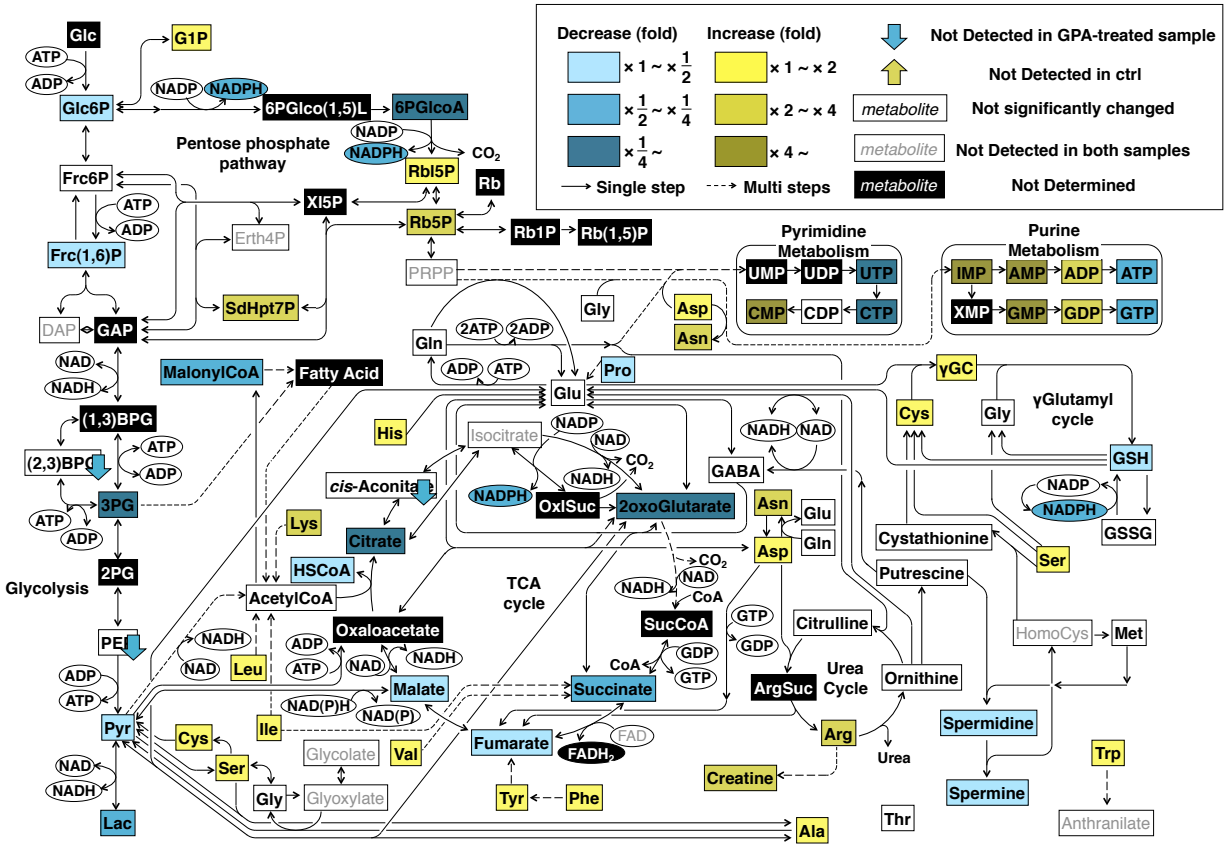

Figure 3-10 Snapshot picture of GPA&PA-changed metabolome.

The global metabolites in GPA&PA-cotreated A431 cells (30 min treatment) were extracted and analyzed by CE-TOFMS, and compared with that of control cells. Substantially decreased metabolites in GPA&PA-cotreated cells are shown as , and (> 50%, > 25%, and < 25%, respectively), and substantially increased metabolites are shown as , and (< 200%, < 400%, and > 400%, respectively). n = 4.

Table 3-4 Effect of GPA on ^{13}C-glucose metabolites

	metabolites	numbers of ^{13}C atom	cellular amounts, μM (s.d.) GPA [nM] 0	5	17	50
glycolysis	cellular glucose		n.d.	n.d.	n.d.	n.d.
	Glc6P	13C-0	0.24 (0.05)	0.21 (0.02)	0.21 (0.05)	0.18 (0.03)
		* 13C-6	4.7 (0.3)	1.2 (0.2)	1.0 (0.1)	1.1 (0.4)
	G1P	13C-0	0.26 (0.03)	0.15 (0.02)	0.17 (0.02)	0.14 (0.02)
		* 13C-6	0.99 (0.20)	0.14 (0.04)	0.11 (0.08)	0.063 (0.082)
	Frc6P	13C-0	0.077 (0.022)	0.035 (0.027)	0.080 (0.028)	0.068 (0.030)
		* 13C-6	0.40 (0.10)	0.085 (0.065)	0.071 (0.067)	0.046 (0.033)
	Frc(1,6)P	13C-0	0.93 (0.04)	0.72 (0.06)	0.58 (0.08)	0.58 (0.05)
		13C-3	0.13 (0.18)	n.d.	n.d.	n.d.
		13C-5	0.66 (0.06)	n.d.	n.d.	n.d.
		* 13C-6	21 (2)	n.d.	n.d.	n.d.
	DHAP candidate-1	13C-0	0.90 (0.06)	0.84 (0.16)	0.51 (0.36)	0.44 (0.30)
		* 13C-3	20 (3)	0.36 (0.26)	0.009 (0.018)	0.087 (0.121)
	DHAP candidate-2	13C-0	0.37 (0.07)	n.d.	n.d.	n.d.
		* 13C-3	18 (2)	1.2 (0.2)	0.41 (0.31)	0.38 (0.38)
	GAP		n.d.	n.d.	n.d.	n.d.
	(1,3) BPG		n.d.	n.d.	n.d.	n.d.
	2,3DPG	13C-0	n.d.	n.d.	n.d.	n.d.
		* 13C-3	2.4 (0.6)	0.43 (0.52)	n.d.	n.d.
	3PG	13C-0	n.d.	n.d.	n.d.	n.d.
		* 13C-3	1.5 (0.6)	0.39 (0.30)	n.d.	0.19 (0.23)
	2PG		n.d.	n.d.	n.d.	n.d.
	PEP		n.d.	n.d.	n.d.	n.d.
	Pyruvate	13C-0	8.7 (3.7)	11 (4)	11 (6)	9.5 (4.4)
		* 13C-3	15 (2)	4.8 (1.1)	1.4 (1.0)	1.7 (1.3)
	Lactate	13C-0	68 (20)	62 (9)	73 (40)	67 (29)
		13C-1	2.0 (0.5)	1.8 (0.1)	2.0 (0.8)	1.9 (0.8)
		* 13C-3	48 (26)	n.d.	n.d.	n.d.
pentose phosphate	6PGluco(1.5)L		n.d.	n.d.	n.d.	n.d.
	6P-gluconate	13C-0	n.d.	n.d.	n.d.	n.d.
		13C-5	0.15 (0.14)	n.d.	n.d.	n.d.
		* 13C-6	5.8 (0.4)	0.73 (0.07)	0.076 (0.151)	n.d.
	Ribulose5P	13C-0	0.20 (0.23)	0.032 (0.065)	0.13 (0.16)	0.14 (0.26)
		* 13C-5	2.2 (0.2)	0.52 (0.08)	0.21 (0.14)	0.14 (0.10)
	Ribose5P	13C-0	n.d.	n.d.	n.d.	0.055 (0.110)
		* 13C-5	1.4 (0.2)	0.50(0.04)	0.33 (0.09)	0.23 (0.03)
	PRPP	13C-0	n.d.	n.d.	n.d.	n.d.
		* 13C-5	0.78 (0.11)	0.69 (0.06)	0.13 (0.25)	0.23 (0.27)
TCA cycle	Acetyl-CoA		n.d.	n.d.	n.d.	n.d.
	Citrate	13C-0	11 (0)	10 (1)	11 (1)	13 (2)
		13C-1	0.78 (0.05)	0.75 (0.08)	0.72 (0.14)	0.85 (0.14)
		13C-2	5.6 (1.2)	1.9 (2.4)	n.d.	n.d.
	cis-Aconiate		n.d.	n.d.	n.d.	n.d.
	isocitrate		n.d.	n.d.	n.d.	n.d.
	2Oxoglutarate	13C-0	6.9 (0.2)	8.0 (0.8)	5.7 (1.0)	5.5 (0.8)
		13C-1	0.16 (0.32)	0.57 (0.09)	n.d.	n.d.
	Succinyl-CoA		n.d.	n.d.	n.d.	n.d.
	Succinate	13C-0	8.7 (0.6)	17 (4)	26 (6)	28 (5)
		13C-1	0.39 (0.05)	0.76 (0.14)	1.1 (0.3)	1.1 (0.2)
	Fumarate		n.d.	n.d.	n.d.	n.d.
	Malate	13C-0	16 (1)	16 (2)	15 (1)	16 (2)
		13C-1	0.62 (0.08)	0.71 (0.07)	0.60 (0.08)	0.63 (0.09)

(*continuing*)

Table 3-4 Effect of GPA on ^{13}C-glucose metabolites (*continued*)

metabolites		numbers of ^{13}C atom	cellular amounts, μM (s.d.) GPA [nM] 0	5	17	50
nucleotide	ADP	13C-0	6.9 (0.7)	7.6 (1.2)	10 (1)	11 (1)
		13C-1	0.89 (0.12)	0.91 (0.16)	1.3 (0.2)	1.4 (0.2)
		13C-2	0.15 (0.09)	0.13 (0.10)	0.27 (0.02)	0.27 (0.05)
		13C-5	0.40 (0.07)	0.38 (0.09)	0.36 (0.06)	0.35 (0.02)
	ATP	13C-0	133 (7)	115 (11)	113 (9)	117 (13)
		13C-1	14 (1)	12 (1)	13 (1)	13 (1)
		13C-2	3.7 (0.2)	3.4 (0.3)	3.2 (0.2)	3.5 (0.5)
		13C-3	0.69 (0.04)	0.62 (0.09)	0.57 (0.14)	0.64 (0.08)
		13C-4	0.33 (0.02)	0.088 (0.176)	n.d.	0.076 (0.152)
		13C-5	7.1 (0.5)	5.7 (0.5)	3.4 (0.4)	3.1 (0.6)
		13C-6	1.1 (0.2)	0.74 (0.09)	0.36 (0.02)	0.32 (0.08)
		13C-7	0.30 (0.13)	0.11 (0.13)	n.d.	n.d.
	GTP	13C-0	19 (1)	17 (2)	17 (2)	17 (2)
		13C-1	2.6 (0.2)	2.3 (0.4)	2.4 (0.4)	2.4 (0.3)
		13C-2	0.73 (0.06)	0.83 (0.15)	0.74 (0.21)	0.56 (0.38)
	UTP	13C-0	36 (3)	35 (5)	33 (6)	32 (5)
		13C-1	3.5 (0.5)	3.3 (0.6)	3.4 (0.6)	3.3 (0.4)
		13C-2	1.3 (0.2)	1.4 (0.2)	1.2 (0.2)	1.2 (0.1)
		13C-3	0.29 (0.21)	0.40 (0.20)	0.23 (0.23)	0.34 (0.13)
		13C-5	12 (1)	9.0 (0.6)	5.8 (0.8)	6.1 (0.9)
		13C-6	0.73 (0.07)	0.58 (0.08)	0.40 (0.07)	0.39 (0.08)
		13C-7	0.26 (0.30)	0.19 (0.22)	0.57 (0.11)	0.12 (0.14)

n.d. not determined

standard deviation in parentheses (n = 4)

* indicates the major isotopomer of each metabolite shown in **Fig. 3-11**

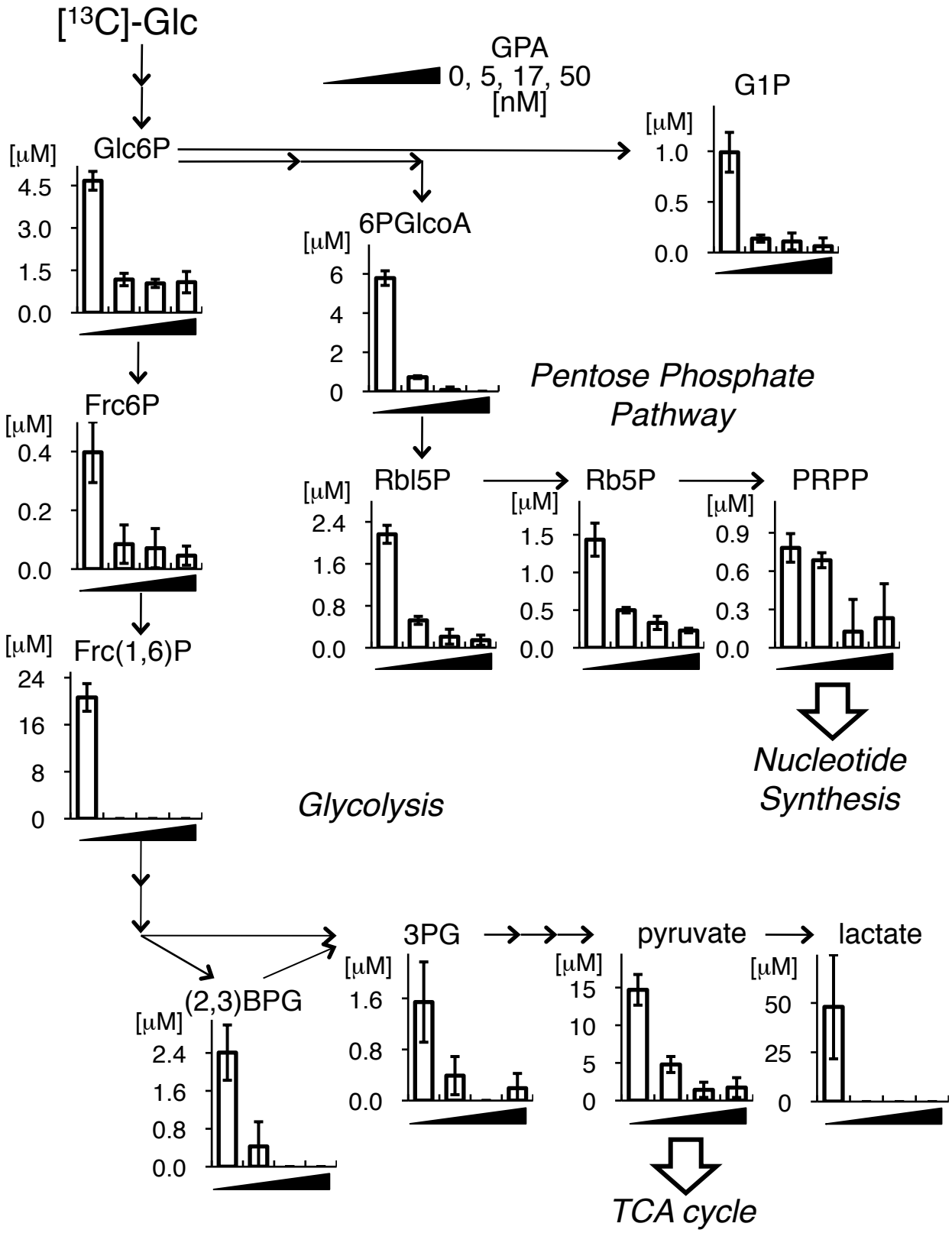

Figure 3-11 [13C]-labeling study.

[13C]-glucose was incorporated into A431 cells for 30 min immediately after GPA-treatment. All detected major isotopomers ([13C]-glucose-6-phosphate and its [13C]-metabolites) were decreased by GPA-treatment (the entire list is shown in **Table 3-4**), indicating that GPA inhibits the step from [13C]-glucose uptake to [13C]-glucose-6-phosphate production. bars: SD (n = 4).

3-2-2 Mode of action of glucopiericidin A

(3) Inhibition of glucose uptake by glucopiericidin A

Since hexokinase catalyzes G6P production, the author examined the effect of GPA on hexokinase activity *in vitro*. Glucose, as a substrate of hexokinase, was mixed with reaction buffer containing partially purified hexokinase, G6PDH, and NADP as a co-enzyme of the G6PDH reaction, and incubated at room temperature[72,73]. In this reaction, the G6P produced by hexokinase is further hydrolyzed by G6PDH, with the accompanying conversion of NADP to NADPH, so that hexokinase activity can be estimated by the spectrophotometric absorbance of NADPH[72]. As shown in **Fig. 3-12**, the assay revealed that addition of glucose led to an increase in the amount of NADPH, which could be negated by the hexokinase inhibitor 2DG. However, GPA at concentrations up to 1.7 μM failed to inhibit the reaction, indicating that the hexokinase reaction step is not the point of inhibition of glycolysis through a decrease in the amount of G6P by GPA.

Another possible step that GPA could act upon to cause a decrease in G6P is glucose uptake. To examine this possibility, cells were treated with [^{3}H]-2DG and evaluated whether GPA would affect glucose uptake. The compound 2DG acts as a glucose-mimic, and is incorporated into cells by glucose transporters. However, 2DG cannot be catabolized in glycolysis; thus, the amount of 2DG that is taken up simply reflects the glucose uptake capacity of a cell's glucose transporters.

In the experiments, GPA inhibited the uptake of [^{3}H]-2DG in a dose dependent

manner (**Fig. 3-13**), with an IC_{50} of 4.9 ± 2.9 nM (mean ± *SE*, n = 3). This concentration was quite similar to the concentration of GPA required to inhibit EGF-induced filopodia protrusion in combination with PA (**Figs. 2-14** and **2-15**). It is reported that GLUT1 is responsible for glucose uptake in A431 cells[74]. Treatment of cells with GPA did not change the expression level of GLUT1 in the plasma membrane (**Fig. 3-13**), which suggests that GPA inhibits GLUT1 function.

To confirm whether GPA does in fact inhibit GLUT1 function, GLUT1 was overexpressed in cells (**Fig. 3-14**), and the sensitivity of cells to GPA upon 2DG uptake was evaluated. Uptake of 2DG was substantially increased (about 4-fold) by GLUT1 overexpression. Although GPA could inhibit 2DG uptake in GLUT1-overexpressing cells, when compared to vector control cells, GLUT1-overexpressing cells became less sensitive to GPA depending on the expression level of GLUT1 (**Fig. 3-14**). The IC_{50} value for 2DG uptake increased with GLUT1 expression (21.6 ± 7.7 nM [mean ± *SE*, n = 3] in vector control cells vs. 108 ± 24 nM [mean ± *SE*, n = 3] in GLUT1--overexpressing cells). These results indicated that GPA inhibits GLUT1 function, and thereby inhibits glycolysis.

To further investigate about the inhibition of glucose uptake by GPA, the effect on GLUT4-mediated glucose uptake was examined. Differentiated Swiss 3T3-L1 adipocytes take up glucose basally via GLUT1[75]. However, when 3T3-L1 adipocytes are stimulated with insulin, GLUT4 is translocated to the membrane, and both GLUT1 and GLUT4 transport glucose into the cells[75]. GPA inhibited both the basal uptake of [^{3}H]-2DG via GLUT1 and the increased uptake of glucose in insulin-stimulated cells

(**Fig. 3-15**), suggesting that GPA inhibits glucose uptake via both GLUT1 and GLUT4.

On the other hand, it is quite important to argue about whether the glucose uptake inhibition was specific to GPA structure. Therefore, the author also examined the effect of PA as the glucose-null derivative of GPA on the glucose uptake in A431 cells. As the result, glucose-null derivative PA failed to inhibit the uptake (**Fig. 3-16**). Thus, it is likely that the glucose uptake inhibition by GPA would be due to its glucopyranoside moiety, perhaps by functioning as a glucose mimic to GLUT1 in A431 cells. This suggests that GLUT1 would be the *bona fide* target of GPA due to GPA's inhibition of glycolysis in A431 cells.

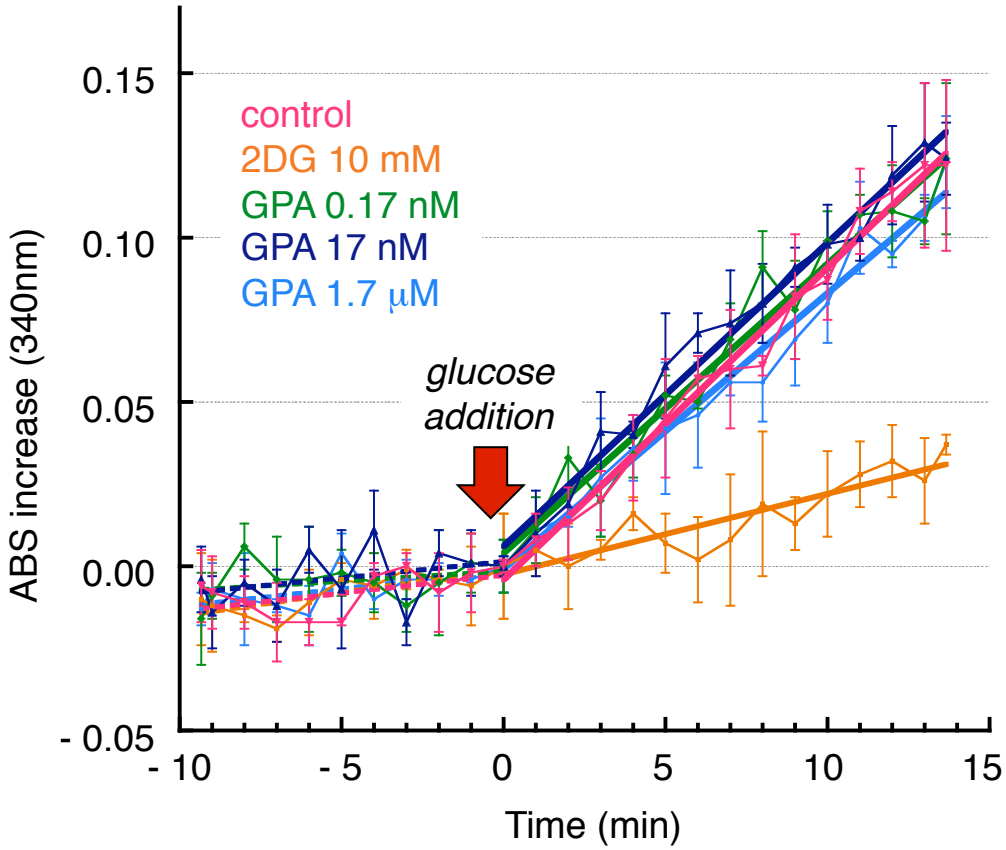

Figure 3-12 GPA failed to inhibit the *in vitro* hexokinase enzyme reaction.

Hexokinase activity was monitored by addition of the hexokinase substrate glucose, resulting in an increase in enzymatic activity (detected by NADPH absorbance at 340 nm), which was inhibited by 2-deoxy-D-glucose. However, GPA could not inhibit this increase in hexokinase activity, indicating that GPA was not a hexokinase inhibitor. bars: SD (n = 3).

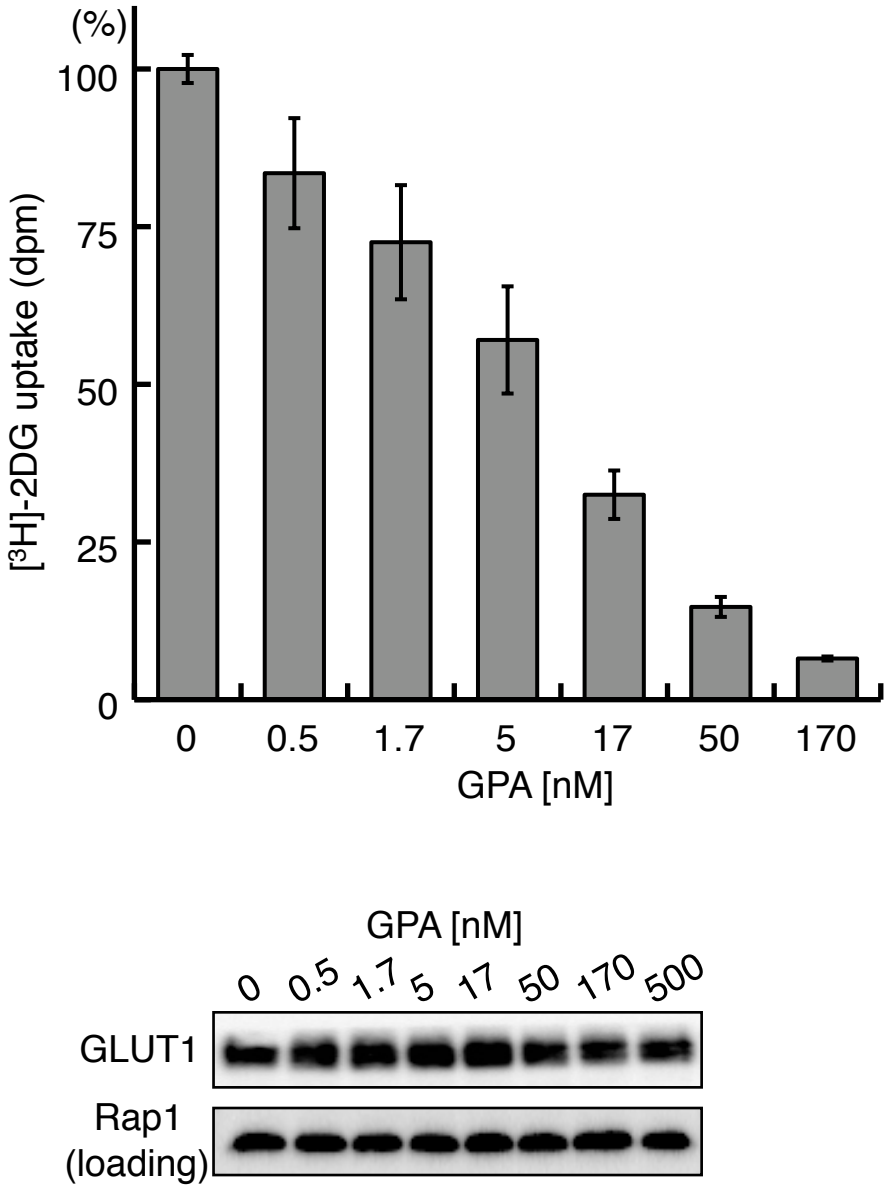

Figure 3-13 Inhibition of glucose uptake by GPA.

GPA inhibited the uptake of the glucose-mimic 2-deoxy-D-glucose (2DG) in a dose dependent manner. bars: SD (n = 3). Similar results were obtained from three individual experiments. These results explain the glucose-6-phosphate decrease depicted in **Fig. 3-11**.

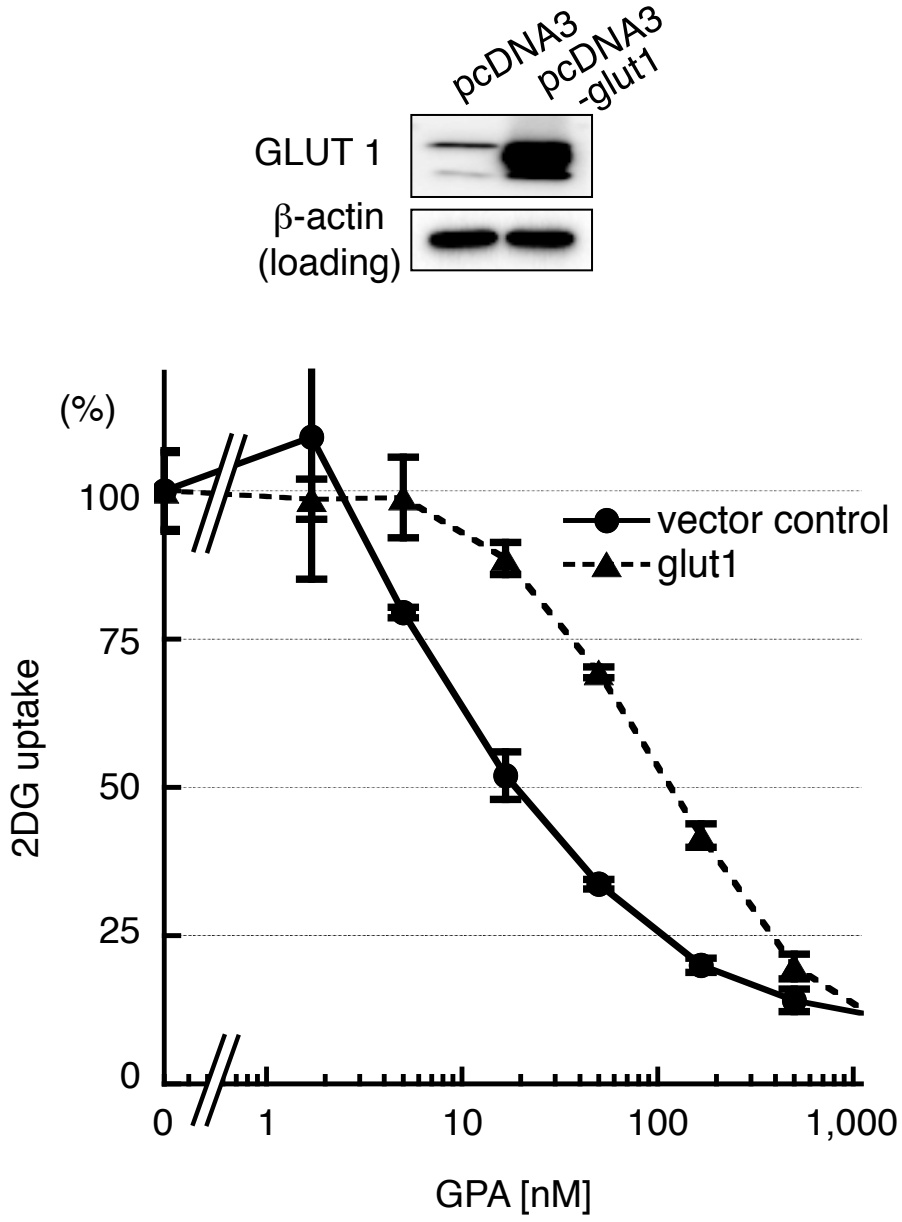

Figure 3-14 Inhibition of GLUT1-mediated glucose uptake by GPA.

The sensitivity of GPA to 2DG uptake was investigated in GLUT1 overexpressed HEK293T cells. The inhibition curve was shifted rightwards by glut1 overexpression, indicating that GLUT1 was the functional target of GPA. bars: SD (n = 3). Similar results were obtained from three individual experiments, and standard error calculated was shown in the main text.

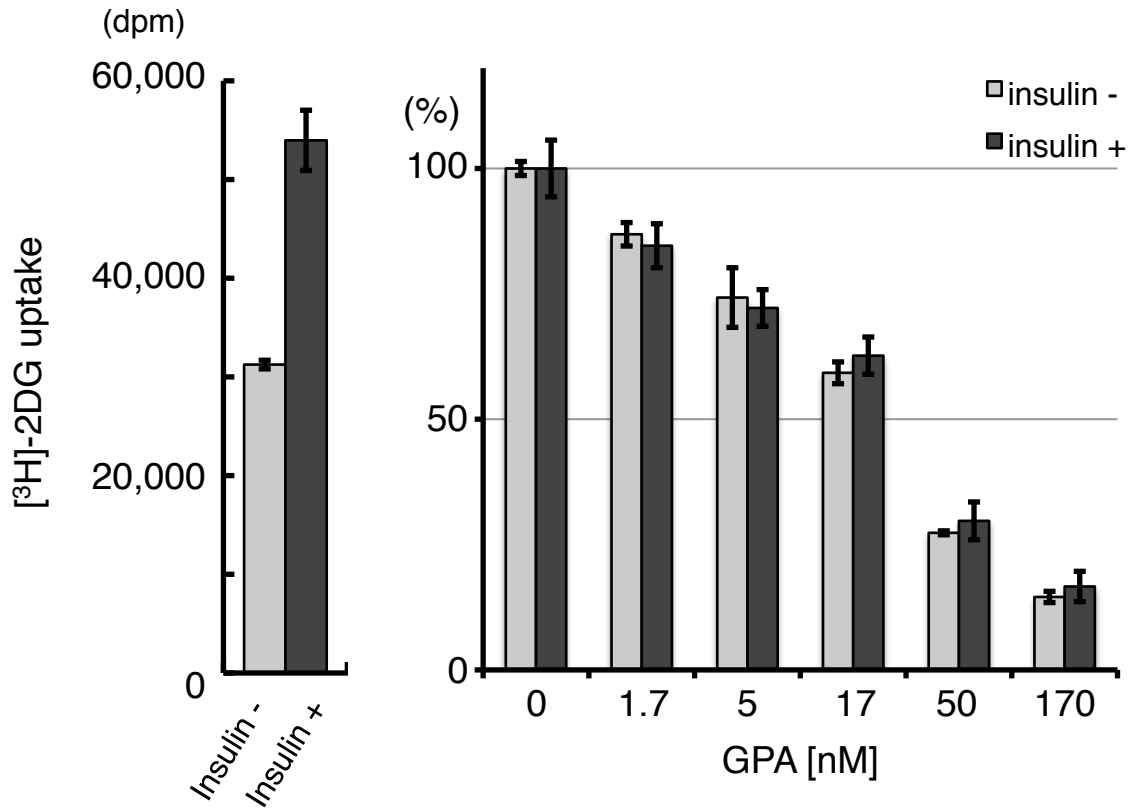

Figure 3-15 Inhibition of both GLUT1- and GLUT4-mediated glucose uptake by GPA.

It was examined whether GPA would also inhibit GLUT4-mediated glucose uptake. Swiss 3T3 were differentiated into adipocytes and treated with insulin to activate GLUT4-mediated glucose uptake. Uptake activity was increased around 2 fold, indicating that assay worked successfully. GPA inhibited both the 2DG uptake in non-stimulated (GLUT1) and insulin-stimulated cells (GLUT1&4). bars: SD (n = 3)

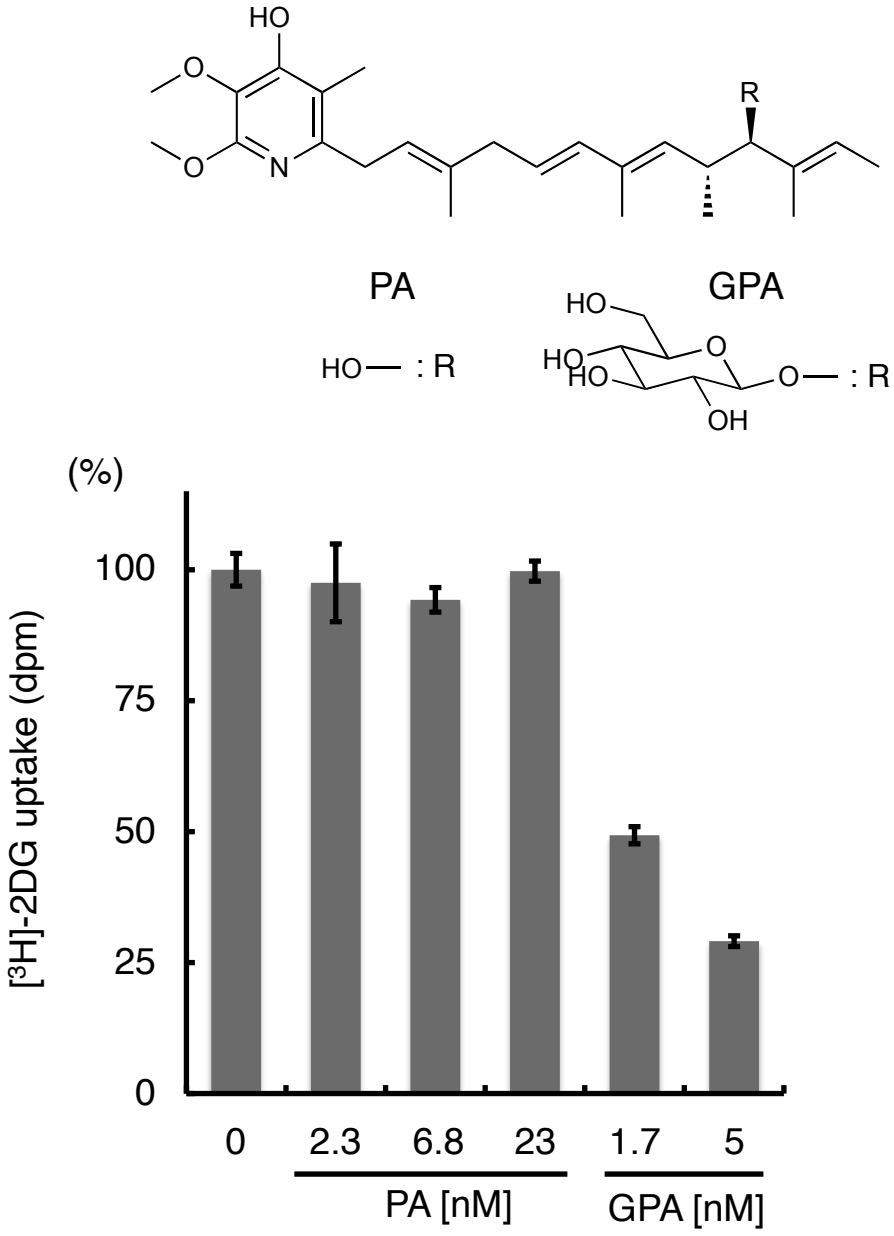

Figure 3-16 Importance of glucose-moiety in GPA structure.

As described in chapter 2, the structure of GPA was quite similar to PA except that glucose-moiety was connected in GPA. Glucose-null PA failed to inhibit the 2DG uptake as shown here, indicating the importance of glucose-moiety in GPA. This suggested that the glycolytic inhibition by GPA would be reasoned from mimicking GLUT1 substrate glucose by glucose-moiety in GPA.

3-3 Discussions

Target of GPA

Glucose transporters comprise a large family of transmembrane proteins characterized by having different affinities for glucose[76,77]. Among glucose transporters, GLUT1 has a high affinity for glucose, and is one of the most abundantly expressed transporters in many types of tumors[77]. Indeed, A431 cells used in this study have been reported to express only GLUT1 as glucose transporter. Although the evidence for direct binding between GPA and GLUT1 is the major issue, however even the present technology does not seem to provide it. Purified GLUT1 can be used for the Surface Plasmon Resonance to show the affinity between GPA and GLUT1, but purification of GLUT1 is not reported, perhaps due to the difficulty of membrane protein preparation in the recombinant expression systems such as *E. coli.* and alternatively *P. pastoris*[78]. Biotin-, flucorescent- or radio-labels of GPA may prove this in a method of direct approach for the target protein identification, however, there are no reports on the labeling GPA and GPA structure is unfortunately unstable. As one possible alternative on this issue, *in vitro* transport assay systems using *Xenopus* oocytes and proteoliposomes will be employed[79,80]. With the great help and critical suggestion from the Prof. Sato at Keio University, the author has challenged the latter since the former would demand too much effort of techniques in the mRNA microinjections. Although the basic liposome preparation and GLUT1 reconstitution into liposomes seemed successful, the glucose uptake function of GLUT1 could not be detected in liposomes, suggesting that the

functional structure of GLUT1 in the cell membrane is disrupted during preparation of the assay materials.

However, data accumulated in these decades suggests that there are only three likely mechanisms that could explain glucose uptake inhibition by GPA: (i) GPA mimics the GLUT1 substrate, (ii) inhibition of GLUT1 translocation into the cell membrane, and (iii) lowering the expression level of GLUT1. The author ruled out the last two possibilities by immunoblotting, as shown in **Fig. 3-13**. The data showing that the level of GLUT1 expression was not changed in the membrane fraction by GPA treatment suggests that uptake inhibition by GPA was not due to an inhibition of GLUT1 translocation or a reduction in GLUT1 expression. Moreover, GPA possesses the glucose moiety, and glucose-null derivative PA failed to inhibit the uptake (**Fig. 3-16**). Thus, it is likely that the glucose uptake inhibition by GPA would be due to its glucopyranoside moiety, perhaps by functioning as a glucose mimic to GLUT1. This suggests that GLUT1 would be the *bona fide* target of GPA due to GPA's inhibition of glycolysis in A431 cells.

As the known glucose transporter inhibitors to date, cytochalasin B and phloritin are reported to suppress glucose uptake at μM and mM concentrations, respectively[81]. GPA, on the other hand, inhibits glucose uptake in A431 cells, Swiss 3T3-L1 adipocytes, and GLUT1-overexpressed HEK293T cells at nM concentrations (**Figs. 3-13** to **3-15**). Thus, GPA is the first report of a GLUT inhibitor capable of suppressing glucose uptake at nM concentrations. The author believes that GPA could be widely applicable as the potent GLUT inhibitor in the other chemical biological study in expansion.

Mechanisms underlying the Synergistic Filopodia Inhibition by PA & GPA

An important question was raised by the results. How does the decrease in cellular ATP caused by the inhibition of glycolysis and mitochondrial respiration by GPA and PA co-treatment result in suppression of EGF-stimulated filopodia protrusions in A431 cells? The molecule Profilin may hold the key to this answer. Profilin has critical role for filopodia protrusion because it promotes polymerization of filamentous actin (F-actin) at the extending ends of filopodia[82]. Profilin binds to ADP-bound actin monomers, promotes exchange of ADP for ATP, and releases ATP-actin at the growing ends of F-actin, leading to polymerization of actin in a straight-lined form[68,82]. The profilin-mediated elongation of F-actin bundles pushes the cell membrane outward, resulting in the protrusion of spike-shaped filopodia. In this regard, ATP molecule is required for Profilin-mediated filopodia protrusion. Moreover, Molitoris *et al.* observed that ATP depletion resulted in punctate dispersion of F-actin from its straight-lined form[83], suggesting that stabilization of straight-lined F-actin depends on the level of ATP in the cell.

Therefore, one possible explanation for the inhibition of filopodia protrusion by GPA and PA co-treatment might be the lowering of intracellular ATP concentration caused by the blockage of glycolysis by GPA and mitochondrial respiration by PA.

Metabolome Analysis for the Chemical Biology

Aside from its influence on glycolysis, GPA treatment also leads to changes in the amounts of TCA cycle intermediates, as well as increases in levels of aspartate and

asparagine (see **Table 3-2**, **Figs. 3-5** and **3-7**). The author believes these changes may be caused in a part by GPA-limited entry of pyruvate into the citrate cycle, which might slow the rate at which oxaloacetate is converted to citrate. Slowing the conversion of oxaloacetate may lead to accumulation of preceding TCA cycle intermediates such as malate, fumarate, and succinate.

Reports suggest that active glutaminolysis takes place in the metabolome of tumor cells[84], described as anaplerotic ATP energy fueling through "truncated" TCA metabolism (from 2-oxoglurate to malate) without pyruvate entry[85,86]. In tumor glutaminolysis, highly incorporated glutamine is converted into glutamate and then into 2-oxoglutarate via aspartate transaminase, with production of aspartate as a byproduct[86]. Thus, the possibility should not be excluded that these changes in the amounts of TCA cycle intermediates and aspartate are caused by glutaminolysis in addition to GPA-suppressed pyruvate entry into the TCA cycle[87].

CE-MS metabolome analysis is a powerful technique that may help elucidate the targets of the chemical substances, in the case the substances impact glycolysis. Glutaminolytic analyses, and labeling studies using [^{13}C]-glutamine in combination with CE-TOFMS—analogous to the studies of GPA's effect on glycolytic pathways described here in this chapter—might clarify the target-unverified chemical substances that disturb glutaminolysis. Therefore chemical metabolomic analyses should be encouraged, not only because they may further understanding of the physiological and pathological effects of many natural products, but also because such studies may enhance development of compounds that may serve as a new class of anticancer drugs

which regulate the tumor metabolome.

Natural Product Screening

This study was based on the screening of crude natural products and bioassay-guided isolation of the components that inhibit filopodia protrusion. Recently, natural product screening has declined in popularity, probably because the isolation and structural determination steps are costly and time-consuming. However, the author strongly believes the use of this technique to isolate compounds acting synergistically to inhibit an important cellular process demonstrates that crude natural product screening is still a valuable technique. Since cellular responses are driven by many complex systems that are often robust due to the presence of rescue and feedback pathways, the best strategy for finding bioactive inhibitors of a particular cellular system may be global screening of crude extracts of natural products. In conclusion, though the approach in this study may be deemed “old-fashioned” and somewhat laborious, the author believes the results provided here have opened the broad avenue of natural products screening for the continued progress in chemical biological research.

3-4 Experimental procedures

General procedures

A431 cells were cultured as described in Chapter 2. HEK293T cells were cultured as same as A431 cells except that FBS was used in exchange of CS for serum. Swiss 3T3 preadipocytes were purchased from ATCC and cultured in CS 10% DMEM containing 4.5 mg ml^{-1} of glucose, 100 U of penicillin G and 100 μg ml^{-1} of streptomycin.

Chemical inhibitors

The chemical inhibitors used in the chemical genomic study contains the SCADS inhibitor kit I & II, a gift from the Screening Committee of Anticancer Drugs supported by Grant-in-Aid for Scientific Research on Priority Area "Cancer" from the Ministry of Education, Culture, Sports, Science and Technology, Japan (kit details can be found online at [http://gantoku-shien.jfcr.or.jp/kit.html]). Other inhibitors were purchased (Sigma, Wako and Calbiochem) or prepared from in-house collection.

Measurement of mitochondrial NADH oxidase activity

For the assay, crude mitochondria were prepared from bovine heart as described by Floridi *et al.*[73] with minor modifications. Small fragments of bovine heart in MSH buffer (210 mM mannitol, 70 mM sucrose, 1 mM EGTA, 1 mM DTT, 0.1% BSA and 10 mM Hepes, pH 7.4) were homogenized with a Dounce Tissue Grinder and centrifuged at 1,000 × g for 10 min. The supernatant was further centrifuged at 8,000 × g for 20 min.

The resulting pellet was homogenized in MSH buffer and centrifuged again. The crude mitochondria pellet was homogenized and stored at -80°C until used.

The mitochondrial NADH oxidase activity was spectrophotometrically determined from the absorption at 340 nm for NADH content as described with minor modification. 0.5 μg protein of bovine heart mitochondria (determined by Bradford method[88]) was added with the test compounds (pre-diluted with the reaction buffer to minimize the organic solvent concentrations at 1%) in 80 μl of the reaction buffer (10 mM phosphate, 250 mM sucrose, 0.5 mM EGTA, 10 mg ml^{-1} BSA, pH7.4) and was pre-incubated at 37°C for 10 min. Reaction was initiated by adding 20 μl of the substrate NADH solution (final 0.3 mM), left at 37°C for 30min and quenched by adding 70 μl of 0.1 N NaOH aq. To subtract the background absorption, the samples treated with NaOH aq. forehead to the addition of NADH solution were prepared.

ATP

Cellular ATP levels were determined using an ATP assay kit (Sigma) after cells had been treated with test compounds for 30 min. After the medium removal, cells were treated with DMSO, frozen completely in deep freezer and thawed for ATP determination. This solution was diluted 10-fold with Milli-Q and mixed with 10-dilution of purchased Luciferin-luciferase solution in kit. Optionally describing, DMSO can be substituted with ice-cold Milli-Q water, which is quite convenient because of no needs of the sample dilution. In this case, over at least 2 hours in deep freezer for freeze is required, and thawed solution should be immediately mixed with

Luciferin-luciferase solution.

Metabolome analysis – sample preparation

Cells grown in 100-mm dishes were incubated in DMEM containing 0.2% CS for 18 h, and then treated with test compounds for 30 min. After washing cells twice with ice-cold 5% mannitol, metabolites were extracted by keeping cells resting on ice for 10 min in 1 ml of ice-cold methanol containing internal standards (25 mM each of 3-aminopyrrolidine [Aldrich], L-methionine sulfone [Wako], trimesate [Wako], and MES [Wako]). Extracts were then transferred to a separate tube and mixed with 500 μl of milli-Q water, and 600 μl of this solution was transferred into another tube, mixed with 400 μl of chloroform, and centrifuged. A 300 μl aliquot of the aqueous layer was centrifugally filtered through a 5 kDa-cutoff membrane (Millipore) to remove proteins from samples. The filtrate was lyophilized, dissolved in 50 μl of milli-Q water, and subjected to CE-TOFMS analysis as described below.

For the [^{13}C]-isotope labeling study, culture media was changed to glucose-depleted DMEM after 18 h incubation in DMEM with 0.2% CS, and cells were treated with 1 mg ml^{-1} of [1,2,3,4,5,6-^{13}C]-glucose (Isotec) immediately after the test compounds addition. Metabolites were extracted after 30 min. For the clear measurement of glucose-6-phosphate, fructose-6-phosphate and glucose-1-phosphate, LC-MS systems were alternatively used.

Metabolome analysis – CE-MS systems conditions

Metabolomic analysis was performed by using an Agilent CE-TOFMS system (Agilent).

CE-TOFMS Conditions for Cationic Metabolite Analysis

Separations were carried out in a fused silica capillary (i.d. 50 μm × 100 cm) filled with 1 M formic acid as the electrolyte. Approximately 3 nl of sample solution were injected at 50 mbar for 15 s, and 30 kV of voltage was applied. The capillary temperature was 20°C. Methanol-water (50% v/v) containing 0.1 μM reserpine was delivered as the sheath liquid at 10 μl min^{-1}. ESI-TOFMS was operated in the positive ion mode, and the capillary voltage was set at 4,000 V. A flow rate of heated dry nitrogen gas (heater temperature, 300°C) was maintained at 5 psig. In TOFMS, the fragmentor, skimmer, and Oct RFV voltage were set at 130, 75, and 175 V, respectively. Automatic recalibration of each acquired spectrum was performed using reference masses of reference standards. The methanol adduct ion ($[2MeOH + H]^+$, m/z 65.0597) and reserpine ($[M + H]^+$, m/z 609.2806) provided the lock mass for exact mass measurements.

CE-TOFMS Conditions for Anionic Metabolite Analysis

A cationic polymer-coated SMILE (+) capillary (Nacalai Tesque, Kyoto, Japan) was used as the separation capillary. A 50 mM ammonium acetate solution (pH 8.5) was used as electrolyte for HPCE. The sample in 30 nl was injected at 50 mbar for 90 s, and 30 kV of voltage was applied. Ammonium acetate (5 mM) in 50% methanol-water (v/v) with 1 μM reserpine was delivered as the sheath liquid at 10 μl min^{-1}. ESI-TOFMS was

conducted in the negative ion mode; the capillary voltage was set at 3,500 V. A flow rate of heated N_2 gas was maintained at 7 psig. For TOFMS, the fragmentor, skimmer, and Oct RFV voltage were set at 105 V, 50 V, and 200 V, respectively. Automatic recalibration of the spectrum was performed using reference masses of standards: i.e., $2CH_3COOH$ ($[M - H]^{-1}$, m/z 119.0350) and reserpine ($[M - H]^{-1}$, m/z 607.2661). Other conditions were identical to those used in cationic metabolite analysis. For the [^{13}C]-isotope labeling study, 0.1 μM of hexakis phosphazene-containing 50% MeOH was delivered as sheath liquid at 10 μl min^{-1}, and automatic recalibration of MS spectra in TOFMS was obtained from the reference: i.e. [^{13}C]-$2CH_3COOH$ (m/z 120.0383) and hexakis-(2,2,-difluorothoxy)-phosphazene + CH_3COOH (m/z 680.0355). Other conditions were identical to the normal anionic analysis.

CE-MSD Conditions for Nucleotides Analysis

Separations were carried out in a fused silica capillary (i.d. 50 μm × 100 cm) with 50 mM ammonium acetate pH 7.5 as the electrolyte. Approximately 30 nl of sample solution were injected at 50 mbar for 30 s, and 30 kV of voltage was applied. The capillary was at 20°C. Sheath liquid was 5 mM ammonium acetate in 50% MeOH at 10 μl min^{-1}. MSD was operated in the negative ion mode, and the capillary voltage was set at 3,500 V. A flow rate of N_2 gas at 300°C was maintained at 10 psig. The fragmentor voltage in MS was at 100 V.

***In vitro* hexokinase assay**

Hexokinase is very active when the enzyme is bound to mitochondria[89,90]; therefore,

hexokinase was isolated from crude mitochondria. The preparation of crude mitochondria was as same as described in the measurement of mitochondrial NADH oxidase above[73].

For the measurement of hexokinase activity, G6PDH (Sigma) was used to generate NADPH from the product of the hexokinase reaction. Hexokinase activity was spectrophotometrically determined from the absorbance of NADPH at 340 nm according to the described method[72]. The reaction mixture contained 30 μg of bovine heart mitochondria, 1 mM ATP, 0.5 mM $NADP^+$, 2 μM rotenone (Calbiochem), 3 μg ml^{-1} oligomycins (Calbiochem), and 0.1 units of G6PDH in 100 μl of PT buffer (10 mM MOPS, 200 mM sucrose, 5 mM succinate, 1 mM P*i*, and 0.01 mM EGTA, pH 7.4). The reaction was initiated by addition of 0.2 mM glucose at room temperature after a 10-min pre-incubation period. The level of NADPH was continuously recorded for 20 min.

Uptake of [^{3}H]-2-deoxyglucose

Serum-starved A431 cells in DMEM containing 1.2 mM glucose were treated with test compounds along with 0.5 μCi of [1,2-^{3}H]-2-deoxy-D-glucose ([^{3}H]-2DG, specific activity 50-60 Ci $mmol^{-1}$, ARC) for 30 min, washed twice with ice-cold PBS, and lysed with 0.5 N NaOH aq. Cell lysate radioactivity was measured on a liquid scintillation counter.

Swiss 3T3-L1 pre-adipocytes were differentiated into adipocytes as described[75]. Adipocytes were pretreated with or without insulin (100 nM, Sigma) for 15 min for

GLUT4 translocation, and then treated with test compounds and [^{3}H]-2DG for 5 min for the glucose uptake study. Other conditions were the same as described above.

To test GPA-sensitivity to GLUT1 overexpression, HEK293T cells were transfected with glut1 (derived from A431 cells) using Lipofectamine. In the uptake study, an HEK293T cell suspension was used because the cells are easily detached from the culture plates and it was quite difficult to wash cells immediately to terminate the uptake reaction. After 36 h from transfection, cells were left in PBS containing 1 mM EDTA for the gentle detachment. A suspension of 2.0×10^5 cells in 200 μl of glucose-free DMEM in a tube was treated with test compounds and [^{3}H]-2DG in a 25°C water bath for 5 min. Glucose uptake was terminated by the addition of ice-cold high glucose solution (final 25 mM), followed by centrifugation at 1,000 × g at 4°C for 5 min. Cell pellets were washed once with ice-cold high glucose solution and lysed with 0.1 N NaOH aq. [^{3}H]-2DG uptake under this condition linearly increased for at least 30 min.

glut1 plasmid

The complete coding region of GLUT1 was amplified by PCR with the cDNA template in A431 cells and ligated in-frame into pcDNA 3, which was verified by DNA-sequencing. Functional expression in HEK293T cells after transfection was confirmed by its expression in membrane and uptake study.

Preparation of membrane fraction and western blot

Plasma-membranous GLUT1 expression levels in A431 cells were determined by

Western blot after membrane fractionation according to the method previously described with modifications. A431 cells, sparsely seeded in 100-mm dishes and incubated in CS 0.2% DMEM for 12 h, were treated with GPA (0-500 nM) for 30 min. Cells were harvested by scraping and collected by centrifugation. Cell pellets were washed once with fractionation buffer (20 mM Tris-HCl, pH 7.5, 1 mM EDTA), resuspended in the same buffer and kept on ice for 30 min. Then pellets were passed 30 times through a syringe needle (gauge 25, Terumo) and centrifuged at 1,000 × g at 4°C for 10 min. The supernatant was further centrifuged at 16,000 × g at 4°C for 30 min to collect the plasma membrane pellet. Pellets were lysed in membrane-solubilization buffer (40 mM Hepes-NaOH, pH 7.5, 300 mM NaCl, 1 mM EDTA, 1% TX-100, 1% NP-40), and the sample protein concentration was normalized according to the Bradford method[88]. Then 3 × SDS buffer (150 mM Tris-HCl, pH 6.8, 30% glycerol, 3% SDS, 0.003% bromophenol blue) and 0.5 mM 2-mercaptoethanol were added and samples were kept on ice for 10 min as described in ref. 91. Proteins were separated by SDS-PAGE, transferred to nitrocellulose membrane, probed by anti-Glut1 (polyclonal, Millipore) and Rap1 (polyclonal, Santa Cruz), and detected by enhanced chemiluminescence (Millipore). To check this fractionation, both enriched tubulin (cytosol marker) in the supernatant of the final centrifugation, and Rap1 (membrane marker) in pellets were confirmed. The same procedure was also done to check the functional expression of A431-derived glut1 by transfection in the membrane fraction in HEK293T cells.

Chapter 4

Application of the Filopodia Protrusion Assay as a New Convenient Cell-based Screening Method for Small Molecule Glycolytic Inhibitors

4-1 Introduction

It is widely recognized that solid tumors exposed to hypoxia can survive and grow aggressively despite low oxygen and limited nutrition. Active glycolysis, as well known as the Warburg effect, plays an important role as a lifeline for tumor survival and growth under these conditions by fueling cancer cells with ATP energy and also supplying bioorganic components, such as nucleotides and fatty acids for growth[84,92]; therefore, glycolysis inhibitors are expected to be candidate drugs for tumor treatment, and thus screening research of these inhibitors has potential for cancer therapy. Many glycolytic inhibitors have been found as the inhibitors of key glycolytic enzymes *in vitro*[93-95], but it is not easy to evaluate whether these glycolytic enzyme inhibitors actually modulate glycolysis in living cells; therefore, the establishment of a new cell-based screening system is required for the discovery of small, cell-permeable molecules that induce glycolysis inhibition in living cells.

In the previous chapter, the author revealed that glucopiericidin A inhibited the glycolysis and showed the synergistic filopodia inhibition in the co-treatment with the mitochondrial respiratory inhibitor. Based on this finding, it is suggested that the filopodia protrusion assay can be applied as the cell-based screening method for the small molecule glycolytic inhibitors.

To find a new glycolytic inhibitor, here in this chapter, the author describes another screening study for a cell membrane-permeable glycolytic inhibitor and simply examined whether the screening hit is able to inhibit the glycolysis.

4-2 Results and discussions

A potential glycolytic inhibitor would inhibit filopodium protrusion only by co-treatment with a mitochondrial respiratory inhibitor according to the results in Chapter 3. Indeed, 2-deoxy-D-glucose (2DG), an inhibitor of glycolytic enzyme hexokinase, inhibited EGF-induced filopodium protrusion only in the presence of rotenone (**Fig. 4-1**), indicating that this assay system works successfully. As the screening source, we used a chemical library composed of 1,069 compounds, mainly cyclohexanepolyols and derivatives thereof. These compounds belong to carbocyclic analogue of hexopyranoses and called carbasugars, one of the members of pseudo-sugars. Carbasugar library was originally prepared in the studies on development of bioactive substances, such as antibacterial and anticancer compounds, sweetener, and enzyme inhibitors by Dr Ogawa et al. Structural features of carbasugars possibly mimic those of glucose or the glycolytic metabolite, and thus would be an attractive screening source for glycolytic inhibitors.

In the first screening run, 10 μg ml^{-1} of compounds (in DMSO) were tested. Hit candidates in the first run were tested again at various concentrations. As a result, we found 2 compounds (sample #**169** [1,4,5,6-tetra-*O*-acetyl-2-*O*-mesyl-3-*O*-benzoyl-*myo*--inositol][96] and sample #**288** [1,2,4,5-tetra-*O*-acetyl-3,6-di-*O*-tosyl-*muco*-inositol][97]) as glycolytic inhibitors that showed filopodium inhibition only in the presence of the mitochondrial respiratory inhibitor rotenone (**Fig. 4-1**). Next we tested whether they indeed suppressed glycolysis. It was described that glycolytic limitation caused a

marked ATP decrease in tumor cells when mitochondria respiration was inhibited[83]. As shown in **Fig. 4-2**, the above candidate glycolytic inhibitors slightly decreased cellular ATP in the absence of the mitochondria respiratory inhibitor. However, in combination with the mitochondria respiratory inhibitor, they indeed decreased intracellular ATP levels in a dose-dependent manner, indicating that they inhibited glycolysis.

To investigate further how they inhibit glycolysis, we examined their effects on the 3 steps of glycolysis, glucose uptake, hexokinase and pyruvate kinase. It was reported that these steps play important roles in accelerated glycolysis in tumor metabolism and a higher expression level of the proteins facilitating these steps is frequently observed[90,93,98,99]. Both #**169** and #**288** did not affect hexokinase and pyruvate kinase reactions up to 30 μg ml^{-1} (**Fig. 4-3**); however, they inhibited the glucose uptake step dose-dependently with IC_{50} values of 4.5 μg ml^{-1} for #**169** and 2.7 μg ml^{-1} for #**288** (**Fig. 4-4**), respectively. Their inhibition of glucose uptake was quite similar to that of decreasing intracellular ATP levels in the presence of rotenone, shown in **Fig. 4-2**, suggesting that both #**169** and #**288** suppressed glycolysis by inhibiting cellular glucose uptake.

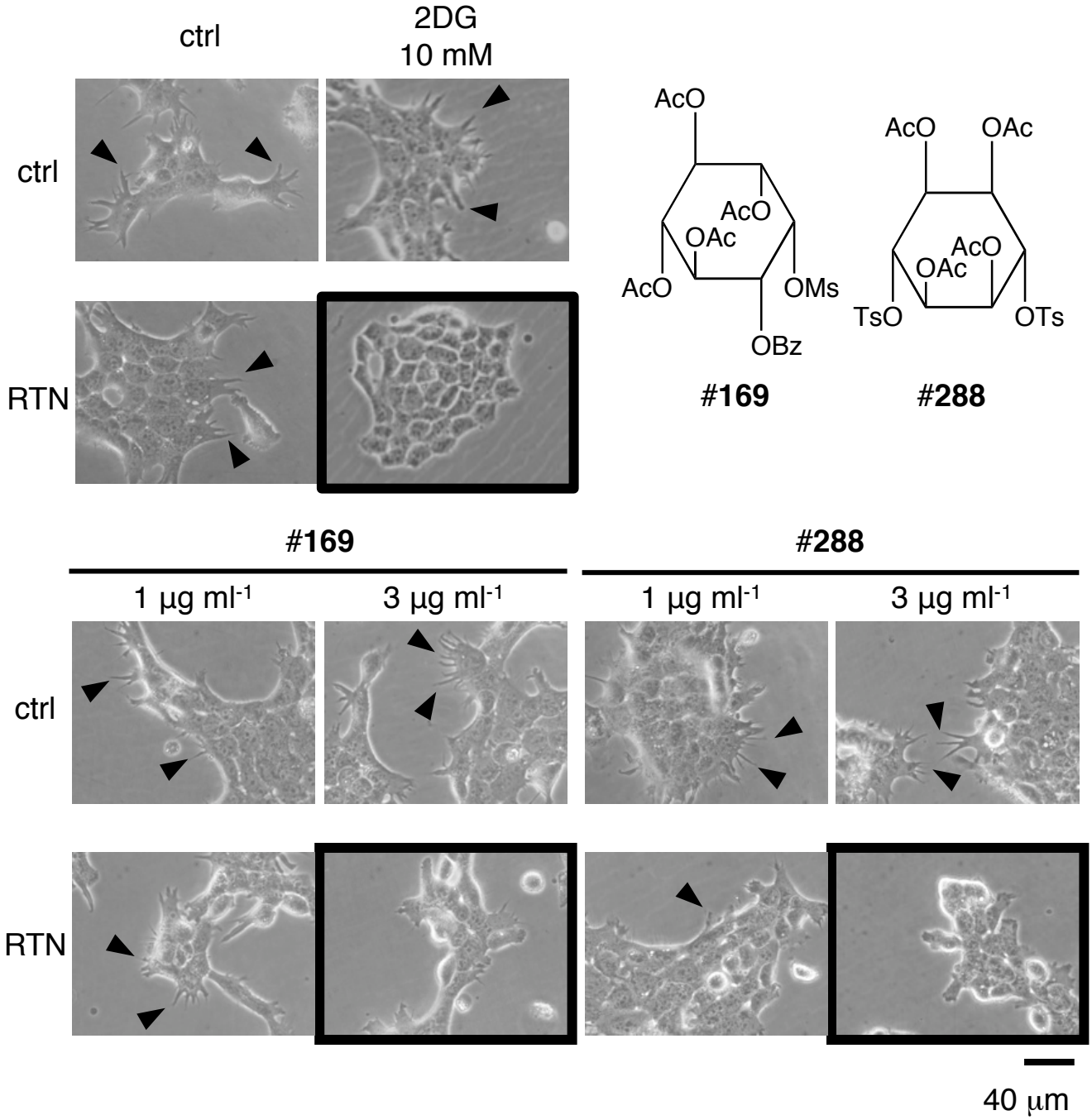

Figure 4-1 Screening results for glycolytic inhibitor

Samples from the pseudo-sugar library were originally prepared and re-crystallized for storage by Dr. Ogawa et al. Two compounds #**169** and #**288** from the library showed the filopodia inhibition only in the presence of mitochondrial respiratory inhibitor. Hexokinase inhibitor 2-deoxy-D-glucose (2DG, 10 mM) as a positive control and rotenone (RTN, 300 nM) to inhibit mitochondrial respiration were used. Arrowhead indicates filopodia and framed photos showed filopodium inhibition. Data represent two independent experiments. Sample purity was confirmed by LC-MS.

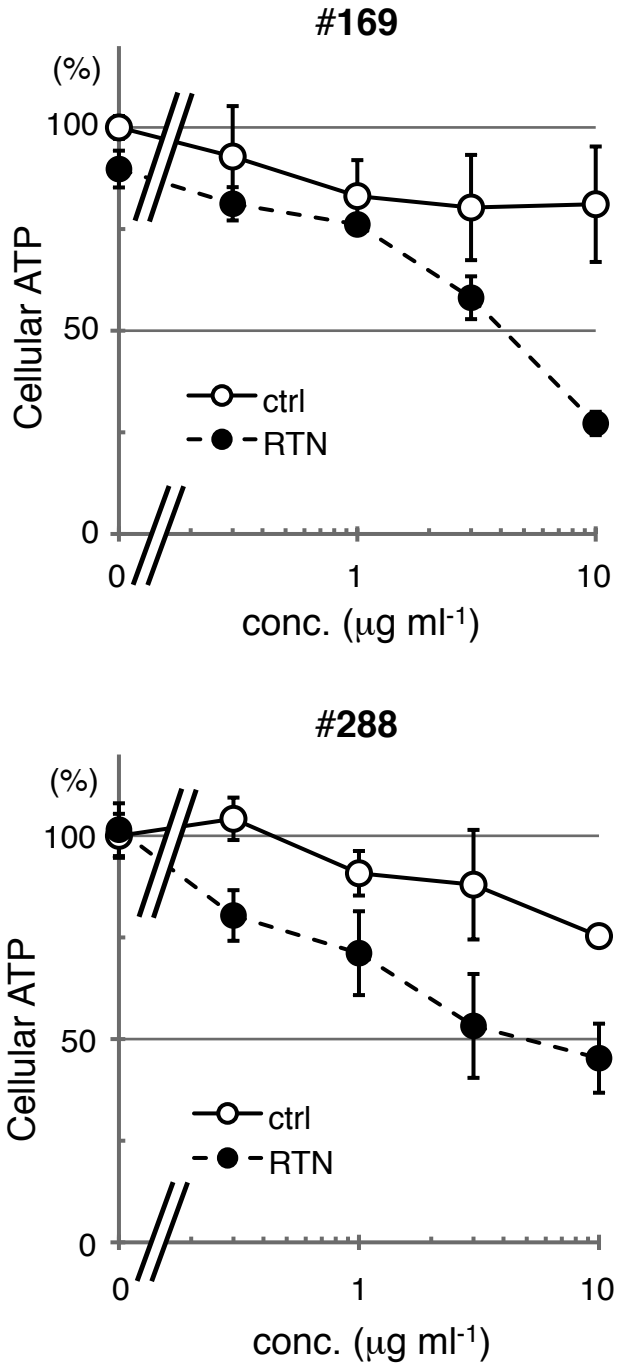

Figure 4-2 Decrease in cellular ATP level by #**169** and #**288** in the presence of mitochondrial respiratory inhibitor.

Cellular ATP level were determined to examine whether #**169** & #**288** indeed suppressed glycolysis in cells. bars: SD (n = 3). RTN: rotenone 300 nM.

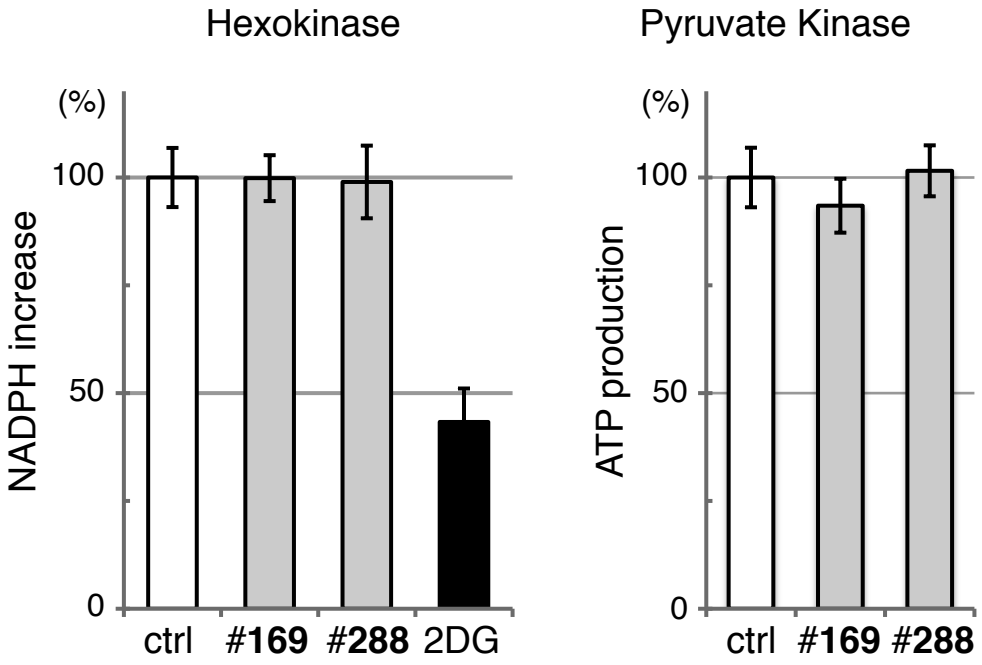

Figure 4-3 No effect of #**169** & #**288** on both Hexokinase and Pyruvate Kinase rate-limiting enzymes activity *in vitro*.

in vitro Hexokinase and Pyruvate Kinase assay were established to examined the effect of #**169** and #**288** on the activity of rate-limiting enzyme in glycolysis. bars: SD (n = 3). #**169** 30 μg ml^{-1}, #**288** 30 μg ml^{-1}.

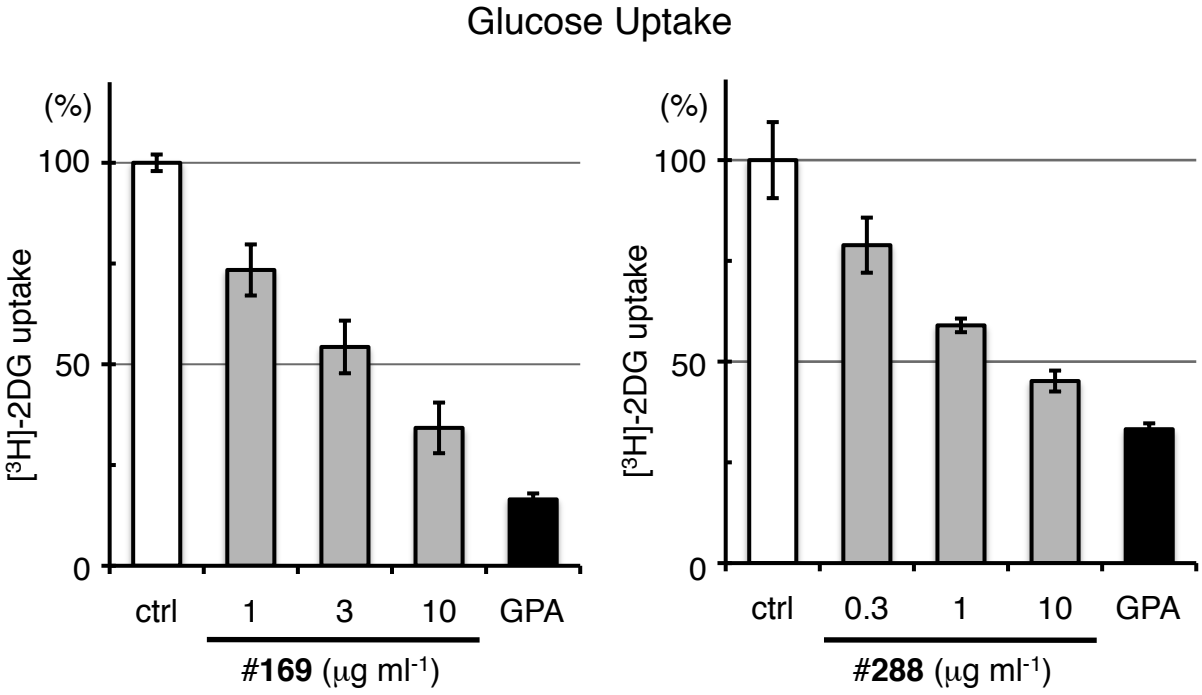

Figure 4-4 Inhibition of glucose uptake by #**169** and #**288**.

Both #**169** and #**288** inhibited the uptake of the 2-deoxy-D-glucose (2DG) in a dose dependent manner. bars: SD (n = 3). IC_{50} values 4.5 μg ml^{-1} (#**169**) and 2.7 μg ml^{-1} (#**288**) were calculated .

4-3 Experimental procedures

Cell culture, filopodia protrusion assay and cellular ATP determination

The same procedures were applied as described in Chapter 2 and 3.

Pyruvate Kinase assay

Purified recombinant human pyruvate kinase 1 was prepared for the assay enzyme. The complete human pyruvate kinase 1 from HeLa cDNA was cloned into *E. coli* expression vector pRSETc. The cell lysate of *E. coli.* transformant was mixed with MagneHis^{TM} Ni-Particles (Promega), from which recombinant 6 x His-Pyruvate kinase was purified by elution with histidine solution. Elute was dialyzed over night and frozen for storage until use. The purity was checked by SDS-PAGE and Coomassie brilliant blue staining, and protein concentration was determined by Bradford method.

The pyruvate kinase produces ATP and pyruvate molecules from the substrate ADP and PEP (phosphoenolpyruvate). In addition the enzyme was activated by F1,6P (fructose 1,6-phosphate). The assay method was as follows; the reaction in the buffer (3 μM ADP and 0.3 μM F1,6P for substrate in PK buffer containing 5 mM $MgCl_2$, 0.1 mg ml^{-1} BSA, 2 mM DTT, 1 mM EDTA, 50 mM KCl, 50 mM Tris [pH7.7]) initiated by addition of 10 μM PEP was carried out at 37°C for 30 min. The reaction was quenched by TCA and neutralized. Enzymatic activity was calculated from ATP production determined by luciferin-luciferase reaction (Sigma). For the test of the inhibitory activity of the compounds, the compounds in the organic solvent (DMSO, MeOH or

EtOH) were first diluted with PK buffer and then mixed in the reaction, so that the final concentration of organic solvent was less than 1%, which cause no effect to the enzyme activity.

Chapter 5

Conclusion

Because of easy-to-use and rapid control over the target protein function, chemical inhibitors are widely applicable for the functional analysis of the proteins in the post genome era. Many chemical inhibitors available, however, are still fewer than the number of the proteins. Thus, the development of new inhibitors contributes to the expansion of the study on the proteins functions. To develop the new chemical inhibitors, two hurdles exist: finding the bioactive compounds and identifying their target proteins. The author challenged these two issues for the development of new chemical inhibitors throughout this thesis.

Chapter 2 described the finding the bioactive compounds from the natural product screening in the cell-based assay. By focusing the filopodia protrusion, the author found one cultured broth of *Lechevalieria* sp. strain that showed the potent filopodia inhibition among over 3,000 screening samples. However, this inhibition disappeared following silica-gel chromatography. Interestingly, the inhibitory activity was almost completely recovered by re-mixing all of the silica-gel chromatography fractions, suggesting that the inhibition required the synergistic effect of two or more compounds contained within the microbial broth that eluted in different fractions. Isolating compounds such as these, which exhibit bioactive properties only when interacting synergistically with other compounds, is technically challenging. However, the author undertook this challenge and isolated the components responsible for inhibition of filopodia protrusion, glucopiericidin A (GPA) and piericidin A (PA). Thus, the author herein found the bioactive compounds and cleared the first hurdle of the development of new chemical inhibitors for the chemical biological study.

In Chapter 3, the author described how GPA & PA combination synergistically inhibited the filopodia, mainly focusing on to the target identification of GPA. The issue directly connects to the second hurdle for the development of the new chemical inhibitor for chemical biology. PA is known as an inhibitor against mitochondrial respiratory chain complex I, and this inhibition would be the cause of synergistic filopodia inhibition by PA since other mitochondrial respiratory inhibitors showed the activity similarly. However, although GPA is structurally related to PA, there are no reports on its target proteins, and GPA showed quite weak inhibition against the same target of PA. This weak inhibition of mitochondrial respiration could not explain the GPA activity on the synergistic filopodia inhibition with PA. For this reason, the author focused on identifying the cellular target protein of GPA. Chemical genomic screening suggested that GPA might affect glycolysis. CE-MS metabolomic analysis showed that GPA does impact glycolysis. Furthermore, metabolomic analyses using [^{13}C]-glucose identified the glucose transporter as the target molecule of GPA. The approach of CE-MS metabolomic identification of GPA's target is the first report to demonstrate the utility of the metabolomic approach to identify the molecular target of a natural product. Afterwards, the author discussed that the synergistic cellular ATP decrease by the simultaneous inhibition of both glycolysis and mitochondrial respiration by GPA and PA, respectively, would cause the synergistic filopodia inhibition. Herein the author cleared the second issue against the development of the new chemical inhibitor and provided the information that GPA is a GLUT inhibitor.

In Chapter 4, the author applied the filopodia protrusion assay as the screening

method for new glycolytic inhibitors, based on the finding of Chapter 2 & 3. By screening the compounds that showed the filopodia inhibition synergistically with the mitochondrial respiratory inhibitor, two new glycolytic inhibitors were found from the chemical synthetic library that was kindly provided from Dr. Ogawa Seiichiro, the emeritus professor at Keio University. The library is mainly composed of cyclohexanepolyols and derivatives thereof that belong to carbocyclic analogue of hexopyranoses and called carbasugars, one of the members of pseudo-sugars. Structural features of carbasugars possibly mimic those of glucose or the glycolytic metabolite, and thus would be an attractive screening source for glycolytic inhibitors. This is not developed on the purpose of this thesis but the kind gift. By the screening study and the further investigation, the author demonstrated the compounds #169 and #288 as the new glycolytic inhibitors, perhaps acting at the step of glucose uptake as similarly to previously found GPA.

As summarized, the findings in this thesis are listed below.

(1) Co-treatment with PA & GPA caused the synergistic filopodia inhibition in A431 cells.

(2) GPA was a glucose transporter inhibitor. GPA is structurally related to PA but its target was different from that of PA.

(3) Metabolomic approach would be worthwhile for the target protein identification of the bioactive compounds, in the case they could impact the metabolisms.

(4) The compounds #169 (1,4,5,6-tetra-*O*-acetyl-2-*O*-mesyl-3-*O*-benzoyl-*myo*--inositol) and #288 (1,2,4,5-tetra-*O*-acetyl-3,6-di-*O*-tosyl-*muco*-inositol) were the

glycolytic inhibitors, probably targeting the glucose uptake step in glycolysis.

(5) The application of the filopodia protrusion assay as the convenient cell-based method for the cell-membrane permeable, small molecule glycolytic inhibitors

In the end, the study of chemical biology would contribute to the understanding the various cellular events and may help towards the discovery of the treatment for the people suffered from diseases. The author hopes if his challenges to develop the chemical inhibitor may help it.

References

1. Pandey, A. & Mann, M. Proteomics to study genes and genomes. *Nature* **405**, 837-846 (2000).
2. Yanagida, M. Functional proteomics; current achievements. *J Chromatogr B Analyt Technol Biomed Life Sci* **771**, 89-106 (2002).
3. Saghatelian, A. & Cravatt, B.F. Assignment of protein function in the postgenomic era. *Nat Chem Biol* **1**, 130-142 (2005).
4. Chanda, S.K. & Caldwell, J.S. Fulfilling the promise: drug discovery in the post-genomic era. *Drug Discov Today* **8**, 168-174 (2003).
5. Alaimo, P.J., Shogren-Knaak, M.A. & Shokat, K.M. Chemical genetic approaches for the elucidation of signaling pathways. *Curr Opin Chem Biol* **5**, 360-367 (2001).
6. Zheng, X.F.S. & Chan, T.-F. Chemical genomics in the global study of protein functions. *Drug Discov Today* **7**, 197-205 (2002).
7. Protein Targeting with Small Molecules, Osada, H.ed. (A John Wiley & Sons, Inc., 2009).
8. Schreiber, S.L. Immunophilin-sensitive protein phosphatase action in cell signaling pathways. *Cell* **70**, 365-368 (1992).
9. Schreiber, S.L. & Crabtree, G.R. The mechanism of action of cyclosporin A and FK506. *Immunol Today* **13**, 136-142 (1992).
10. Schreiber, S.L. Chemistry and biology of the immunophilins and their immunosuppressive ligands. *Science* **251**, 283-287 (1991).
11. Liu, J. *et al.* Calcineurin is a common target of cyclophilin-cyclosporin A and FKBP-FK506 complexes. *Cell* **66**, 807-815 (1991).
12. Clipstone, N.A. & Crabtree, G.R. Identification of calcineurin as a key signalling enzyme in T-lymphocyte activation. *Nature* **357**, 695-697 (1992).
13. Fenteany, G. *et al.* Inhibition of proteasome activities and subunit-specific amino-terminal threonine modification by lactacystin. *Science* **268**, 726-731 (1995).
14. Jensen, T.J. *et al.* Multiple proteolytic systems, including the proteasome, contribute to CFTR processing. *Cell* **83**, 129-135 (1995).
15. Lee, D.H. & Goldberg, A.L. Proteasome inhibitors: valuable new tools for cell biologists. *Trends Cell Biol* **8**, 397-403 (1998).
16. Schreiber, S.L. Chemical genetics resulting from a passion for synthetic organic chemistry. *Bioorg Med Chem* **6**, 1127-1152 (1998).

17. Osada, H. Introduction of new tools for chemical biology research on microbial metabolites. *Biosci Biotechnol Biochem* **74**, 1135-1140.
18. Wagner, B.K. & Clemons, P.A. Connecting synthetic chemistry decisions to cell and genome biology using small-molecule phenotypic profiling. *Curr Opin Chem Biol* **13**, 539-548 (2009).
19. Koehn, F.E. & Carter, G.T. The evolving role of natural products in drug discovery. *Nat Rev Drug Discov* **4**, 206-220 (2005).
20. Newman, D.J. & Cragg, G.M. Natural products as sources of new drugs over the last 25 years. *J Nat Prod* **70**, 461-477 (2007).
21. Kino, T. *et al.* FK-506, a novel immunosuppressant isolated from a Streptomyces. I. Fermentation, isolation, and physico-chemical and biological characteristics. *J Antibiot (Tokyo)* **40**, 1249-1255 (1987).
22. Omura, S. *et al.* Lactacystin, a novel microbial metabolite, induces neuritogenesis of neuroblastoma cells. *J Antibiot (Tokyo)* **44**, 113-116 (1991).
23. DeBoer, C., Meulman, P.A., Wnuk, R.J. & Peterson, D.H. Geldanamycin, a new antibiotic. *J Antibiot (Tokyo)* **23**, 442-447 (1970).
24. Luesch, H. *et al.* A functional genomics approach to the mode of action of apratoxin A. *Nat Chem Biol* **2**, 158-167 (2006).
25. Sin, N. *et al.* The anti-angiogenic agent fumagillin covalently binds and inhibits the methionine aminopeptidase, MetAP-2. *Proc Natl Acad Sci U S A* **94**, 6099-6103 (1997).
26. Shang, S. & Tan, D.S. Advancing chemistry and biology through diversity-oriented synthesis of natural product-like libraries. *Curr Opin Chem Biol* **9**, 248-258 (2005).
27. Eguchi, M., Nguyen, C., Lee, S.C. & Kahn, M. ICG-001, a novel small molecule regulator of TCF/beta-catenin transcription. *Med Chem* **1**, 467-472 (2005).
28. Zhu, S., Mc Henry, K.T., Lane, W.S. & Fenteany, G. A chemical inhibitor reveals the role of Raf kinase inhibitor protein in cell migration. *Chem Biol* **12**, 981-991 (2005).
29. Kawatani, M. *et al.* The identification of an osteoclastogenesis inhibitor through the inhibition of glyoxalase I. *Proc Natl Acad Sci U S A* **105**, 11691-11696 (2008).
30. Zenitani, S. *et al.* Gerfelin, a novel inhibitor of geranylgeranyl diphosphate synthase from Beauveria felina QN22047. I. Taxonomy, fermentation, isolation, and biological activities. *J Antibiot (Tokyo)* **56**, 617-621 (2003).
31. Faix, J. & Rottner, K. The making of filopodia. *Curr Opin Cell Biol* **18**, 18-25 (2006).
32. Mattila, P.K. & Lappalainen, P. Filopodia: molecular architecture and cellular functions. *Nat Rev Mol Cell Biol* **9**, 446-454 (2008).

33. Dent, E.W. *et al.* Filopodia are required for cortical neurite initiation. *Nat Cell Biol* **9**, 1347-1359 (2007).
34. Geraldo, S. *et al.* Targeting of the F-actin-binding protein drebrin by the microtubule plus-tip protein EB3 is required for neuritogenesis. *Nat Cell Biol* **10**, 1181-1189 (2008).
35. Schaefer, A.W., Kabir, N. & Forscher, P. Filopodia and actin arcs guide the assembly and transport of two populations of microtubules with unique dynamic parameters in neuronal growth cones. *J Cell Biol* **158**, 139-152 (2002).
36. Geraldo, S. & Gordon-Weeks, P.R. Cytoskeletal dynamics in growth-cone steering. *J Cell Sci* **122**, 3595-3604 (2009).
37. Lidke, D.S. *et al.* Reaching out for signals: filopodia sense EGF and respond by directed retrograde transport of activated receptors. *J Cell Biol* **170**, 619-626 (2005).
38. Ruan, G., Agrawal, A., Marcus, A.I. & Nie, S. Imaging and tracking of tat peptide-conjugated quantum dots in living cells: new insights into nanoparticle uptake, intracellular transport, and vesicle shedding. *J Am Chem Soc* **129**, 14759-14766 (2007).
39. Smith, J.L., Lidke, D.S. & Ozbun, M.A. Virus activated filopodia promote human papillomavirus type 31 uptake from the extracellular matrix. *Virology* **381**, 16-21 (2008).
40. Zamudio-Meza, H., Castillo-Alvarez, A., Gonzalez-Bonilla, C. & Meza, I. Cross-talk between Rac1 and Cdc42 GTPases regulates formation of filopodia required for dengue virus type-2 entry into HMEC-1 cells. *J Gen Virol* **90**, 2902-2911 (2009).
41. Ng, L.G. *et al.* Migratory dermal dendritic cells act as rapid sensors of protozoan parasites. *PLoS Pathog* **4**, e1000222 (2008).
42. Neumann, A.K., Thompson, N.L. & Jacobson, K. Distribution and lateral mobility of DC-SIGN on immature dendritic cells--implications for pathogen uptake. *J Cell Sci* **121**, 634-643 (2008).
43. Jacinto, A. *et al.* Dynamic actin-based epithelial adhesion and cell matching during Drosophila dorsal closure. *Curr Biol* **10**, 1420-1426 (2000).
44. Millard, T.H. & Martin, P. Dynamic analysis of filopodial interactions during the zippering phase of Drosophila dorsal closure. *Development* **135**, 621-626 (2008).
45. Bacon, C., Lakics, V., Machesky, L. & Rumsby, M. N-WASP regulates extension of filopodia and processes by oligodendrocyte progenitors, oligodendrocytes, and Schwann cells-implications for axon ensheathment at myelination. *Glia* **55**, 844-858 (2007).
46. Shulman, Z. *et al.* Lymphocyte crawling and transendothelial migration require chemokine triggering of high-affinity LFA-1 integrin. *Immunity* **30**, 384-396 (2009).

47. Rabinovitz, I., Toker, A. & Mercurio, A.M. Protein kinase C-dependent mobilization of the alpha6beta4 integrin from hemidesmosomes and its association with actin-rich cell protrusions drive the chemotactic migration of carcinoma cells. *J Cell Biol* **146**, 1147-1160 (1999).
48. Matsumoto, M. *et al.* New piericidin glucosides, glucopiericidins A and B. *J Antibiot (Tokyo)* **40**, 149-156 (1987).
49. Hall, C. *et al.* Piericidin A: a new inhibitor of mitochondrial electron transport. *Biochem Biophys Res Commun* **25**, 373-377 (1966).
50. Hart, C.P. Finding the target after screening the phenotype. *Drug Discov Today* **10**, 513-519 (2005).
51. Cuatrecasas, P., Wilchek, M. & Anfinsen, C.B. Selective enzyme purification by affinity chromatography. *Proc Natl Acad Sci U S A* **61**, 636-643 (1968).
52. Spencer, D.M., Wandless, T.J., Schreiber, S.L. & Crabtree, G.R. Controlling signal transduction with synthetic ligands. *Science* **262**, 1019-1024 (1993).
53. Fenteany, G. *et al.* A beta-lactone related to lactacystin induces neurite outgrowth in a neuroblastoma cell line and inhibits cell cycle progression in an osteosarcoma cell line. *Proc Natl Acad Sci U S A* **91**, 3358-3362 (1994).
54. Luesch, H. Towards high-throughput characterization of small molecule mechanisms of action. *Mol Biosyst* **2**, 609-620 (2006).
55. Kamiyama, H. *et al.* Epoxyquinol B, a naturally occurring pentaketide dimer, inhibits NF-kappaB signaling by crosslinking TAK1. *Biosci Biotechnol Biochem* **72**, 1894-1900 (2008).
56. Takemoto, Y. *et al.* Chemistry and biology of moverastins, inhibitors of cancer cell migration, produced by Aspergillus. *Chem Biol* **12**, 1337-1347 (2005).
57. Yaguchi, S. *et al.* Antitumor activity of ZSTK474, a new phosphatidylinositol 3-kinase inhibitor. *J Natl Cancer Inst* **98**, 545-556 (2006).
58. Peterson, J.R., Lebensohn, A.M., Pelish, H.E. & Kirschner, M.W. Biochemical suppression of small-molecule inhibitors: a strategy to identify inhibitor targets and signaling pathway components. *Chem Biol* **13**, 443-452 (2006).
59. Hoon, S. *et al.* An integrated platform of genomic assays reveals small-molecule bioactivities. *Nat Chem Biol* **4**, 498-506 (2008).
60. Monton, M.R.N. & Soga, T. Metabolome analysis by capillary electrophoresis-mass spectrometry. *J Chromatogr A* **1168**, 237-246 (2007).
61. Soga, T. *et al.* Quantitative metabolome analysis using capillary electrophoresis mass spectrometry. *J Proteome Res* **2**, 488-494 (2003).

62. Hirayama, A. *et al.* Quantitative metabolome profiling of colon and stomach cancer microenvironment by capillary electrophoresis time-of-flight mass spectrometry. *Cancer Research* **69**, 4918-4925 (2009).
63. Ishii, N. *et al.* Multiple high-throughput analyses monitor the response of E. coli to perturbations. *Science* **316**, 593-597 (2007).
64. Soga, T. *et al.* Differential metabolomics reveals ophthalmic acid as an oxidative stress biomarker indicating hepatic glutathione consumption. *J Biol Chem* **281**, 16768-16776 (2006).
65. Sugimoto, M. *et al.* Capillary electrophoresis mass spectrometry-based saliva metabolomics identified oral, breast and pancreatic cancer-specific profiles. *Metabolomics* **6**, 78-95 (2009).
66. Gutman, M., Singer, T.P., Beinert, H. & Casida, J.E. Reaction sites of rotenone, piericidin A, and amytal in relation to the nonheme iron components of NADH dehydrogenase. *Proc Natl Acad Sci USA* **65**, 763-770 (1970).
67. Bachelard, H.S., Clark, A.G. & Thompson, M.F. Cerebral-cortex hexokinase. Elucidation of reaction mechanisms by substrate and dead-end inhibitor kinetic analysis. *Biochem J* **123**, 707-715 (1971).
68. Le Clainche, C. & Carlier, M.-F. Regulation of actin assembly associated with protrusion and adhesion in cell migration. *Physiol Rev* **88**, 489-513 (2008).
69. Korn, E.D., Carlier, M.F. & Pantaloni, D. Actin polymerization and ATP hydrolysis. *Science* **238**, 638-644 (1987).
70. Homma, K. & Ikebe, M. Myosin X is a high duty ratio motor. *J Biol Chem* **280**, 29381-29391 (2005).
71. Miccoli, L. *et al.* Intracellular pH governs the subcellular distribution of hexokinase in a glioma cell line. *Biochem J* **313 (Pt 3)**, 957-962 (1996).
72. Methods of enzymatic analysis (3rd edition), Bergmeyer, H.U. ed. (Academic Press, New York, 1983).
73. Floridi, A. *et al.* Effect of lonidamine on the energy metabolism of Ehrlich ascites tumor cells. *Cancer Research* **41**, 4661-4666 (1981).
74. Aloj, L. *et al.* Glut-1 and hexokinase expression: relationship with 2-fluoro-2-deoxy-D-glucose uptake in A431 and T47D cells in culture. *Cancer Research* **59**, 4709-4714 (1999).
75. Saito, T. *et al.* The interaction of Akt with APPL1 is required for insulin-stimulated Glut4 translocation. *J Biol Chem* **282**, 32280-32287 (2007).
76. Mueckler, M. *et al.* Sequence and structure of a human glucose transporter. *Science* **229**, 941-945 (1985).

77. Scheepers, A., Joost, H.G. & Schurmann, A. The glucose transporter families SGLT and GLUT: molecular basis of normal and aberrant function. *JPEN J Parenter Enteral Nutr* **28**, 364-371 (2004).
78. Cai, J. & Gros, P. Overexpression, purification, and functional characterization of ATP-binding cassette transporters in the yeast, Pichia pastoris. *Biochim Biophys Acta* **1610**, 63-76 (2003).
79. Colville, C.A. *et al.* Kinetic analysis of the liver-type (GLUT2) and brain-type (GLUT3) glucose transporters in Xenopus oocytes: substrate specificities and effects of transport inhibitors. *Biochem J* **290 (Pt 3)**, 701-706 (1993).
80. Wheeler, T.J. & Hinkle, P.C. Kinetic properties of the reconstituted glucose transporter from human erythrocytes. *J Biol Chem* **256**, 8907-8914 (1981).
81. Hsu, S.C. & Molday, R.S. Glycolytic enzymes and a GLUT-1 glucose transporter in the outer segments of rod and cone photoreceptor cells. *J Biol Chem* **266**, 21745-21752 (1991).
82. Witke, W. The role of profilin complexes in cell motility and other cellular processes. *Trends Cell Biol* **14**, 461-469 (2004).
83. Molitoris, B.A., Geerdes, A. & McIntosh, J.R. Dissociation and redistribution of Na+,K(+)-ATPase from its surface membrane actin cytoskeletal complex during cellular ATP depletion. *J Clin Invest* **88**, 462-469 (1991).
84. Deberardinis, R.J. *et al.* Beyond aerobic glycolysis: transformed cells can engage in glutamine metabolism that exceeds the requirement for protein and nucleotide synthesis. *Proc Natl Acad Sci USA* **104**, 19345-19350 (2007).
85. Parlo, R.A. & Coleman, P.S. Enhanced rate of citrate export from cholesterol-rich hepatoma mitochondria. The truncated Krebs cycle and other metabolic ramifications of mitochondrial membrane cholesterol. *J Biol Chem* **259**, 9997-10003 (1984).
86. Piva, T.J. & McEvoy-Bowe, E. Oxidation of glutamine in HeLa cells: role and control of truncated TCA cycles in tumour mitochondria. *J Cell Biochem* **68**, 213-225 (1998).
87. Kovacević, Z., Popović, J., Brkljac, O. & Lelas, S. Interaction of metabolism of aspartate and inosine and energy state of malignant cells. *Biochem J* **247**, 47-51 (1987).
88. Bradford, M.M. A rapid and sensitive method for the quantitation of microgram quantities of protein utilizing the principle of protein-dye binding. *Anal Biochem* **72**, 248-254 (1976).
89. Bustamante, E., Morris, H.P. & Pedersen, P.L. Energy metabolism of tumor cells. Requirement for a form of hexokinase with a propensity for mitochondrial binding. *J Biol Chem* **256**, 8699-8704 (1981).
90. Mathupala, S.P., Ko, Y.H. & Pedersen, P.L. Hexokinase II: cancer's double-edged sword acting

as both facilitator and gatekeeper of malignancy when bound to mitochondria. *Oncogene* **25**, 4777-4786 (2006).

91. Membrane transport: a practical approach, Baldwin, S.A.ed. (Oxford University Press, 2000).
92. Hsu, P.P. & Sabatini, D.M. Cancer cell metabolism: Warburg and beyond. *Cell* **134**, 703-707 (2008).
93. Madhok, B.M. *et al.* Targeting Glucose Metabolism: An Emerging Concept for Anticancer Therapy. *Am J Clin Oncol* (in print).
94. Shanmugam, M., McBrayer, S.K. & Rosen, S.T. Targeting the Warburg effect in hematological malignancies: from PET to therapy. *Curr Opin Oncol* **21**, 531-536 (2009).
95. Vander Heiden, M.G. *et al.* Identification of small molecule inhibitors of pyruvate kinase M2. *Biochem Pharmacol* **79**, 1118-1124 (2010).
96. Suami, T., Lichtenthaler, F. & Ogawa, S. Aminocyclitols. VIII. A Synthesis of Inosamines and Inosadiamines. *Bull Chem Soc Jpn* **39**, 170-178 (1966).
97. Ogawa, S., Oki, S. & Suami, T. Inositol Derivatives. 11. Synthesis of Dianhydroinositols. *Bull Chem Soc Jpn* **52**, 1095-1101 (1979).
98. Airley, R.E. & Mobasheri, A. Hypoxic regulation of glucose transport, anaerobic metabolism and angiogenesis in cancer: novel pathways and targets for anticancer therapeutics. *Chemotherapy* **53**, 233-256 (2007).
99. Mazurek, S., Boschek, C.B., Hugo, F. & Eigenbrodt, E. Pyruvate kinase type M2 and its role in tumor growth and spreading. *Semin Cancer Biol* **15**, 300-308 (2005).

謝辞

本研究を遂行するにあたり、終始御懇篤なる御指導、御鞭撻賜りました慶應義塾大学理工学部教授 井本正哉博士に謹んで感謝の意を表します。

また本研究に際し、常々御指導、御助言賜りました慶應義塾大学理工学部専任講師 田代悦博士に深謝致します。

本論文の執筆にあたり、御教示、御高配賜りました慶應義塾大学理工学部教授 上村大輔博士、慶應義塾大学理工学部教授 佐藤智典博士、慶應義塾大学理工学部教授 岡浩太郎博士、慶應義塾大学理工学部准教授 土居信英博士に厚く感謝致します。

メタボローム解析に際し、多大なる御指導、御鞭撻頂きました慶應義塾大学環境情報学部教授 曽我朋義博士に深謝致します。

解糖代謝抑制物質の探索研究に際し、御助言ならびに貴重な化合物を御提供頂きました慶應義塾大学理工学部名誉教授 小川誠一郎博士に心より感謝致します。

glucopiericidin A, piericidin A の生産菌の同定、発酵生産、構造解析に際し、御指導、御助言頂きました微生物化学研究センター 高橋良和博士、澤竜一博士、五十嵐雅之博士、木下直子氏に厚く感謝致します。また、微生物化学研究センターよりスクリーニングサンプルを御供与頂きました。重ねて御礼申し上げます。

SCAD kit library を用いた glucopiericidin A の標的探索研究に際し、御協力を頂きました癌研究会癌化学療法センター分子薬理部部長 矢守隆夫博士、微生物化学研究センター 川田学博士をはじめ文部科学省がん特定領域研究化学療法基盤情報支援班の先生方に厚く御礼申し上げます。

glucopiericidin A の標的同定に際し、結果が得られず本論文に記載できませんでしたが GLUT との直接相互作用の証明研究にて終始御助言、御尽力下さいました慶應義塾大学理工学部教授 佐藤智典博士に改めて御礼申し上げます。

メタボローム解析に際し、池田五月氏、紙健次郎氏をはじめ慶應義塾大学先端生命科学研究所の皆様に御協力、御助言頂きました。御礼申し上げます。

解糖代謝抑制物質の探索研究に際し、慶應義塾大学理工学部応用細胞生物学研究室卒業生 三澤茉由子さんに大変な御助力を頂きました。心より感謝致します。

本研究に際し、理化学研究所 竹本靖博士より語り尽くせぬ御恩を拝受致しました。心より御礼申し上げます。また、親身に御助言、御激励下さいました理化学研究所 二村友史博士をはじめ応用細胞生物学研究室の諸先輩方ならびに卒業生の皆様に感謝致します。

最後に、様々な面でサポートして頂きました応用細胞生物学研究室秘書 梅崎秀香さん、幾多の面で御助力頂きました早稲田大学 金井麻衣博士、ならびに御協力下さいました揖場郷君、道下真衣さんをはじめ研究室の後輩に深く感謝致します。